Identification and analysis of genes involved in bone formation

- a genetic approach in zebrafish -

Kirsten Mireille Spoorendonk

The research described in this thesis was performed at the Hubrecht Institute of the Royal Netherlands Academy of Arts and Sciences (KNAW), within the Graduate School of Cancer Genomics and Developmental Biology, Utrecht, the Netherlands.

Cover: modified image of five times the opercle of an *osx:mCherry* zebrafish embryo counterstained with calcein.

ISBN: 978-90-393-5241-0
Printed by: Digital Printing Partners, Houten

Identification and analysis of genes involved in bone formation

- a genetic approach in zebrafish -

Identificatie en analyse van genen betrokken bij botvorming
- *een genetische benadering in de zebravis* -

(met een samenvatting in het Nederlands)

PROEFSCHRIFT

ter verkrijging van de graad van doctor aan de Universiteit Utrecht op gezag van de rector magnificus, prof. dr. J.C. Stoof, ingevolge het besluit van het college voor promoties in het openbaar te verdedigen op donderdag 17 december 2009 des ochtends te 10.30 uur

door
Kirsten Mireille Spoorendonk

geboren op 22 augustus 1982 te Hendrik-Ido-Ambacht

Promotoren: Prof. dr. E. Cuppen
Prof. dr. S. Schulte-Merker

The following financial sponsors are gratefully acknowledged:
- Schering-Plough
- J. E. Jurriaanse stichting

CONTENTS

CHAPTER 1

Zebrafish as a unique model system in bone research: the power of genetics and *in vivo* imaging

Kirsten M. Spoorendonk, Christina L. Hammond, Leonie F.A. Huitema, Jo Vanoevelen, and Stefan Schulte-Merker

Journal of Applied Ichthyology, in press.

SUMMARY

For many years bone research has been mainly performed in mice, chicken, cell culture systems or human material from the clinic. In this review, we describe the features of zebrafish (*Danio rerio*), a relatively new model system in this field. This small teleost offers possibilities which makes it a great complement to the mouse: forward genetic screens are possible in fish due to extrauterine development and large brood size, and the recent generation of osteoblast-specific reporter lines allows visualization of osteoblasts *in vivo*. As key regulators of bone formation are highly conserved between mammals and teleosts, findings in fish likely apply to mammalian osteogenesis and tissue mineralization.

Bone and cartilage are specialized tissues that make up the skeleton of the vertebrate body. Bones shape and support body structures and are indispensable for several mechanical and metabolic functions. Development of bone can occur via two distinct mechanisms, intramembranous and chondral bone formation. During intramembranous (or dermal) ossification, mesenchymal cells condense and differentiate into osteoblasts, the bone-forming cells. In contrast, during chondral ossification, mesenchymal cells condense and differentiate into chondrocytes to form a cartilage template. Subsequently, this template is either replaced by bone (endochondral ossification) or it becomes surrounded by bone (perichondral ossification).

Osteoporosis and osteoarthritis are skeletal diseases affecting a huge part of the human population above 55 years of age. Osteoporosis is characterized by a gradual reduction of bone mass, leading to bone fragility. Patients with osteoarthritis suffer from articular cartilage mineralization, leading to cartilage destruction. Less common but leading to similar or even greater disabilities, are bone diseases where patients show skeletal abnormalities or overgrowth, such as cleidocranial dysplasia (CCD) and fibrodysplasia ossificans progressiva (FOP). These pathologies have recently been linked to mutations in Runx2 (a key regulator of both chondrocyte and osteoblast differentiation) (Otto et al., 2002) and BMP dysregulation (Kaplan et al., 2006), respectively.
Unfortunately, for many other bone diseases the underlying genetic cause remains unknown and only a few effective treatments for chronic skeletal diseases are available. Therefore, it is desirable to gain more insight in the molecular mechanisms underlying bone development and diseases, and to identify new genes essential in bone formation and bone homeostasis.

The majority of studies in the areas of osteogenesis and mineral research have been performed in mice and chicken, or using *in vitro* cell culture systems. Until now the zebrafish (*Danio rerio*) has not been used extensively as a model system in bone research. Several characteristics, like the absence of haematopoietic bone marrow tissue (Witten and Huysseune, 2009) and the lack of osteocytes in most species (Hall and Witten, 2007), distinguish teleost bone from that of mammals. These features have undoubtedly contributed to fish being sidelined when studying bone formation and osteoblast function. Nevertheless, key regulators of bone formation are highly conserved between mammals and teleosts, and the corresponding orthologs share significant sequence similarities and an overlap in expression patterns (Flores et al., 2004; Li et al., 2009; Yan et al., 2005) when compared to mammals.

Due to its rapid generation time, large offspring numbers, external development, transparency and the availability of genetic maps, the zebrafish is a very attractive model system to study the function of genes involved in bone formation. In this

review we will discuss the use of zebrafish in forward genetic screens to identify specific bone mutants. Furthermore, we will address the use of transgenic zebrafish lines representing unique tools to follow osteoblasts *in vivo* and to analyze their function in wild type or mutant backgrounds.

Screen set up

Forward genetic screens in zebrafish have resulted in the identification of mutants encompassing a wide range of developmental processes. The random and therefore unbiased way of inducing mutations via N-ethyl-N-nitrosourea (ENU), followed by phenotypic screening and positional cloning of the affected genes has been proven to be an effective method to identify novel gene functions (Driever et al., 1996; Haffter et al., 1996).

Large scale genetic screens are typically set up as follows (see figure 1): males are mutagenized with ENU, an alkylating agent considered as one of the most potent mutagens to induce point mutations. These parental males are outcrossed with wild-type females resulting in F1 offspring where every fish carries a unique set of heterozygous mutations. F1 individuals are then outcrossed with F1 fish stemming from an unrelated mutagenesis event, thereby giving rise to F2 families in which 50% of the fish carry the mutation. F2 families are then incrossed (brother-sister matings), followed by phenotypic screening of the F3 progeny. Per F2 family, usually an attempt is made to screen egglays from at least four separate matings, as this will result in a 68% probability to homozygose all mutations in that particular family (Driever et al., 1996).

In zebrafish, ossification of the craniofacial skeleton starts around 3 days post fertilization (dpf) with the fifth branchial arch and the opercle as the first two elements to mineralize (Cubbage and Mabee, 1996). Centra of the axial skeleton are formed sequentially, starting with the third and fourth centrum around 6 dpf (Bird and Mabee, 2003; Du et al., 2001). To screen for bone mutants in zebrafish the F3 progeny is raised to 8 dpf, as this is a stage advanced enough to analyze a number of different bone elements, whilst avoiding the need to feed the larvae (and thereby avoiding variabilities introduced within an F3 dish through feeding). At 8dpf, larvae are fixed and histologically stained for bone using alizarin red. Bone formation is a relatively late process in development and partly dependent on cartilage formation, at least for chondral bone. Therefore, to be able to pick up specific bone mutants that do not exhibit cartilage defects, bone stainings are combined with alcian blue stainings for cartilage (Walker and Kimmel, 2007). Afterwards the embryos can be analyzed through visual inspection on a standard dissecting microscope.

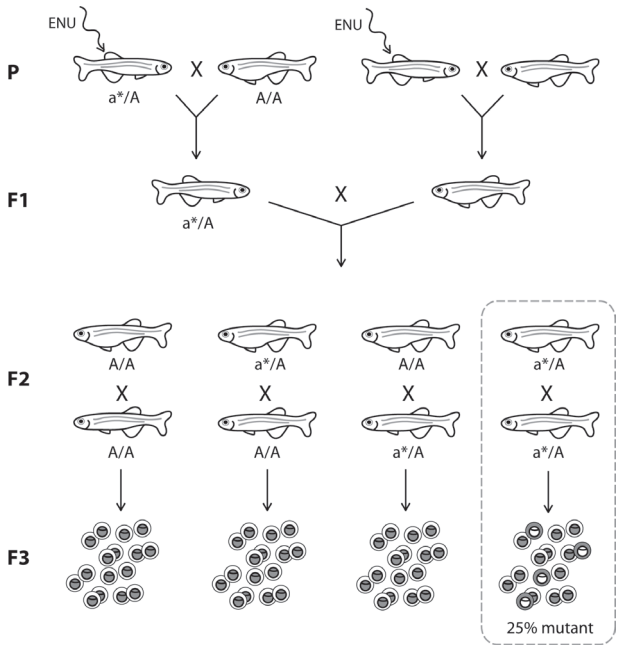

Figure 1: **Crossing scheme for a forward genetic screen.** Parental ENU mutagenized males are outcrossed with wild-type females. Non-related F1 individuals are crossed with each other, giving rise to F2 families. Crosses between F2 siblings produce F3 clutches that can be screened for phenotypes. In this scheme, for simplicity, only one mutation (a*) is considered, while every mutagenesis event leads to many induced mutations.

Distinct classes of bone mutants

If a certain phenotype of interest is picked up in 25% of an F3 egglay, the parental F2 fish will be kept and used to establish a line.

Identified bone mutants can be categorized according to the intensity and localization of the alizarin red stain, which provides information about the amount of bone present and the type of bone affected. In general, four classes of bone mutants can be distinguished (see figure 2).

Class I: generally less or no bone

The first group of mutants is identified by a complete absence of alizarin red staining, or a significantly lower amount of it. All other structures (particularly cartilage), size and overall appearance of the embryo, should appear comparable to siblings. In most boneless mutants bone osteoid is formed, but mineralization does not occur or is delayed (fig 2, class I: arrow is pointing to the tip of the notochord which is formed but is not mineralized).

Occasionally, it is observed that mutants contain smaller or no otoliths, structures which will be part of the hearing and balance system. Otoliths consist of calcium carbonate (Hughes et al., 2006), which is a different mineral crystal than hydroxyapatite in bone (Buckwalter and Cooper, 1987). This suggests that in mutants with aberrant otoliths, the affected gene might possibly play a rather general role in calcium transport and calcium homeostasis in the zebrafish embryo. In mutants where otoliths are calcified normally the mutated gene is more likely to play a more specific role in

bone development. Another subgroup of mutants in this first class shows alizarin red staining only in the teeth. As the case with otoliths, teeth contain a different biomineral composition than bone (Butler and Ritchie, 1995). Therefore it is expected that, also for these mutants without affected teeth, the affected gene plays a specific role in bone formation.
A concern with this particular class of mutants is a possible delay of development due to a mutation in housekeeping genes or an effect on heart beat, the vasculature, etc.: such a delay could easily result in a slow onset of ossification, and be misinterpreted as a lack in mineralization. Therefore, exact stage comparisons between mutants and siblings are essential.

Class II: ectopic overossifcation
The second class comprises mutants that show ossification at additional and ectopic places, where in wildtype siblings no bone is formed. This excessive amount of mineralization can originate either from an overproduction of bone in regions where bone is expected to be formed, or it can arise at completely ectopic sites leading to pathological mineralization.
An example of the former group is the *stocksteif* mutant, characterized by overossification in the region of the notochord, resulting in fusion of the vertebral centra. In older mutants boundaries between adjacent centra are only occasionally retained and haemal and neural arches are misshaped as well (Spoorendonk et al., 2008). The mutated gene, *cyp26b1*, has been proposed to regulate, through controlling retinoic acid levels within osteoblasts, the activity of osteoblasts especially in the axial skeleton (Laue et al., 2008; Spoorendonk et al., 2008).
In addition, fish carrying the *chihuahua* mutation belong to this group. *Chihuahua* is a dominant mutation in type I collagen, resulting in a phenotype in which all bones appear to be misshapen and numerous spots of uneven mineralization can be observed (Fisher et al., 2003).
Touchtone/nutria mutants, exhibiting a phenotype that results from mutations in *trpm7*, provide an example of the latter group: here, mutant embryos show ectopic mineralization within mesonephric tubules (Elizondo et al., 2005), leading to kidney stone formation, a classic example of pathological mineralization.

Class III: more perichondral bone, but normal dermal bone
In the last two classes only perichondral bone, but not dermal bone is affected. Where normally mineralization of the ceratohyal has just started at 8 dpf and mineralization of the first four branchial arches only begins around 12 dpf, mutants in class III display ossified ceratohyal and branchial arches already by 8 dpf (arrows in fig 2, class III). However, dermal bone formation is unaffected. Since mineralization is achieved through combined activities of two populations of cells, namely hypertrophic chondrocytes and osteoblasts, premature differentiation of either chondrocytes or osteoblasts (or both) could be responsible for the phenotype.

Class IV: less perichondral bone, but normal dermal bone
Mutants in class IV also give a phenotype affecting only chondral bone, but different to the mutants from class III: this phenotype is characterized by a lack or delay of perichondral bone formation. Again, dermal bone development is not perturbed in these mutants. While the phenotypes of the first three classes of bone mutants can be readily detected by 8 dpf, this final class becomes steadily more apparent after two weeks of age, since at 8 dpf the only perichondral bones which are already fully mineralized are the fifth branchial arch and the basioccipital. While after this stage in wild type larvae other cartilage elements, such as the ceratohyal, Meckel's cartilage, branchial arches, and chondrocranium, begin to mineralize, in mutants these elements remain purely cartilaginous. This phenotype, as in the case of class III mutants, could be due to changes in the differentiation potential or function of chondrocytes or osteoblasts.

In addition to the four classes that are outlined above there are a few reported zebrafish bone mutants, which rather than showing altered levels of ossification instead display misshapen bone elements. Since often these are identified in conjunction with other craniofacial abnormalities, it appears likely that the bone phenotypes are secondary to earlier patterning defects rather than an osteoblast specific misregulation. Examples in this subclass include the *fused somites* mutant (van Eeden et al., 1996), the *endothelin 1* mutant (Kimmel et al., 2003), and *fgf8* heterozygous phenotypes (Albertson and Yelick, 2007).

Zebrafish share many similarities with higher vertebrates in terms of the origins of the cells that contribute to the various bone elements. Cell labeling studies have demonstrated that much of the craniofacial skeleton derives from cranial neural crest cells, the skeletogenic population of which is spatially separated from neurogenic neural crest cells even prior to migration (Schilling and Kimmel, 1994). The pharyngeal skeleton which includes the jaw, branchial arches and gill structures and which is formed on a cartilage model is derived solely from cranial neural crest (Knight and Schilling, 2006; Yelick and Schilling, 2002), while the neurocranium is derived from both cranial neural crest and mesoderm (Yelick and Schilling, 2002). Most likely the other dermal bone elements (e.g. cleithrum and opercle) also originate from the latter two lineages. It is possible that the phenotypes of class III and class IV mutants arise from earlier changes to the timing of neural crest differentiation or specification.

Eventually, when a certain phenotype has been identified, positional cloning can clarify the genetic lesion of the mutants. The procedure how to achieve this is described elsewhere (Geisler, 2002), and will therefore not be covered here.
Most mouse mutants with a defect in bone formation are embryonic lethal or die at birth because of respiratory distress. Initial data seem to indicate that this is not necessarily true for fish mutants (C.H., L.H. and S.S.-M, unpublished), possibly due

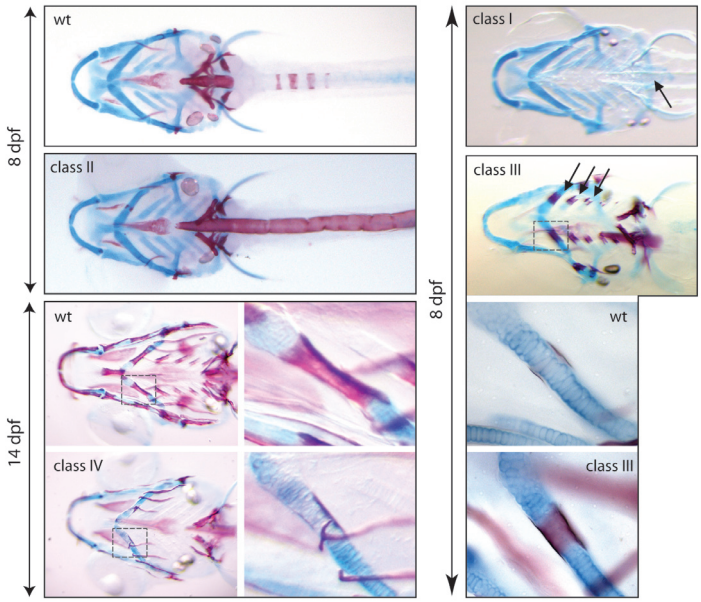

Figure 2: **Classification of bone mutants.** Four distinct classes of bone mutants can be specified. All embryos shown are stained for both bone (alizarin red) and cartilage (alcian blue). Mutants of class I show no bone at all or severely reduced bone formation. Note that bone structures are formed but ossification does not occur (arrow is pointing to the tip of the notochord which is formed but not mineralized). Class II mutants are characterized by ectopic overossification. In this example the notochord is enwrapped by alizarin red positive matrix resulting from fusion of the future vertebrae. Mutants of class III have excess perichondral bone, but a normal amount of dermal bone, while mutants of class IV have less perichondral bone, while retaining normal amounts of dermal bone. Magnifications of the ceratohyal are shown. Arrows are pointing to the ceratohyal and the first two branchial arches, which are already ossified in this particular class III mutant.

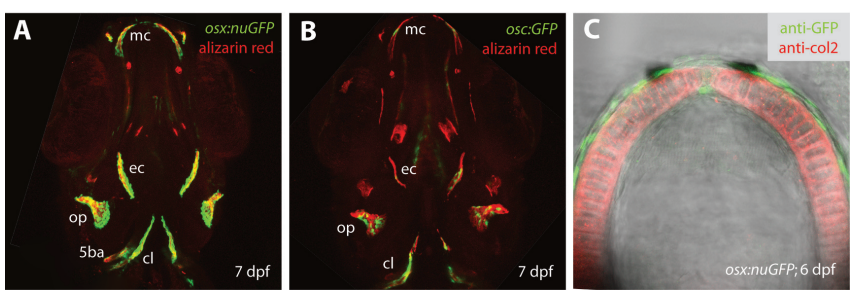

Figure 3: **Imaging osteoblasts by *in vivo* analysis of transgenic lines.** (A-B) *osx:nuclearGFP* (A) and *osc:GFP* (B) expressing osteoblasts in the head (ventral view) of a 7 day old transgenic zebrafish embryo, counterstained with alizarin red. 5ba = fifth branchial arch, cl = cleithrum, ec = ectopterygoid, mc = Meckel's cartilage, op = opercle, *osc =osteocalcin, osx =osterix.*
(C) Ventral view of Meckel's cartilage in an *osx:nuGFP* embryo with chondrocytes (stained with anti-collagenII in red) and osteoblasts (stained with anti-GFP). Note that the osteoblasts that form the bone collar are surrounding the cartilage cells.

to a lower weight-bearing demand on the skeleton in aquatic animals. Many zebrafish bone mutants are sub-viable and can survive to early adulthood, possibly enabling analysis not only of embryonic but also larval or adult effects on osteogenesis in these mutants. For example, mutants of the Hedgehog signaling pathway such as the *Indian Hedgehog* null mutant which in mice die at birth (St-Jacques et al., 1999), but in zebrafish can survive to adulthood (Hammond and Schulte-Merker, 2009). Furthermore, *Patched1* mutants which in mice die at E9.5 (Goodrich et al., 1997) but in zebrafish survive to late larval stages, thus allowing bone development to be studied (Hammond and Schulte-Merker, 2009).
Although until now not many zebrafish bone mutants have been positionally cloned, this will certainly change in the future and contribute significantly to our understanding of bone development and homeostasis not only during embryonic stages but also throughout life.

Imaging and analyzing osteoblasts *in vivo*
In addition to the advantages as a model for genetic analysis, zebrafish have always been heralded for the transparency of its embryos and larvae, and for the opportunities this particular feature offers in terms of life imaging. Initially this was used to follow individual, dye-injected cells for lineage tracings and fate mapping studies (Kimmel et al., 1990), but very quickly it was appreciated that cell- or tissue-specific promoters controlling expression of bioluminescent chromophores such as GFP or RFP are powerful reagents to study gene expression and to analyze cells *in vivo*. Today, dozens of transgenic lines exist that make use of this strategy, and fortunately, some of those pertain to osteogenesis research.
Very recently, *twist:eGFP, osteocalcin:dsRed* (Inohaya et al., 2007), and *osterix:mCherry* (Renn and Winkler, 2009; Spoorendonk et al., 2008) transgenic medaka lines have been reported. *Twist* is expressed in mesenchymal cells and has been shown to be a specific marker, within somites, for sclerotome tissue in zebrafish (Morin-Kensicki and Eisen, 1997) as well as in medaka (Renn et al., 2006). These mesenchymal cells can differentiate into either chondrocytes or osteoblast, the latter process driven by the master regulator *osterix* (Nakashima et al., 2002). *Osteocalcin*, on the other hand, is a marker for differentiated cells producing bone matrix (Gavaia et al., 2006). Inohaya et al. (2007) were able to show that *twist:eGFP* positive cells in the axial skeleton differentiated into mature osteoblasts, expressing *osteocalcin:dsRed.* Furthermore, Renn and colleagues (Renn and Winkler, 2009) showed in *osterix:mCherry* and *osteocalcin:eGFP* double transgenic medaka that early osteoblasts expressing mCherry are *osteocalcin* negative initially, but become positive during later differentiation. Taken together, these lines make it possible, for the first time, to follow and analyze sclerotomal cells and osteoblasts *in vivo*.

Since zebrafish and medaka have highly similar and conserved modes of ossification (Inohaya et al., 2007), it has been possible to generate stable transgenic zebrafish

lines for *osterix* (figure 3A) and *osteocalcin* (figure 3B) by injecting the medaka promoter constructs into one cell stage embryos. As in medaka, zebrafish *osterix* expression precedes *osteocalcin* expression. Eventually, both genes are expressed in all mineralized elements of the zebrafish skeleton. Both lines are extremely useful to analyze the behaviour and function of osteoblasts, not only in the wild type situation but also in mutant backgrounds. For example, we recently found that, upon retinoic acid treatment, localization and numbers of osteoblasts are not changed: retinoic acid most likely causes increased activity of axial osteoblasts, resulting in an overproduction of bone matrix and fusion of vertebrae (Spoorendonk et al., 2008).

In a field where *in vitro* analysis is made inherently difficult by the vary nature of the cells under study and by the long culturing times, it is important to explore ways to follow cells *in vivo*. For example, there are conflicting ideas about the relationship of hypertrophic chondrocytes and osteoblasts: in general it is believed that chondrocytes degenerate and die during endochondral bone development. It is suggested that they are replaced by osteoblasts, the cells eventually responsible for bone matrix deposition. However, other reports have claimed that hypertrophic chondrocytes do survive and transdifferentiate into osteoblasts (Wlodarski et al., 2006). This hypothesis is supported by microscopic examinations of cells present at the chondro-osseous junctions in the growth plate (Bianco et al., 1998; Galotto et al., 1994; Riminucci et al., 1998). It is speculated that there are two subpopulations of chondrocytes, one which becomes apoptotic, while the other population transdifferentiates into osteoblasts. However, all these studies where carried out *in vitro* or in fixed specimen. An alternative and possibly much more informative approach would be to use double transgenic fish lines that mark chondrocytes (e.g. through *collagenII:RFP*) as well as osteoblasts (e.g., via *osterix:GFP*). If trans-differentiation were indeed to contribute significantly to bone formation, then one should be able to identify chondrocytes that express both RFP and GFP *in vivo*. This indeed appeared to be the case, as very recently shown by Hammond and Schulte-Merker (2009). Figure 3C shows a six day old *osx:nuGFP* embryo immuno-stained with anti-GFP and anti-collagenII, demonstrating the single cell resolution obtainable with this technology.

In summary, the zebrafish has been demonstrated to be a powerful model especially in forward genetics to identify novel gene functions and to study their role in numerous processes including osteogenesis. The zebrafish can be used as a tool to complement genetic and embryological studies in mice and avians in order to clarify the molecular mechanisms underlying bone development and disease. In addition, zebrafish and medaka are ideally suited and currently the only model system available to allow visualization of chondrocytes and osteoblasts *in vivo* over time. The combination of these advantageous features will greatly contribute to our understanding of osteogenesis in the future.

REFERENCES

Albertson, R. C. and Yelick, P. C. (2007). Fgf8 haploinsufficiency results in distinct craniofacial defects in adult zebrafish. Dev Biol 306, 505-15.

Bianco, P., Cancedda, F. D., Riminucci, M. and Cancedda, R. (1998). Bone formation via cartilage models: the “borderline” chondrocyte. Matrix Biol 17, 185-92.

Bird, N. C. and Mabee, P. M. (2003). Developmental morphology of the axial skeleton of the zebrafish, Danio rerio (Ostariophysi: Cyprinidae). Dev Dyn 228, 337-57.

Buckwalter, J. A. and Cooper, R. R. (1987). Bone structure and function. Instr Course Lect 36, 27-48.

Butler, W. T. and Ritchie, H. (1995). The nature and functional significance of dentin extracellular matrix proteins. Int J Dev Biol 39, 169-79.

Cubbage, C. C. and Mabee, P. M. (1996). Development of the Cranium and Paired Fins in the Zebrafish Danio rerio (Ostariophysi, Cyprinidae). Journal of Morphology 229, 121-160.

Driever, W., Solnica-Krezel, L., Schier, A. F., Neuhauss, S. C., Malicki, J., Stemple, D. L., Stainier, D. Y., Zwartkruis, F., Abdelilah, S., Rangini, Z. et al. (1996). A genetic screen for mutations affecting embryogenesis in zebrafish. Development 123, 37-46.

Du, S. J., Frenkel, V., Kindschi, G. and Zohar, Y. (2001). Visualizing normal and defective bone development in zebrafish embryos using the fluorescent chromophore calcein. Dev Biol 238, 239-46.

Elizondo, M. R., Arduini, B. L., Paulsen, J., MacDonald, E. L., Sabel, J. L., Henion, P. D., Cornell, R. A. and Parichy, D. M. (2005). Defective skeletogenesis with kidney stone formation in dwarf zebrafish mutant for trpm7. Curr Biol 15, 667-71.

Fisher, S., Jagadeeswaran, P. and Halpern, M. E. (2003). Radiographic analysis of zebrafish skeletal defects. Dev Biol 264, 64-76.

Flores, M. V., Tsang, V. W., Hu, W., Kalev-Zylinska, M., Postlethwait, J., Crosier, P., Crosier, K. and Fisher, S. (2004). Duplicate zebrafish runx2 orthologues are expressed in developing skeletal elements. Gene Expr Patterns 4, 573-81.

Galotto, M., Campanile, G., Robino, G., Cancedda, F. D., Bianco, P. and Cancedda, R. (1994). Hypertrophic chondrocytes undergo further differentiation to osteoblast-like cells and participate in the initial bone formation in developing chick embryo. J Bone Miner Res 9, 1239-49.

Gavaia, P. J., Simes, D. C., Ortiz-Delgado, J. B., Viegas, C. S., Pinto, J. P., Kelsh, R. N., Sarasquete, M. C. and Cancela, M. L. (2006). Osteocalcin and matrix Gla protein in zebrafish (Danio rerio) and Senegal sole (Solea senegalensis): comparative gene and protein expression during larval development through adulthood. Gene Expr Patterns 6, 637-52.

Geisler, R. (2002). Mapping and cloning. In: Zebrafish, a practical approach. Eds: C. Nusslein-Volhard and R. Dahm, pp. 175-210.

Goodrich, L. V., Milenkovic, L., Higgins, K. M. and Scott, M. P. (1997). Altered neural cell fates and medulloblastoma in mouse patched mutants. Science 277, 1109-13.

Haffter, P., Granato, M., Brand, M., Mullins, M. C., Hammerschmidt, M., Kane, D. A., Odenthal, J., van Eeden, F. J., Jiang, Y. J., Heisenberg, C. P. et al. (1996). The identification of genes with unique and essential functions in the development of the zebrafish, Danio rerio. Development 123, 1-36.

Hall, B. K. and Witten, P. E. (2007). Plasticity of and transitions between skeletal tissues in vertebrate evolution and development. In: Major transitions in vertebrate evolution. Eds: J. S. Anderson and H. Sues, pp. 13-56.

Hammond, C. L. and Schulte-Merker, S. (2009). Two populations of endochondral osteoblasts

with differential sensitivity to Hedgehog signalling. Development, in press.

Hughes, I., Thalmann, I., Thalmann, R. and Ornitz, D. M. (2006). Mixing model systems: using zebrafish and mouse inner ear mutants and other organ systems to unravel the mystery of otoconial development. Brain Res 1091, 58-74.

Inohaya, K., Takano, Y. and Kudo, A. (2007). The teleost intervertebral region acts as a growth center of the centrum: in vivo visualization of osteoblasts and their progenitors in transgenic fish. Dev Dyn 236, 3031-46.

Kaplan, F. S., Fiori, J., LS, D. L. P., Ahn, J., Billings, P. C. and Shore, E. M. (2006). Dysregulation of the BMP-4 signaling pathway in fibrodysplasia ossificans progressiva. Ann N Y Acad Sci 1068, 54-65.

Kimmel, C. B., Ullmann, B., Walker, M., Miller, C. T. and Crump, J. G. (2003). Endothelin 1-mediated regulation of pharyngeal bone development in zebrafish. Development 130, 1339-51.

Kimmel, C. B., Warga, R. M. and Schilling, T. F. (1990). Origin and organization of the zebrafish fate map. Development 108, 581-94.

Knight, R. D. and Schilling, T. F. (2006). Cranial neural crest and development of the head skeleton. Adv Exp Med Biol 589, 120-33.

Laue, K., Janicke, M., Plaster, N., Sonntag, C. and Hammerschmidt, M. (2008). Restriction of retinoic acid activity by Cyp26b1 is required for proper timing and patterning of osteogenesis during zebrafish development. Development 135, 3775-87.

Li, N., Felber, K., Elks, P., Croucher, P. and Roehl, H. H. (2009). Tracking gene expression during zebrafish osteoblast differentiation. Dev Dyn 238, 459-66.

Morin-Kensicki, E. M. and Eisen, J. S. (1997). Sclerotome development and peripheral nervous system segmentation in embryonic zebrafish. Development 124, 159-67.

Nakashima, K., Zhou, X., Kunkel, G., Zhang, Z., Deng, J. M., Behringer, R. R. and de Crombrugghe, B. (2002). The novel zinc finger-containing transcription factor osterix is required for osteoblast differentiation and bone formation. Cell 108, 17-29.

Otto, F., Kanegane, H. and Mundlos, S. (2002). Mutations in the RUNX2 gene in patients with cleidocranial dysplasia. Hum Mutat 19, 209-16.

Renn, J., Schaedel, M., Volff, J. N., Goerlich, R., Schartl, M. and Winkler, C. (2006). Dynamic expression of sparc precedes formation of skeletal elements in the Medaka (Oryzias latipes). Gene 372, 208-18.

Renn, J. and Winkler, C. (2009). Osterix-mCherry transgenic medaka for in vivo imaging of bone formation. Dev Dyn 238, 241-8.

Riminucci, M., Bradbeer, J. N., Corsi, A., Gentili, C., Descalzi, F., Cancedda, R. and Bianco, P. (1998). Vis-a-vis cells and the priming of bone formation. J Bone Miner Res 13, 1852-61.

Schilling, T. F. and Kimmel, C. B. (1994). Segment and cell type lineage restrictions during pharyngeal arch development in the zebrafish embryo. Development 120, 483-94.

Spoorendonk, K. M., Peterson-Maduro, J., Renn, J., Trowe, T., Kranenbarg, S., Winkler, C. and Schulte-Merker, S. (2008). Retinoic acid and Cyp26b1 are critical regulators of osteogenesis in the axial skeleton. Development 135, 3765-74.

St-Jacques, B., Hammerschmidt, M. and McMahon, A. P. (1999). Indian hedgehog signaling regulates proliferation and differentiation of chondrocytes and is essential for bone formation. Genes Dev 13, 2072-86.

van Eeden, F. J., Granato, M., Schach, U., Brand, M., Furutani-Seiki, M., Haffter, P., Hammerschmidt, M., Heisenberg, C. P., Jiang, Y. J., Kane, D. A. et al. (1996). Mutations affecting somite formation and patterning in the zebrafish, Danio rerio. Development 123, 153-64.

Walker, M. B. and Kimmel, C. B. (2007). A two-color acid-free cartilage and bone stain for zebrafish larvae. Biotech Histochem 82, 23-8.

Witten, P. E. and Huysseune, A. (2009). A comparative view on mechanisms and functions of skeletal remodelling in teleost fish, with special emphasis on osteoclasts and their function. Biol Rev Camb Philos Soc 84, 315-46.

Wlodarski, K. H., Wlodarski, P. K. and Brodzikowska, A. (2006). Metaplasia of chondrocytes into osteoblasts. Folia Biol (Krakow) 54, 75-80.

Yan, Y. L., Willoughby, J., Liu, D., Crump, J. G., Wilson, C., Miller, C. T., Singer, A., Kimmel, C., Westerfield, M. and Postlethwait, J. H. (2005). A pair of Sox: distinct and overlapping functions of zebrafish sox9 co-orthologs in craniofacial and pectoral fin development. Development 132, 1069-83.

Yelick, P. C. and Schilling, T. F. (2002). Molecular dissection of craniofacial development using zebrafish. Crit Rev Oral Biol Med 13, 308-22.

CHAPTER 2

General introduction

I. Bone development
II. Vertebral development
III. Outline of this thesis

I. BONE DEVELOPMENT

Ossification is an essential requirement for normal skeletal development, which is generally accomplished through the function of two cell types, osteoblasts and chondrocytes. Both cell types are derived from common mesenchymal precursors. To establish their final identity the cells go through multiple stages, which are often regulated by specific transcription factors.
Bone formation can occur in two distinct ways (Karsenty and Wagner, 2002; Kobayashi and Kronenberg, 2005): intramembranous and chondral bone formation. During intramembranous (or dermal) ossification, mesenchymal cells condense and directly differentiate into bone-forming osteoblast. In contrast, during chondral ossification, mesenchymal cells condense and differentiate as chondrocytes. These chondrocytes form a cartilage template, which will be later on replaced by bone.

Other than osteoblasts and chondrocytes, a third cell type, the osteoclast, is responsible for bone homeostasis. Osteoclasts are multinucleated giant cells derived from hematopoietic precursors whose main role is bone resorption and remodeling (Bar-Shavit, 2007). They are derived from hematopoietic precursors and characterized by the expression and secretion of tartrate-resistant acid phosphatase (TRAP)(Lamp and Drexler, 2000). Thus, three distinct cell types (chondrocytes, osteoblasts, and osteoclasts) from two cell lineages direct the formation and remodeling of bone (see figure 1) (Karsenty and Wagner, 2002; Kobayashi and Kronenberg, 2005).

Intramembranous ossification
Clavicles and bone in the regions of the craniofacial skeleton develop by intramembranous ossification. During this process mesenchymal cells differentiate into osteoblasts. This is a stepwise process (Hall and Miyake, 2000) which starts with the migration of mesenchymal cells to the sites of future skeletogenesis. Subsequently, the interaction with epithelial tissue leads to the formation of condensations. The condensed mysenchymal cells grow out and differentiate into osteoblasts forming the skeletal elements. One condensation gives rise to a single bone element or sometimes to multiple elements.
Osteoblasts are responsible for the secretion of organic extracellular matrix, called osteoid, which consists, among other proteins and proteoglycans, mainly of type I collagen (Mackie, 2003). Subsequently, the osteoid matrix will be mineralized. The generation of inorganic phosphate during the process of osteoblast differentiation is one of the signals facilitating the coordination of multiple factors necessary for mineralization (Beck, 2003). Mature bone consist for 30% of organic compounds (mostly collagens) and for 70% of the inorganic mineral hydroxyapatite ($Ca_5(PO_4)_3OH$) (Buckwalter and Cooper, 1987), which gives bone its firmness.
Eventually, osteoblasts either stay at the surface of the bone matrix continuing with the deposition of osteoid, they undergo apoptosis, or they transform into osteocytes,

which are entrapped in mineralized matrix (Franz-Odendaal et al., 2006). Osteocytes cease producing matrix but keep communicating with each other and with the osteoblasts at the bone surface via their dendritic canalicular system. Gap junctions are present between all cells for direct communication (Franz-Odendaal et al., 2006). However, in advanced bony fishes including the zebrafish, bone formation results in a type of bone where entrapment of osteoblasts does not occur (Ekanayake and Hall, 1987; Witten et al., 2001). Consequently, their bone does not contain any osteocytes and is therefore known as acellular bone.

Two transcription factors, *Runx2* (also known as *Cbfa1*) and *Osterix* (*Osx*; also known as *Sp7*) are absolutely required for osteoblast differentiation. *Runx2* is expressed in the lateral mesoderm, in mesenchymal condensations, and in chondrocytes in addition to osteoblasts. *Runx2* target genes include genes expressed by mature osteoblasts, such as *osteocalcin, osteopontin*, and *type I collagen* (Ducy et al., 1997). Bone tissue is completely missing in *Runx2* null mice (Komori et al., 1997). *Osx* is specificially expressed in osteoblasts in all developing bones. Analysis of *Osx* null mice shows that *Osx* is genetically downstream of *Runx2*, since *Runx2* is expressed in *Osx* null mice, while *Osx* is not expressed in *Runx2* null mice (Nakashima et al., 2002).
Several signaling molecules were found to be expressed during specific stages of dermal bone formation. For example, bone morphogenetic proteins (BMPs) positively regulate the commitment to the osteogenic pathway, while *Indian hedgehog* (*Ihh*) negatively regulates the transition from pre-osteoblast to osteoblast (Abzhanov et al., 2007).

Chondral ossification
Vertebrate long bones form through a process called chondral ossification. Formation of the cartilage anlage starts with mesenchymal condensations (Hall and Miyake, 2000). Then, cells start proliferating and differentiate into chondrocytes. Early chondrocytes are small and produce mainly type II collagen. Subsequently, chondrocytes turn flat and columnar, and will finally differentiate into hypertrophic chondrocytes (Kobayashi and Kronenberg, 2005). This last switch is reflected by expression of *type X collagen* (Karsenty and Wagner, 2002). Eventually, the cartilage template is either replaced by bone (endochondral ossification) or it becomes surrounded by bone (perichondral ossification).

The transcription factor *Sox9* is mainly expressed in resting and proliferating chondrocytes, but not anymore in hypertrophic chondrocytes (Goldring et al., 2006). *Sox9* is required for formation of normal mesenchymal condensations, for conversion of mesenchymal cells to chondrocytes, for proliferation of chondrocytes, and for suppression of premature conversion of these chondrocytes to hypertrophic chondrocytes (Akiyama et al., 2002; Bi et al., 1999). Furthermore, *Sox9* directly

regulates expression of genes important for chondrocyte function, such as *collagen type II, IX,* and *XI* (Goldring et al., 2006; Olsen et al., 2000).
Besides its function in osteoblast maturation, *Runx2* is also the major transcription factor controlling a crucial step of chondrocyte maturation because chondrocytes stop dividing and become hypertrophic after they start expressing *Runx2*. Mice lacking *Runx2* function show a defect in chondrocyte maturation, with a lack of hypertrophic chondrocytes in many bones (Inada et al., 1999).
Furthermore, similar to intramembranous ossification, signaling molecules are required for the differentiation of chondrocytes as well: among others, BMPs are necessary for the differentiation of condensed mesenchymal cells into pre- and early chondrocytes, while *Ihh* regulates the differentiation step into flat, columnar chondroctyes (Kobayashi and Kronenberg, 2005).

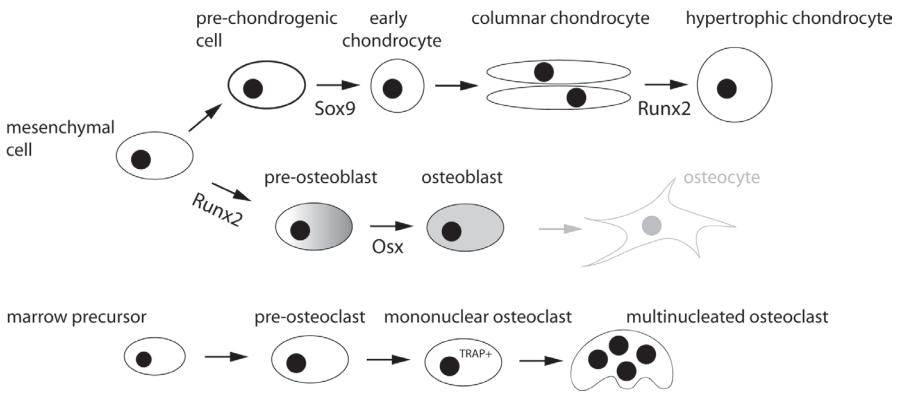

Figure 1: **Differentiation pathways of the cells involved in bone formation.**
During chondral bone formation, mesenchymal cells condense and differentiate into chondrocytes. The cartilage template formed by these chondrocytes is later on replaced by bone. *Sox9* plays an important role in commitment and maintenance of the chondrocyte phenotype. *Runx2* expression stimulates terminal differentiation into hypertrophic chondrocytes. During intramembranous ossification mesenchymal cells condense and directly differentiate into osteoblasts. *Runx2* and *Osx* are both required for osteoblast differentiation. Osteocytes (shaded in grey) are present in mammals, but zebrafish exhibit acellular bone without osteocytes. Osteoclasts, the bone resorbing cells, express and secrete *TRAP* and originate from a marrow precursor. *Figure adapted from Kobayashi and Kronenberg (2005).*

II. VERTEBRAL DEVELOPMENT

The vertebrate body is supported by the vertebral column, a series of segmental bony elements that both provide stability and allow mobility. The functional segmental unit of the vertebral column, the vertebra, is composed (figure 2), in the simplest form, of the vertebral body (or centrum) that develops around the embryonic notochord, of dorsally extending neural arches and spines, and of ventrally extending ribs (or, in more posterior positions, haemal arches and spines).
In zebrafish, ossification starts at three days post fertilization (dpf) in the craniofacial skeleton (Cubbage and Mabee, 1996). From 6 dpf onwards, centra of the axial skeleton are formed sequentially, starting with the third and fourth ones, where after additional centra are added bi-directionally (Bird and Mabee, 2003; Du et al., 2001). Mineralization of the neural and haemal arches follows later from 17dpf onwards (Fleming et al., 2004; Spoorendonk et al., 2008).

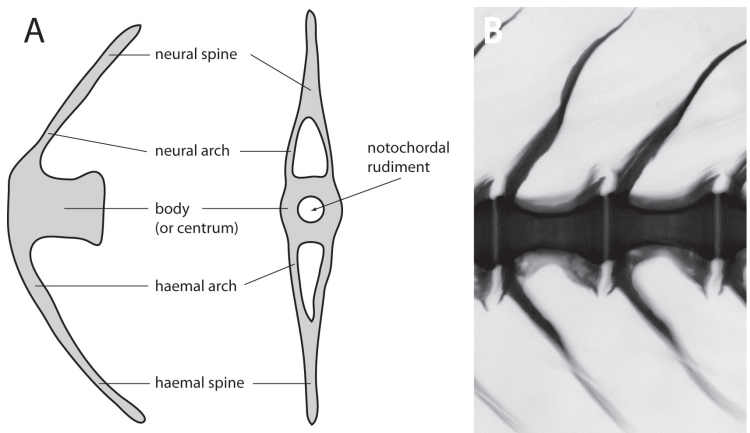

Figure 2: **Composition of a zebrafish vertebra.** (A) Schematic drawings of a vertebra: lateral (left) and frontal view. The vertebral body, or centrum, develops around the embryonic notochord. Neural arches extend dorsally, while haemal arches extend ventrally. Distal to those places where the two sides of an arch fuse together it is called a spine. Note that this is a caudal vertebra: pre-caudal vertebrae exhibit ventrally extending ribs (instead of haemal arches) from each vertebral body. (B) Lateral view of two consecutive alizarin red stained vertebrae in the vertebral column of a 5 week old wild type zebrafish.

Here, we will discuss the development of the axial skeleton in zebrafish and other teleosts in the context of bone matrix formation. How does the formation of the axial skeleton in zebrafish form compared to this process in other species such as mice and chick? We will address similarities and differences between species and highlight some of the open questions still unanswered.

From somites to vertebrae

The overall process of somite development in zebrafish is similar to that of amphibians, birds, and mammals (Kimmel et al., 1995). The first pairs of somites in a zebrafish embryo form approximately 10.5 hours post fertilization, just after tailbud closure. Somites, the segmental units of the paraxial mesoderm, will give rise to parts of the axial skeleton, the skeletal muscles of the trunk, and the connective tissue of the skin, and will therefore subdivide in sclerotome, myotome, and dermatome, respectively (Stickney et al., 2000).

In amniotes, the ventral half of each somite comprises of sclerotomal cells which migrate ventrally to surround the notochord, where they form the vertebral body, and dorsolaterally to form the neural arch (Monsoro-Burq et al., 1994). Experimental studies in predominantly avian embryos have shown that the posterior sclerotome of one somite pair recombines with the anterior sclerotome of the adjacent posterior somite pair to form the vertebral column. In this resegmentation model, the original boundary between somites ultimately aligns near the midline of one vertebral segment (Brand-Saberi and Christ, 2000; Christ et al., 2000; Saga and Takeda, 2001).
The fish somite however, consists predominantly of myotome cells, with sclerotome constituting a relatively minor component only found at the ventromedial edge of each somite. Nevertheless, in zebrafish (Morin-Kensicki and Eisen, 1997; Morin-Kensicki et al., 2002) as well as in medaka (Inohaya et al., 2007), it has been shown that cells of this ventromedial portion of each somite migrate dorsally around the notochord and contribute to vertebral components similar as in amniotes. However, the contribution of the sclerotome to the vertebral column in fish is apparently not completely predictable according to the anterior and posterior somite-domain of origin, as the resegmentation model has suggested for other species. Instead, Morin-Kensicki (2002) and colleagues could show that cells derived from individual anterior or posterior sclerotome cells in zebrafish do not distribute along the AP axis in a manner strictly according to their origin, thereby indicating a “leaky” resegmentation model. In fact, individual anterior and posterior sclerotome cells were each capable of contributing progeny to either anterior or posterior vertebral positions and in some cases to both positions.

Sclerotome differentiation

The notochord is the primary embryonic component implicated in inductive signaling to the sclerotome. The diffusible signaling molecules Noggin and Sonic hedgehog (Shh) that are secreted from the floorplate and notochord have been shown to initiate sclerotome formation and play a role in its maintainenance, respectively (Dockter, 2000). For most sclerotome-specific genes such as *Pax1, Pax9, Bapx1*, and *Twist*, which have been characterized in mouse and chicken, homologues have been identified in fish.

Pax1 and Pax9

In both chicken and mouse *Pax9* is expressed mainly in the dorsal and lateral parts of the sclerotome. *Pax1* is expressed mainly in the ventro-medial part of the mouse sclerotome, while almost all sclerotome cells of the chicken express *Pax1* (Muller et al., 1996; Neubuser et al., 1995; Peters et al., 1995). In *Pax1/Pax9* double mutant mice, the derivatives of the medial part of the sclerotome are missing: vertebral bodies, intervertebral discs, and proximal parts of the ribs are all absent (Peters et al., 1999). The *Pax1* homozygotes exhibit more restricted defects of the vertebral bodies and intervertebral discs (Wilm et al., 1998), while the *Pax9* homozygous mutants are not affected in their axial skeleton (Peters et al., 1998). Therefore, the *Pax1/Pax9* double mutant mice reveal that *Pax1* and *Pax9* synergistically regulate vertebral column development. Interestingly, the neural arches of *Pax1/Pax9* double mutant mice, which are derived from the lateral regions of the sclerotomes, do form and are connected by ectopic elements of cartilage.

In medaka, expression of both *pax* genes have also been detected in the sclerotome, but no spatial differences could be shown (Mise et al., 2008). Larvae injected with morpholinos for either *pax1* or *pax9* gave similar, concentration-dependent results: neural arches were defective or missing and scoliosis was observed. Double knockdown larvae showed a dramatic increase in the severity of this phenotype (Mise et al., 2008). Thus, as in amniotes, in teleosts *pax1* and *pax9* function synergistically in sclerotome development. However, the phenotypes affect different components of the vertebral column (amniotes: bodies, teleost: neural arches). Mise and colleagues conclude that after gene duplication of the ancestral *Pax1/9* gene, *Pax1* and *Pax9* subfunctionalized their developmental roles in the sclerotome independently in teleosts and amniotes.

Bapx1

A similar phenotype as seen in the *Pax1/Pax9* double knock out mice has also been observed in *Bapx1* null mutant mice. Loss of *Bapx1* results in a markedly reduced number of sclerotomal cells that end up ventro-medially around the notochord. Subsequently, both the intervertebral discs and the centra of the vertebral bodies fail to form (Lettice et al., 1999). Rodrigo et al. showed that expression of *Bapx1* in the scelerotome requires the presence of *Pax1* and *Pax9*, in a gene dose-dependent manner. Moreover, *Pax1* can substitute for *Shh* in inducing *Bapx1* to initiate differentiation into skeletal cells, which strongly suggest that *Bapx1* is a direct target of *Pax1* and *Pax9* (Rodrigo et al., 2003).

Also in fish, *bapx1* is expressed in the sclerotome: expression has been observed at the ventro-medial part of each somite (Yasutake et al., 2004). In zebrafish, the general pattern of *bapx1* expression in the posterior notochord, centra, and neural and haemal arches and spines is maintained for approximately three weeks (Crotwell and Mabee, 2007). No knock-down studies for *bapx1* in teleosts have been performed so far.

Twist

Another gene commonly employed as a sclerotome marker is *Twist*, a basic helix-loop-helix transcription factor. In vertebrates, *Twist* is mainly expressed in mesoderm-derived tissues, including the head mesenchyme, branchial arches, limb buds and sclerotome (Morin-Kensicki and Eisen, 1997; Wolf et al., 1991; Yasutake et al., 2004). In *Twist* heterozygous mutant mice, the vertebral column is normally developed, but abnormalities are observed in the craniofacial structures and the phalanges (Bourgeois et al., 1998). Homozygous *Twist* null mutant mice, however, fail to undergo closure of the cephalic neural tube and die at E11.5 (Chen and Behringer, 1995). Therefore, development of the vertebral column cannot be studied.

In *twist:eGFP* transgenic medaka, eGFP-positive cells were first reported to appear in the sclerotome. Eventually, these cells became distributed around the notochord. By using a double transgenic medaka line (*twist:eGFP* and *osteocalcin:dsRed*), it has been shown that some eGFP-positive cells in the sclerotome were able to differentiate into mature osteoblasts, expressing *osteocalcin:dsRed* (Inohaya 2007). Larvae injected with morpholinos against medaka *twist* (Yasutake 2004) resulted in embryos with defective or missing neural arches. However, expression patterns of sclerotomal markers *pax9* and *bapx1* were normal in *twist* morphants, suggesting that the sclerotome was present even in the absence of *twist* function. Moreover, vertebral bodies and haemal arches developed normally.

These results are similar to the ones observed for the double knockdown of *pax1* and *pax9* in medaka. However, compared to the embryonic lethality of the homozygous *Twist* null mutant mice, the teleost *twist* phenotype observed is less severe than expected.

Do different cells contribute to arches versus centra?

One remarkable aspect that emerges from the described studies is the possibility that arches and vertebral bodies originate from different populations of cells, and that these two groups of cells are individually regulated by different molecular mechanisms.

In mice, the *Pax1/Pax9* pathway involving *Bapx1* has been revealed to control the vertebral body development. Unfortunately, mutants lacking the other elements of the vertebral column have not been described so far. In teleosts, however, all sclerotome-specific genes analyzed so far have been shown to play a role in neural arch development. Next to proposing the hypothesis of a different molecular regulation for arches and vertebral bodies, these observations moreover suggest that sclerotomal cells might actually not be involved in the formation of teleosts vertebral bodies.

Endochondral versus dermal vertebral bodies

In both mouse and chick the vertebral column forms as a cartilaginous template that is later converted into bone by endochondral ossification (Monsoro-Burq, 2005).

In teleosts however, cartilage templates at places where centra develop are not observed: throughout the zebrafish vertebral column, a few cartilage structures can be observed by alcian blue staining, but only as templates for the Weberian apparatus and the rib-heads, and never for centra (Bird and Mabee, 2003; Du et al., 2001; Fleming et al., 2004). In medaka, cartilage is not observed throughout the vertebral column at all (Ekanayake and Hall, 1987; Ekanayake and Hall, 1988). Remarkably, the first structures to form within the salmon axial skeleton are the cartilage materials of the neural and haemal arches. After these cartilage templates are replaced by bony tissue, the future vertebral bodies are formed as ring-shaped mineralized zones within the acellular notochordal sheath, as in zebrafish and medaka, by direct bone formation without a cartilage template (Nordvik et al., 2005).
Thus, while in amniotes the vertebral column is completely formed by endochondral ossification, in teleosts at least the centra are formed by intramembranous ossification. This is also the mode of ossification for the neural and haemal arches for zebrafish and medaka. In salmon, arches do pass a cartilage stage while centra do not: another clear example that the development of centra and arches most likely is differentially regulated.

Four types of vertebral bodies

Additionaly, evolutionary studies showed that a persistent notochord with paired neural and haemal arches, but lacking vertebral bodies, might in fact be the primitive homologous feature that was present 450 million years ago in the last common ancestor of all vertebrates. Arches are the primary elements that are always present in every vertebrate. The secondary elements are the centra or bodies, which may be absent (Arratia et al., 2001).

Four morphologically different types of vertebral bodies have evolved, based on the origin of the cells producing mineralized matrix. In general, in primitive groups such as the salmoids, all these types are present and eventually form one compact vertebral body, whereas in advanced groups, some of the types are reduced (Arratia et al., 2001). A derived character of teleosts, for example, is the chordacentrum, which does not form in avian and mammalian species. Mineralization of a chordacentrum starts in the middle fibrous part of the notochordal sheath. Studies in salmon showed that initially, notochordal segments are formed within the chordoblast layer by metameric changes in the axial orientation of groups of chordoblasts. Formation of the chordoblast segments closely precedes formation of the chordacentra, which form as calcified rings within the adjacent notochordal sheath (Grotmol et al., 2003). Eventually, sclerotomal osteoblasts then differentiate on the surface of these chordacentra, using them as foundations to form autocentra for further vertebral growth (Arratia et al., 2001; Grotmol et al., 2003). The two other types of centra that can be found in other species are the arcocentrum, formed by ossification of cartilage extensions from the arches (arculia), and the holocentrum, initiated by proliferation of cartilage cells around the notochord (Arratia et al., 2001).

The dual segmentation model

The notochord plays a central role in the formation of vertebrae. In amniotes, it are the signals given by the notochord which initiate sclerotome differentiation. *Shh*, which is secreted by the notochord, has been shown to be the key molecule required for sclerotomal expression of *Pax1* and *Pax9*. Indeed, *Pax1* expression is rapidly lost and no skeletal elements of the vertebral column are formed at all in *Shh*-deficient mice (Chiang et al., 1996).

With the presence of the chordacentrum in teleosts, it is proposed that in this group the notochord has a more prominent and direct role in regulating vertebral development independent of the differentiation of the sclerotome. When notochord cells are laser-ablated prior to centrum formation (4 dpf), at 12 dpf centra from ablated regions were absent, whereas those being immediately adjacent were normal (Fleming et al., 2004). This suggests that indeed the bone matrix forming the centra is secreted directly by the notochord cells. As described above, teleosts exhibit two types of centra: chordacentra and autocentra. Grotmol and colleagues have proposed a dual segmentation model: the segmentation of vertebral bodies arises as a primary pattern within the chordoblast layer of the notochord (chordacentrum), while the segmental appearance of neural and haemal arches appears to arise from the sclerotome (autocentrum) (Grotmol et al., 2003). Because of this latter process, it could also be shown, as described above, that cells of the teleost sclerotome contribute to vertebral components (Inohaya et al., 2007).

In the zebrafish *fused somites* mutants (*fss*), sclerotome patterning is abnormal (van Eeden et al., 1996). And indeed, according to the dual segmentation model, the subsequent patterning of the neural and haemal arches is disorganized, yet the centra develop normal in number and shape. Taken together, in teleosts it is clear that vertebral bodies and arches are differently regulated: the notochord is responsible for the segmentation of the centra, while sclerotomal cells form the arches.

Future research will be necessary to answer important questions raised by these observations, such as the molecular differences between the cell types responsible for the matrix deposition and mineralization of chordacentra and autocentra, and whether other vertebrates share this mechanism of bone formation.

Teleosts as a unique model system to study bone development

Osteoblasts of intramembranous bone on one hand and of chondral bone on the other hand share at least some molecular identity and both express characteristic osteoblast markers such as *Runx2, Osx, Collagen type I,* and *Osteocalcin*. Interestingly*, Sox9,* and *Collagens type II and IX*, generally thought of as cartilage markers, have also been reported to be expressed in pre-osteoblasts (Abzhanov et al., 2007). Therefore, although the vertebrae of teleosts are formed by direct ossification without a cartilage template, the eventually formed bone is most likely similar in composition to mammalian and avian vertebrae formed via endochondral ossification. Moreover, it has been shown that key regulators of bone formation and

their transcriptional hierarchy required for mammalian osteoblast differentiation are highly conserved in zebrafish dermal as well as chondral bone (Li et al., 2009).

Additionally, teleosts offer possibilities which make them a great complement to other model systems: first, due to their rapid generation time, extra-uterine development and the genetic maps available, forward genetic screens to identify novel genes in bone development are possible.
Second, their transparency have allowed the generation of osteoblast-specific transgenic lines which make it possible to study the behaviour of osteoblasts *in vivo*. Together with fluorescent histological bone stainings such as alizarin red and calcein, which both can be performed on live embryos, these transgenic lines are unique tools to study bone development and disease.

III. OUTLINE OF THIS THESIS

In the research described in this thesis we used the zebrafish (*Danio rerio*), a small freshwater teleost, as a model system to study bone formation. An introduction to this relatively new model system in the field was given in **chapter 1**, where after an introduction to bone and vertebral development followed in **chapter 2**.

In **chapter 3** we describe and discuss the set up of the forward genetic ENU-mutagenesis screen, which we performed in order to identify novel genes involved in bone development and disease. We report the identification of 27 bone specific mutants after screening 700 zebrafish families. One of the mutants with a delay in bone formation, p.03.14 or *lenny*, was studied further and a detailed analysis of this mutant is presented in this chapter.
In **chapter 4** we report the analysis and positional cloning of the *stocksteif* mutant. This mutant is characterized by over-ossification around the embryonic notochord resulting in fused vertebrae. *stocksteif* encodes *cyp26b1*, a retinoic acid metabolizing enzyme. We show that *cyp26b1* is expressed in osteoblasts and examine the effects of retinoic acid on osteoblasts *in vivo*. In **chapter 5** we describe the expression of *cyp26b1* in developing centra preceding the onset of mineralization. Surprisingly, *osterix* is not expressed here. Our data suggest a role for *cyp26b1* in the formation of the teleost chordacentrum.
In **chapter 6** we report the analysis of the *dragonfish* mutant. This mutant shows an over-ossification phenotype similar to the *stocksteif* mutant. Additionally, in *dragonfish* mutants also ectopic mineralization in the head and in the neural tube is observed. We show that *dragonfish* functions in a pathway distinct from that of retinoic acid.
Finally, **chapter 7** gives a summarizing discussion of all the results presented in this thesis.

REFERENCES

Abzhanov, A., Rodda, S. J., McMahon, A. P. and Tabin, C. J. (2007). Regulation of skeletogenic differentiation in cranial dermal bone. Development 134, 3133-44.

Akiyama, H., Chaboissier, M. C., Martin, J. F., Schedl, A. and de Crombrugghe, B. (2002). The transcription factor Sox9 has essential roles in successive steps of the chondrocyte differentiation pathway and is required for expression of Sox5 and Sox6. Genes Dev 16, 2813-28.

Arratia, G., Schultze, H. P. and Casciotta, J. (2001). Vertebral column and associated elements in dipnoans and comparison with other fishes: development and homology. J Morphol 250, 101-72.

Bar-Shavit, Z. (2007). The osteoclast: a multinucleated, hematopoietic-origin, bone-resorbing osteoimmune cell. J Cell Biochem 102, 1130-9.

Beck, G. R., Jr. (2003). Inorganic phosphate as a signaling molecule in osteoblast differentiation. J Cell Biochem 90, 234-43.

Bi, W., Deng, J. M., Zhang, Z., Behringer, R. R. and de Crombrugghe, B. (1999). Sox9 is required for cartilage formation. Nat Genet 22, 85-9.

Bird, N. C. and Mabee, P. M. (2003). Developmental morphology of the axial skeleton of the zebrafish, Danio rerio (Ostariophysi: Cyprinidae). Dev Dyn 228, 337-57.

Bourgeois, P., Bolcato-Bellemin, A. L., Danse, J. M., Bloch-Zupan, A., Yoshiba, K., Stoetzel, C. and Perrin-Schmitt, F. (1998). The variable expressivity and incomplete penetrance of the twist-null heterozygous mouse phenotype resemble those of human Saethre-Chotzen syndrome. Hum Mol Genet 7, 945-57.

Brand-Saberi, B. and Christ, B. (2000). Evolution and development of distinct cell lineages derived from somites. Curr Top Dev Biol 48, 1-42.

Buckwalter, J. A. and Cooper, R. R. (1987). Bone structure and function. Instr Course Lect 36, 27-48.

Chen, Z. F. and Behringer, R. R. (1995). twist is required in head mesenchyme for cranial neural tube morphogenesis. Genes Dev 9, 686-99.

Chiang, C., Litingtung, Y., Lee, E., Young, K. E., Corden, J. L., Westphal, H. and Beachy, P. A. (1996). Cyclopia and defective axial patterning in mice lacking Sonic hedgehog gene function. Nature 383, 407-13.

Christ, B., Huang, R. and Wilting, J. (2000). The development of the avian vertebral column. Anat Embryol (Berl) 202, 179-94.

Crotwell, P. L. and Mabee, P. M. (2007). Gene expression patterns underlying proximal-distal skeletal segmentation in late-stage zebrafish, Danio rerio. Dev Dyn 236, 3111-28.

Cubbage, C. C. and Mabee, P. M. (1996). Development of the Cranium and Paired Fins in the Zebrafish Danio rerio (Ostariophysi, Cyprinidae). Journal of Morphology 229, 121-160.

Dockter, J. L. (2000). Sclerotome induction and differentiation. Curr Top Dev Biol 48, 77-127.

Du, S. J., Frenkel, V., Kindschi, G. and Zohar, Y. (2001). Visualizing normal and defective bone development in zebrafish embryos using the fluorescent chromophore calcein. Dev Biol 238, 239-46.

Ducy, P., Zhang, R., Geoffroy, V., Ridall, A. L. and Karsenty, G. (1997). Osf2/Cbfa1: a transcriptional activator of osteoblast differentiation. Cell 89, 747-54.

Ekanayake, S. and Hall, B. K. (1987). The development of acellularity of the vertebral bone of the Japanese medaka, Oryzias latipes (Teleostei; Cyprinidontidae). J Morphol 193, 253-61.

Ekanayake, S. and Hall, B. K. (1988). Ultrastructure of the osteogenesis of acellular vertebral bone in the Japanese medaka, Oryzias latipes (Teleostei, Cyprinidontidae). Am J

Anat 182, 241-9.
Fleming, A., Keynes, R. and Tannahill, D. (2004). A central role for the notochord in vertebral patterning. Development 131, 873-80.
Franz-Odendaal, T. A., Hall, B. K. and Witten, P. E. (2006). Buried alive: how osteoblasts become osteocytes. Dev Dyn 235, 176-90.
Goldring, M. B., Tsuchimochi, K. and Ijiri, K. (2006). The control of chondrogenesis. J Cell Biochem 97, 33-44.
Grotmol, S., Kryvi, H., Nordvik, K. and Totland, G. K. (2003). Notochord segmentation may lay down the pathway for the development of the vertebral bodies in the Atlantic salmon. Anat Embryol (Berl) 207, 263-72.
Hall, B. K. and Miyake, T. (2000). All for one and one for all: condensations and the initiation of skeletal development. Bioessays 22, 138-47.
Inada, M., Yasui, T., Nomura, S., Miyake, S., Deguchi, K., Himeno, M., Sato, M., Yamagiwa, H., Kimura, T., Yasui, N. et al. (1999). Maturational disturbance of chondrocytes in Cbfa1-deficient mice. Dev Dyn 214, 279-90.
Inohaya, K., Takano, Y. and Kudo, A. (2007). The teleost intervertebral region acts as a growth center of the centrum: in vivo visualization of osteoblasts and their progenitors in transgenic fish. Dev Dyn 236, 3031-46.
Karsenty, G. and Wagner, E. F. (2002). Reaching a genetic and molecular understanding of skeletal development. Dev Cell 2, 389-406.
Kimmel, C. B., Ballard, W. W., Kimmel, S. R., Ullmann, B. and Schilling, T. F. (1995). Stages of embryonic development of the zebrafish. Dev Dyn 203, 253-310.
Kobayashi, T. and Kronenberg, H. (2005). Minireview: transcriptional regulation in development of bone. Endocrinology 146, 1012-7.
Komori, T., Yagi, H., Nomura, S., Yamaguchi, A., Sasaki, K., Deguchi, K., Shimizu, Y., Bronson, R. T., Gao, Y. H., Inada, M. et al. (1997). Targeted disruption of Cbfa1 results in a complete lack of bone formation owing to maturational arrest of osteoblasts. Cell 89, 755-64.
Lamp, E. C. and Drexler, H. G. (2000). Biology of tartrate-resistant acid phosphatase. Leuk Lymphoma 39, 477-84.
Lettice, L. A., Purdie, L. A., Carlson, G. J., Kilanowski, F., Dorin, J. and Hill, R. E. (1999). The mouse bagpipe gene controls development of axial skeleton, skull, and spleen. Proc Natl Acad Sci U S A 96, 9695-700.
Li, N., Felber, K., Elks, P., Croucher, P. and Roehl, H. H. (2009). Tracking gene expression during zebrafish osteoblast differentiation. Dev Dyn 238, 459-66.
Mackie, E. J. (2003). Osteoblasts: novel roles in orchestration of skeletal architecture. Int J Biochem Cell Biol 35, 1301-5.
Mise, T., Iijima, M., Inohaya, K., Kudo, A. and Wada, H. (2008). Function of Pax1 and Pax9 in the sclerotome of medaka fish. Genesis 46, 185-92.
Monsoro-Burq, A. H. (2005). Sclerotome development and morphogenesis: when experimental embryology meets genetics. Int J Dev Biol 49, 301-8.
Monsoro-Burq, A. H., Bontoux, M., Teillet, M. A. and Le Douarin, N. M. (1994). Heterogeneity in the development of the vertebra. Proc Natl Acad Sci U S A 91, 10435-9.
Morin-Kensicki, E. M. and Eisen, J. S. (1997). Sclerotome development and peripheral nervous system segmentation in embryonic zebrafish. Development 124, 159-67.
Morin-Kensicki, E. M., Melancon, E. and Eisen, J. S. (2002). Segmental relationship between somites and vertebral column in zebrafish. Development 129, 3851-60.
Muller, T. S., Ebensperger, C., Neubuser, A., Koseki, H., Balling, R., Christ, B. and Wilting, J. (1996). Expression of avian Pax1 and Pax9 is intrinsically regulated in the pharyngeal endoderm, but depends on environmental influences in the paraxial mesoderm. Dev Biol 178, 403-17.

Nakashima, K., Zhou, X., Kunkel, G., Zhang, Z., Deng, J. M., Behringer, R. R. and de Crombrugghe, B. (2002). The novel zinc finger-containing transcription factor osterix is required for osteoblast differentiation and bone formation. Cell 108, 17-29.

Neubuser, A., Koseki, H. and Balling, R. (1995). Characterization and developmental expression of Pax9, a paired-box-containing gene related to Pax1. Dev Biol 170, 701-16.

Nordvik, K., Kryvi, H., Totland, G. K. and Grotmol, S. (2005). The salmon vertebral body develops through mineralization of two preformed tissues that are encompassed by two layers of bone. J Anat 206, 103-14.

Olsen, B. R., Reginato, A. M. and Wang, W. (2000). Bone development. Annu Rev Cell Dev Biol 16, 191-220.

Peters, H., Doll, U. and Niessing, J. (1995). Differential expression of the chicken Pax-1 and Pax-9 gene: in situ hybridization and immunohistochemical analysis. Dev Dyn 203, 1-16.

Peters, H., Neubuser, A., Kratochwil, K. and Balling, R. (1998). Pax9-deficient mice lack pharyngeal pouch derivatives and teeth and exhibit craniofacial and limb abnormalities. Genes Dev 12, 2735-47.

Peters, H., Wilm, B., Sakai, N., Imai, K., Maas, R. and Balling, R. (1999). Pax1 and Pax9 synergistically regulate vertebral column development. Development 126, 5399-408.

Rodrigo, I., Hill, R. E., Balling, R., Munsterberg, A. and Imai, K. (2003). Pax1 and Pax9 activate Bapx1 to induce chondrogenic differentiation in the sclerotome. Development 130, 473-82.

Saga, Y. and Takeda, H. (2001). The making of the somite: molecular events in vertebrate segmentation. Nat Rev Genet 2, 835-45.

Spoorendonk, K. M., Peterson-Maduro, J., Renn, J., Trowe, T., Kranenbarg, S., Winkler, C. and Schulte-Merker, S. (2008). Retinoic acid and Cyp26b1 are critical regulators of osteogenesis in the axial skeleton. Development 135, 3765-74.

Stickney, H. L., Barresi, M. J. and Devoto, S. H. (2000). Somite development in zebrafish. Dev Dyn 219, 287-303.

van Eeden, F. J., Granato, M., Schach, U., Brand, M., Furutani-Seiki, M., Haffter, P., Hammerschmidt, M., Heisenberg, C. P., Jiang, Y. J., Kane, D. A. et al. (1996). Mutations affecting somite formation and patterning in the zebrafish, Danio rerio. Development 123, 153-64.

Wilm, B., Dahl, E., Peters, H., Balling, R. and Imai, K. (1998). Targeted disruption of Pax1 defines its null phenotype and proves haploinsufficiency. Proc Natl Acad Sci U S A 95, 8692-7.

Witten, P. E., Hansen, A. and Hall, B. K. (2001). Features of mono- and multinucleated bone resorbing cells of the zebrafish Danio rerio and their contribution to skeletal development, remodeling, and growth. J Morphol 250, 197-207.

Wolf, C., Thisse, C., Stoetzel, C., Thisse, B., Gerlinger, P. and Perrin-Schmitt, F. (1991). The M-twist gene of Mus is expressed in subsets of mesodermal cells and is closely related to the Xenopus X-twi and the Drosophila twist genes. Dev Biol 143, 363-73.

Yasutake, J., Inohaya, K. and Kudo, A. (2004). Twist functions in vertebral column formation in medaka, Oryzias latipes. Mech Dev 121, 883-94.

CHAPTER 3

The identification of genes required for bone development in zebrafish using a forward genetic approach

Kirsten M. Spoorendonk
Maja M. Paciejewska
Stefan Schulte-Merker

SUMMARY

Bone formation is a complex process which involves three different cell types: chondrocytes, osteoblasts, and osteoclasts. Many transcription factors and signaling molecules regulate this process. However, a lot of questions still remain regarding bone development and disease. Identifying novel gene functions critical for bone formation and studying their role in this process would provide answers to these questions. To this end, we used forward genetic screens in zebrafish and analyzed 700 families in order to identify mutants with defects in bone formation. In total we identified 27 specific bone mutants, which comprise a maximum of 23 genetic loci. Here, we report the analysis and positional cloning of one mutant exhibiting a general delay in all mineralization processes. The affected gene most likely encodes a novel gene involved in calcium homeostasis.

INTRODUCTION

There are two types of bone, chondral bone and dermal (or intramembranous) bone. During chondral bone formation, mesenchymal cells condense and differentiate into chondrocytes. These chondrocytes form a cartilage template that is later on replaced or surrounded by osteoblasts which ossify the cartilaginous template. Dermal bone, on the other hand, forms without a cartilage intermediate: mesenchymal cells directly differentiate into osteoblasts (Karsenty and Wagner, 2002; Kobayashi and Kronenberg, 2005). Osteoblasts produce osteoid, an organic extracellular matrix which is mainly composed of type I collagen (Mackie, 2003). Mineralization of the osteoid matrix is the final step in the ossification process. The production of inorganic phosphate by osteoblasts during their differentiation has been implicated as one of the signals facilitating the coordination of multiple factors necessary for mineralization (Beck, 2003). The precise mechanisms behind this complex process, however, remain unclear.
A third cell type, the osteoclast, is responsible for the resorption and remodeling of bone tissue. Thus, eventually, the formation of bone matrix is the net result of the combined activity of bone producing osteoblasts and bone resorbing osteoclasts. In zebrafish, osteoclasts have not been observed before 20 days of development (Witten et al., 2001), which makes the zebrafish larvae an excellent model to study osteoblast function in a context where osteoclasts are not interfering.
Moreover, large-scale forward genetic screens in the zebrafish have proven to be an effective method to reveal important developmental regulatory genes and their functions (Driever et al., 1996; Haffter et al., 1996). For this purpose, we screened for zebrafish mutants that display specific defects in bone formation.

Both chondrocytes as well as osteoblasts are derived from mesenchymal cells. Non-differentiating chondrocytes are characterized by the expression of *col2a1* (encoding collagen type II) (Karsenty and Wagner, 2002). When the process of chondral ossification starts, chondrocytes in the core of the mesenchymal condensate become hypertrophic, a transition reflected by the switch from *col2a1* to *col10a1* (collagen type X) expression (Karsenty and Wagner, 2002). Osteoblasts are maturing in a small layer around the cartilage template (perichondrium or periosteum) or, in the case of dermal ossification, in independent condensations. They express *col1a1* (collagen type I), and, at least in zebrafish, also *col10a1* (Avaron et al., 2006).
Many transcription factors are involved in both ossification processes, with *runx2* being a key regulator for both chondrocyte and osteoblast differentiation (Flores et al., 2004; Komori, 2002), and *osterix* being a specific marker and regulator of the osteoblast lineage (Nakashima et al., 2002). Furthermore, the processes of proliferation and differentiation of chondrocytes and osteoblasts, eventually leading to bone mineralization, are controlled by the activity of several signaling molecules such as *ihh* (indian hedgehog), FGFs (fibroblasts growth factors), and members

of the wnt and BMP signaling pathways (Colnot, 2005; Karsenty and Wagner, 2002). Eventually, mature bone, formed via either chondral or dermal ossification, is characterized among others by the expression of the non-collagenous proteins osteopontin (also called spp1) (Kawasaki et al., 2004) and osteocalcin (or bone Gla protein) (Inohaya et al., 2007).

The transcriptional hierarchy required for mammalian osteoblast differentiation is highly conserved in zebrafish dermal as well as chondral bone formation (Li et al., 2009). Therefore, identifying novel genes important in bone formation in zebrafish will also help us to understand mammalian bone development and disease. Previously, several screens have been performed looking at the development of the cartilaginous head skeleton (Kimmel et al., 2001; Neuhauss et al., 1996; Piotrowski et al., 1996; Schilling et al., 1996). Forward genetic screens to identify novel bone-specific genes, however, have not been described yet.
Here, we report the screening of 700 zebrafish families in which we found 27 bone-specific mutants. These mutants fall into three different classes, categorized according to the amount of bone and the type of bone affected. For one of the mutants of the first class (a general decrease in the amount of bone matrix present), p.03.14 or *lenny*, the phenotypic analysis and positional cloning is described. We show *in vivo* that osteoblasts are present in these mutants and that osteoid matrix is produced, but that there is a defect in mineralization.

MATERIALS & METHODS

Mutagenesis and screening. ENU mutagenesis was performed as previously described for the creation of the Hubrecht Institute target selected mutagenesis library (Wienholds et al., 2002). Mutagenized TL males were out-crossed to wild-type TL female fish. F1 progeny of these matings (a kind gift from E. de Bruijn and E. Cuppen) were out-crossed to transgenic *fli1a:EGFP* individuals (Lawson and Weinstein, 2002) from an AB background, to generate 700 F2 families. From these families a maximum of 10 matings was set up, and a maximum of 4 egg-lays was selected for further analysis (more details can be found in the results section).

Skeletal staining. Embryos were fixed at 8 dpf and simultaneously stained for bone and cartilage as described before (this thesis, chapter 4: Spoorendonk et al., 2008). Embryos were analyzed and photographed with a Leica 480C camera on a Zeiss Axioplan microscope. In the pilot screen, 8 days old embryos were stained only for bone: the alcian blue step in the staining process was omitted.
Bone stainings *in vivo* (analysis of transgenic embryos) were carried out with 0.005 % alizarin red (Sigma) in embryo medium for 10 min. Subsequently, embryos were analyzed on a Leica TCS SPE confocal system.

Rescue experiment. Embryos were raised in E3 embryo medium with an extra addition of 10mM Ca^{2+}.

Meiotic mapping. Positional cloning of the lenny mutation was carried out as previously described (Geisler, 2002). Briefly, linkage was determined using a genome wide simple sequence length polymorphism (SSLP) panel. This panel with 192 markers was tested on genomic DNA of 48 pooled mutants and 48 pooled siblings. SSLPs z1202 and z14143 showed linkage and were determined at a single embryo level as flanking markers. Fine mapping was performed with additional SSLPs and single nucleotide polymorphisms (SNPs).
Primer sequences for SNP7 are as follows; SNP7_FW: GGAGAAGGCTGAAATTCTGG, SNP7_RV: GCTGACTTCCATATAGTATTCC.

Zebrafish transgenic lines. *osx:nuGFP* was used as previously described (Renn and Winkler, 2009; Spoorendonk et al., 2008).

RESULTS

In order to identify novel gene functions that are involved in bone development we performed a forward genetic screen in zebrafish. We first set up a pilot screen, in which we screened the F3 generation of 100 F2 families. Zebrafish embryos of these F3 clutches where raised to 8 dpf, fixed, and stained with alizarin red for bone.

Screen set up

For a typical forward genetic screen, males are mutagenized with ENU and out-crossed to wild-type females. The F1 individuals that are heterozygous for the randomly induced mutations in the parental (P) generation are crossed with F1 individuals stemming from an unrelated mutagenesis event, giving rise to F2 families, which will be crossed (via brother-sister matings) to produce F3 offspring (Driever et al., 1996; Haffter et al., 1996). In our screen, F1 individuals were crossed with the endothelial-specific transgenic *fli1a:EGFP* fish from an AB background (figure 1, line 2), as this enabled us to screen F3 embryos for vasculature defects as well. Since mutagenesis was performed in fish from a TL background (figure 1, line 1), this out-cross step can be considered as a map-cross as well. Therefore, we could directly collect screened F3 embryos for mapping of the mutation.
Any mutation within the original F1 fish will be inherited by 50% of the F2 progeny. Statistically, 25% of the crosses among F2 siblings are between heterozygous mutant carriers for any given mutation in that family, and will lead to phenotypes in 25% of the F3 embryos in all cases where a particular mutation can give rise to a phenotype. The probability of finding a mutation in a family is $P = (1-(0.75)^n)$, where n is the number of successful crosses per F2 family (Driever et al., 1996). We made an attempt to screen four egglays per F2 family since this will results in a 68% probability to find all the mutations in a particular family. Screening a fifth dish would increase this probability by 8%, but the additional screening time would have increased by 25%.

After the positive outcome of the pilot screen with three identified mutants, we decided to continue screening another 600 F2 families. Two minor changes were implemented in the screening protocol: first, after fixation of the F3 embryos at 8 dpf, we now carried out skeletal stainings for bone (alizarin red) and cartilage (alcian blue) simultaneously. Second, we stopped using chorion+ as an embryo medium, but instead raised the embryos in E3 medium.

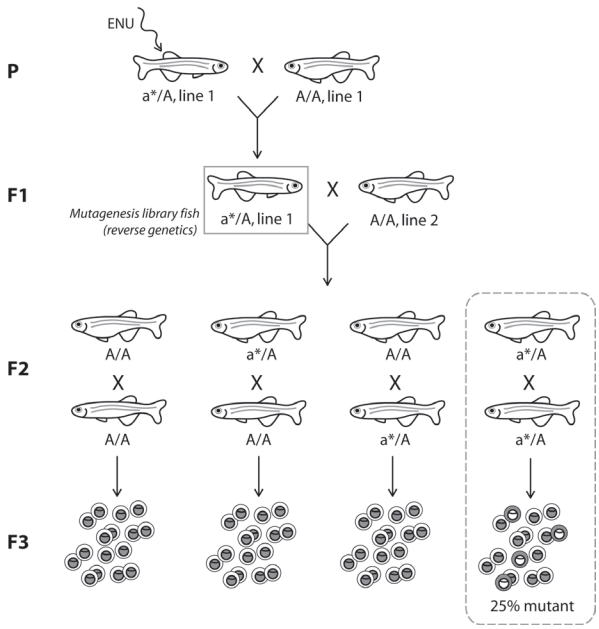

Figure 1: **Screen set up of the Hubrecht forward genetic screen.** Parental males are ENU mutagenized and outcrossed to wild type females with the same genetic background (line 1, in our case TL). F2 families are generated by out-crossing the F1 individuals to fish stemming from a different genetic background (line 2, in our case *fli1a:EGFP* fish from an AB background). F3 progeny is screened at 8 dpf for defects in bone development.

Bone elements in the zebrafish larva

In wild-type zebrafish larvae, the first bony elements arise at 3 dpf (Cubbage and Mabee, 1996). Two days later, at 5 dpf, when the cartilage skeleton is already completely formed, a few bone structures can be distinguished: the opercle, the cleithrum, the fifth branchial arch, the parasphenoid, and the tip of the notochord.
In the 8 days old wild-type zebrafish larvae, also the ectopterygoid, entopterygoid, the middle part of the ceratohyal, the basioccipital, and a few of the anterior future vertebrae are mineralized. Therefore, this is a stage that is advanced enough to analyze bone development in the zebrafish larva. Figure 2 shows all the described bone elements in a ventral (figure 2A-B) as well as a lateral (figure 2C) view of the zebrafish head. Furthermore, in figure 2D we have depicted the structures ossifying via chondral ossification (fifth branchial arch, basioccipital, ceratohyal) versus dermal ossification.

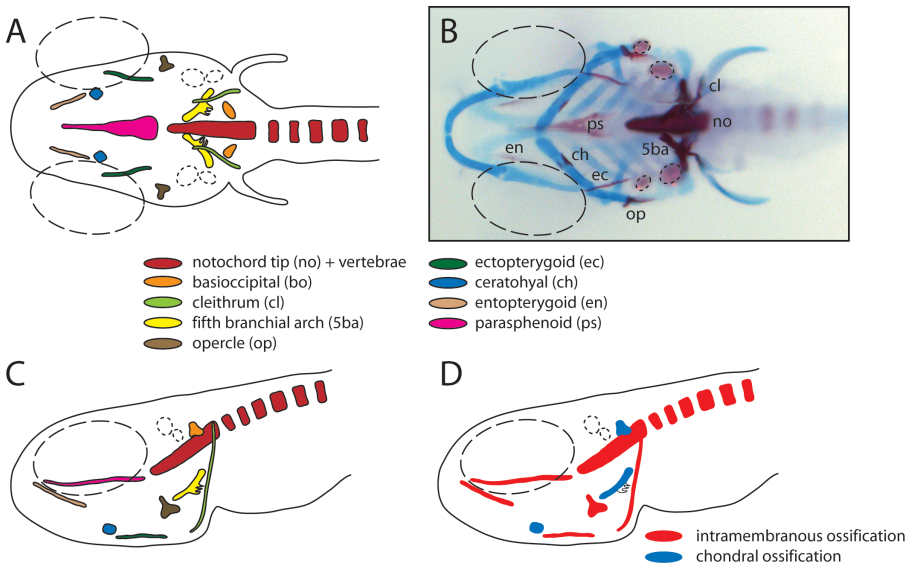

Figure 2: **Bone elements in the 8 day old zebrafish embryo.** (A, C-D) Ventral (A) and lateral (C-D) view of a schematic representation of all bone elements in an 8dpf zebrafish embryo. (B) Ventral view of a zebrafish embryo stained for both bone (alizarin red) and cartilage (alcian blue). The colored bone elements in A and C and the abbreviations in B are listed in the legend in the middle. In D, the two different types of bone formation are depicted (dermal in red or chondral in blue). Big and small dotted circles represent the outlines of the eyes and otoliths, respectively.

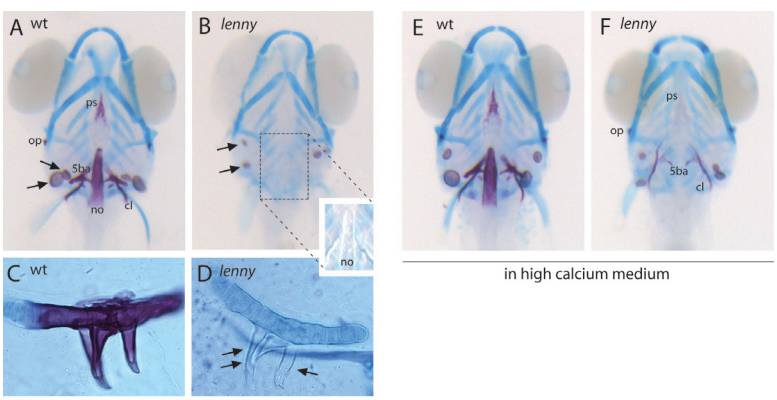

Figure 3: ***lenny* mutants are delayed in bone formation and can be partly rescued with an excess of calcium.** (A-B) Ventral views of the head skeleton of a wild type sibling (A) and a *lenny* mutant embryo (B). Arrows are pointing to the otoliths, which are smaller in mutants. Inset in B shows that the matrix of the notochord is formed in mutants but that it is not mineralized. (C-D) Flat-mounted fifth branchial arches of a wild type sibling (C) and a *lenny* mutant (D). Arrows are pointing to the teeth. (E-F) Ventral views of a wild type sibling (E) and a mutant (F) raised in E3 medium enriched for calcium show that mutants can be partly rescued. All embryos shown are stained for both bone (alizarin red) and cartilage (alcian blue) at 8 dpf. 5ba = fifth branchial arch, cl = cleithrum, no = notochord tip, op = opercle, ps = parasphenoid.

Forward genetic screen results in 27 bone specific mutants

Zebrafish bone mutants can be categorized in four different classes as previously described (this thesis, chapter 1), according to the amount of alizarin red stain and the type of bone affected:

I. generally less bone, or no bone at all
II. ectopic over-ossification
III. excess of perichondral bone, but normal amounts of dermal bone
IV. reduced formation of perichondral bone, but normal amounts of dermal bone

In our screen we identified mutants of the first three classes, but did not find mutants that we could characterize as class IV mutants. Table 1 gives an overview of all the mutants we found during the screen. The first character of the ID number stands for the part of the screen in which the mutant was identified: mutants with ID numbers starting with "p" were found in the pilot screen, while mutants with ID numbers starting with 1, 2, or 3, where found in the three consecutive parts of the screen that followed. In the pilot screen we screened 100 families and identified 3 mutants, all falling into class I. In the ensuing screen (part 1: 150 families, part 2: 150 families, part 3: 300 families) we also identified mutants in class II and III.

Only mutants that could be confirmed after an additional re-screening of the F2 carrier pair are listed. All mutants are specific bone mutants with a normal cartilage skeleton and no other obvious additional phenotypes, except for three mutants of class III: these mutants also exhibit less cartilage. In total, after screening 700 families, we found 27 specific bone mutants: 10 class I mutants, 8 class II mutants, and 9 class III mutants.

27 mutations fall into a maximum of 23 complementation groups

Complementation analysis was performed within each group. In class I, the alleles with ID numbers 1.018, 2.04.23, and 3.03.28 did not complement each other (table 1, column 'remarks': one asterisk) and also alleles 2.01.23 and 3.01.05 did not complement each other (table 1, column 'remarks': +). Furthermore, alleles 1.027 and 1.093 from class II did not complement each other (table 1, column 'remarks': two asterisks). Therefore, the 27 isolated mutations represent a maximum of 23 genes. One of the mutants in class I which we decided to study further was p.03.14 or *lenny*. Results, including the positional cloning, will be described below. The analysis and positional cloning of *dragonfish* (IDs 1.027 and 1.093), a class II mutant, is discussed in chapter 6 of this thesis.

Table 1 (right): **List of mutants identified in the Hubrecht forward genetic screen.**
ID numbers of mutants are listed, including a short description of the phenotype. Alleles that did not complement each other are marked with one asterisk (class I: 3 alleles), a plus (+) (class I: 2 alleles) or two asterisks (class II: 2 alleles).

ID number	name	phenotypic description	remarks
class I (generally less or no bone)			
p.01.15		less bone: only notochord, cleithrum, and teeth mineralized	
p.03.14	***lenny***	**delayed onset of ossification**	
p.05.01		less bone: 5th branchial arch not ossified	
1.018		no bone, except teeth	*
2.01.23		delayed onset of ossification	+
2.04.23		no bone, except teeth	*
3.01.05		delayed onset of ossification	+
3.03.28		no bone, except teeth	*
3.05.22		delayed onset of ossification	
3.09.02		delayed onset of ossification	
class II (ectopic overossification)			
1.027	***dragonfish***	**overossification of notochord (fused vertebrae) + ectopic mineralization**	**
1.037		ectopic specs of bone behind cleithrum	
1.093	***dragonfish***	**overossification of notochord (fused vertebrae) + ectopic mineralization**	**
2.05.01		overossification of notochord (fused vertebrae)	
3.01.13		overossification of notochord (fused vertebrae)	
3.04.13		spotted ossification of notochord	
3.06.26		overossification of notochord (fused vertebrae)	
3.07.30		overossification of notochord (fused vertebrae)	
3.09.20		ectopic mineralization in head and trunk (along dorsal site of notochord)	
class III (more perichondral bone, but normal dermal bone)			
1.019		more perichondral bone: in ceratohyal and 1st 2 branchial arches	less cartilage
1.024		more perichondral bone	
1.062		more perichondral bone	
1.102		more perichondral bone, but not in branchial arches	less cartilage
1.114		more perichondral bone	
2.01.07		more perichondral bone	less cartilage
2.02.08		more perichondral bone: all branchial arches ossified	
3.06.08		more perichondral bone	
3.06.24		more perichondral bone: all branchial arches ossified	

***lenny* mutants are delayed in bone formation**

Until 8 dpf almost all *lenny* mutants completely lack alizarin red staining in the bony skeleton (figure 3B). Although most mutants do not develop a swim bladder, they are comparable in size and external features to the siblings. Interestingly, the outline of the elements, which will normally be ossified in wild type zebrafish larvae, can be easily observed in *lenny* mutants. For example, the slightly different lightning in the inset in figure 3B shows that the matrix of the notochord is formed. In situ hybridizations with markers for matrix proteins such as *type X collagen* did not show any alterations between mutants and siblings (data not shown), suggesting that the osteoid matrix has formed correctly in mutants. However, mineralization does not occur.

Magnifications of the fifth branchial arch in figure 3C-D furthermore show that cartilage formation and differentiation is normal in lenny mutants. However, similar to the structures that normally ossify via dermal bone formation, these chondral elements do not mineralize.

Moreover, also the teeth of *lenny* mutants do not mineralize (arrows in figure 3D are pointing to the teeth), and the otoliths are smaller than those of their wild type siblings (arrows in figure 3A-B are pointing to the otoliths).

In a few cases mutants do show a faint alizarin red staining in the cleithrum, opercle, parasphenoid, and fifth branchial arch. These mutants are sub-viable and are eventually able to ossify their complete skeleton (preliminary data, not shown). These results indicate that the *lenny* mutant phenotype does not represent a complete absent of ossification but possibly a delay in bone formation.

The *lenny* mutant phenotype can be partly rescued with extra calcium

In *lenny* mutants, mineralization processes are delayed and also otoliths are smaller than in wild type siblings. Therefore, we hypothesized that the affected gene might rather play a more general role in calcium homeostasis and not have a very specific function related to bone formation. To test this, we raised a clutch of embryos from an egglay of two *lenny* carriers in a medium enriched for calcium: we added 10 mM $CaCl_2$ to the E3 embryo medium (which normally contains a concentration of 0.33 mM $CaCl_2$). Embryos were fixed and stained for bone and cartilage at 8 dpf. This resulted in 77% (50 out of 65) of the embryos showing a normal wild type staining pattern for both bone and cartilage (figure 3E), and 23% (15 out of 65) showing a staining that completely resembled the staining of the few 8 day old *lenny* mutants that where able to mineralize some elements (figure 3F): while the cartilage skeleton is normal, a faint alizarin red staining is observed in the cleithrum, opercle, parasphenoid, and fifth branchial arch (figure 3F). Genotyping (with the nearest z-markers) showed that the embryos of the latter group were indeed all mutants, and thus were partly rescued. Surprisingly, staining in the tip of the notochord was never observed in these mutants.

Positional cloning of the *lenny* mutation

To identify the responsible affected gene in the *lenny* mutant, genetic mapping was performed with simple sequence length polymorphism markers (SSLPs). Linkage was established to a region on linkage group 5 between markers z14143 and z1202. A single nucleotide polymorphism (SNP) in the *her1* gene (SNP7) and an additional SSLP (z1454) were found to be the closest flanking markers in the proximity of the *lenny* mutation (20 recombinants in 1030 meiosis and 3 recombinants in 654 meiosis, respectively) (figure 4). According to Ensembl Zv8 (release 54), these flanking markers are situated at a distance of approximately 2 Mb from each other, still enclosing more than 40 genes.

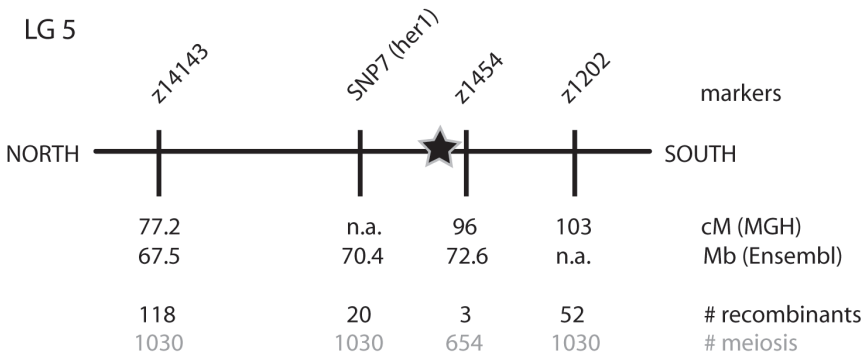

Figure 4: **Schematic overview of the area of linkage group 5 to which the *lenny* mutation was mapped.** SSLP and SNP markers are depicted including the number of recombinants and the number of meioses tested. SSLP z1454 was found closest to the mutation. The estimated position of the mutation is indicated by the star. n.a. = not annotated.

Osteoblasts are present in *lenny* mutants

In order to study the behaviour of osteoblasts *in vivo* in *lenny* mutants, we analyzed lenny mutant embryos in the background of an osteoblast-specific transgenic line: *osterix:nuclearGFP* (*osx:nuGFP*) (Renn and Winkler, 2009; Spoorendonk et al., 2008). In wild type siblings, *osx:nuGFP* expressing osteoblasts are observed around all mineralized elements in the 5 day old zebrafish head skeleton (figure 5A-D). Even though *lenny* mutants do not show any mineralized matrix (figure 5F), *osx:nuGFP* expression is found at the very same spots as where it is observed in wild type siblings (figure 5E; compare with 5A). Thus, in *lenny* mutants *osx:nuGFP* expressing osteoblasts are present.

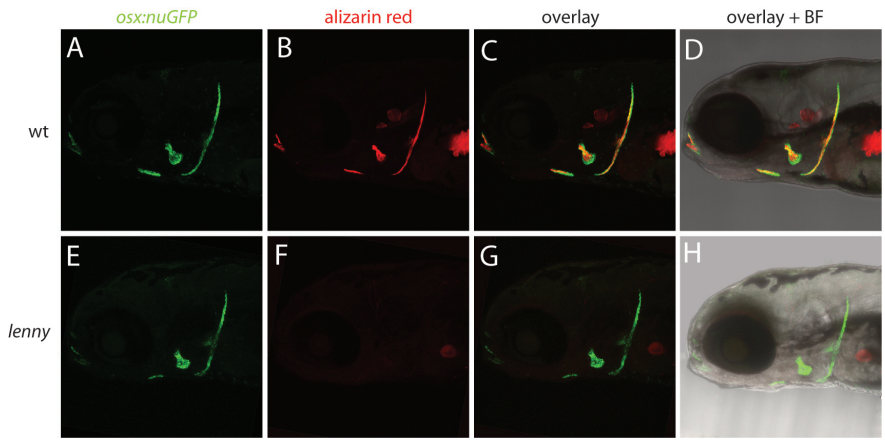

Figure 5: **Osteoblasts are present in *lenny* mutants.** Lateral views of the head of a 5 day old *osx:nuGFP* transgenic wild type sibling (A-D) and a *lenny* mutant embryo (E-H) are shown. While alizarin red staining (F) is completely absent in this mutant, *osx:nuGFP* expressing osteoblasts (E) are present at the correct places. BF = bright field.

DISCUSSION

Screen characteristics

In this study, we performed a large forward genetic screen in zebrafish to identify novel gene functions in bone development. Usually, F2 families are generated by crossings between F1 individuals, where both F1 fish originate from different males. Thus, in this situation both F1 individuals carry a unique set of heterozygous mutations (Driever et al., 1996; Haffter et al., 1996)(see also this thesis, chapter 1, figure 1). Here, however, we generated the F2 families by out-crossing F1 individuals to wild type *fli1a:EGFP* transgenic fish. This approach has the following advantages: first, parallel with our bone screen, a screen for genes playing a role in lymphangiogenesis could be performed (Hogan et al., 2009), and for this particular assay the *fli1a:EGFP* transgene needed to be introduced. Second, we could directly collect F3 embryos for mapping: since mutagenesis was performed in fish with a TL background, while the *fli1a:EGFP* fish have an AB background, this outcross step is actually a map-cross.

On the other side, it will also mean that theoretically the screening work is half as efficient, since, according to the more common set up with two heterozygous F1 fish stemming from independent mutagenesis events, in our set up only one of the F1 parents is derived from a mutagenized background. Fortunately, it turned out that our mutagenesis rate was so high that it effectively allowed us to compensate for this: while others have reported a mutation frequency of approximately 1 in 500.000

bp (Draper et al., 2004), our ENU mutagenesis was very effective and resulted in a mutation frequency (analyzed in the F1 generation) of at least 1 in 150.000 bp (E. de Bruijn and E. Cuppen, personal communication).
The fact that in our screen for 21 of the 24 affected loci only a single allele has been found indicates that this screen has not approached saturation, which makes it impossible to reliably estimate the total number of genes required for the control of bone formation in zebrafish. Given that we screened 700 families this is not surprising, as previous screens with much larger numbers (Driever et al., 1996; Haffter et al., 1996) also did not claim to have reached saturation.
Additionally, genes are often represented in large families and many zebrafish genes in particular have been duplicated during evolution (Otto and Yong, 2002; Robinson-Rechavi et al., 2001). Consequently, several genes can have partially or completely overlapping developmental functions. Mutations in individual genes might therefore have only subtle or no phenotypes and will not be picked up for this reason in a screen, while some of these genes could be very important for the regulation of bone development.
Nevertheless, preliminary positional cloning data have so far indicated that all the genes we have identified in our screen are genes with a novel function in bone development. Therefore, we conclude that forward genetic screens in fish present an efficient and effective way to identify genes with previously unappreciated roles in osteogenesis.

Pilot versus main screen
In the pilot screen, in which we screened 100 families, we found 3 mutants. We characterized all these three mutants into class I: less bone formation, or no bone formation at all. In the three parts of the screen that followed we identified mutants from classes I, II, and III.
There are two differences between the pilot screen and main screen: First, 8 day old F3 embryos were only stained for bone in the pilot screen, while they were stained for both bone and cartilage in the main screen. This latter staining procedure allowed us to make a better judgement whether or not mutants exhibited additional phenotypes (for example, whether the morphology of branchial arches was affected).
Second, embryos were raised in chorion+ water in the pilot screen, while they were raised in E3 embryo medium in the main screen. Chorion+ water (diluted sea-salt solution) contains approximately 0,01 mM $CaCl_2$. E3 embryo medium, on the other hand, contains 0,33 mM $CaCl_2$. Calcium is, together with phosphate, the main component of bone (hydroxyapatite, $Ca_5(PO_4)_3OH$) and therefore crucial for ossification. It turned out that the calcium concentration in chorion+ water was too low, resulting in a great variability of ossification at 8 dpf. Raising embryos in E3 embryo medium prevents this specific problem. This might explain why, in the pilot screen, we have only found class I mutants and did not identify a single mutant showing over-ossification.

In our screen we did not find mutants that we could characterize as class IV mutants. Class IV mutants (which we know to exist from screen results in other labs: Torsten Trowe, personal communication) show less perichondral bone, but a normal amount of dermal bone. The first perichondral structures to ossify are the basioccipital and the fifth branchial arch, which are mineralized by 5 dpf. From 8 dpf onwards the ceratohyal and the first four branchial arches start to ossify. Thus, this is a phenotype with a very late onset and therefore not reasonably to be picked up in a screen performed at 8 dpf. To screen specifically for class IV mutants one should screen a few days later around 10 to 12 dpf. Then, however, variabilities will be introduced because the larvae need to be fed, which makes the screening considerably more difficult.

The *lenny* mutant phenotype

For one of the mutants in class I, p.03.14 or *lenny*, we undertook further characterization of the phenotype. Mutants exhibit a delay of mineralization in dermal as well as chondral bone elements. Interestingly, the outline of the structures that would normally be ossified can be clearly observed in mutants. Since in situ hybridisations with markers for matrix components such as *type X collagen* did not show any alterations between mutants and siblings, we suggest that *lenny* mutants are able to produce osteoid matrix but that they fail to mineralize the matrix.
Consistent with this notion, indeed *osx:nuGFP* expressing cells are observed (figure 5E-G) at the right places in *lenny* mutants. Thus, osteoblasts are present but, since alizarin red staining is absent, their mineralization activity is most likely impaired.

Additionally, the teeth of *lenny* mutants are not mineralized and the otoliths are smaller then those of their wild type siblings. Teeth are formed by odontoblasts and ameloblasts producing dentin and enamel, respectively (Butler and Ritchie, 1995). Otoliths, the structures that will be part of the hearing and balance stystem, consist of calcium carbonate (Hughes et al., 2006). Thus, both tissues contain a different biomineral composition than the hydroxyapatite typical for bone and therefore we propose that the affected gene most likely plays a general role in calcium homeostasis or transport, rather then a specific role in bone development. Indeed, raising mutants in embryo medium with a high concentration of calcium could partly rescue the *lenny* mutant phenotype. Occasionally mutants can exhibit some alizarin red positive material, resulting in bone stainings similar to the situation of mutants rescued with extra calcium. These results suggest that the *lenny* gene is important, but not essential for bone formation.
Surprisingly, in both scenarios described above the tip of the notochord was never mineralized. This might suggests that either the material of the notochord or the developmental process resulting in depositing this material is different compared to other bone elements. Elucidating the molecular lesion of *lenny* mutants will be very helpful in answering this question and will give us more insight into the mechanisms

of mineralization, which are until now mostly unclear.

Prospects

Preliminary data of the analysis of other boneless mutants suggests a scenario where in most of the class I mutants osteoblasts are present but unable to form or mineralize bone tissue (L. Huitema and S. Schulte-Merker, personal communication). In order to identify mutants in which osteoblasts are either missing, or present in higher numbers, it is possible in the future to implement a two-step screening protocol: first, perform screening *in vivo* in embryos within an *osx:nuGFP* background that will permit counting of osteoblasts. Then, subsequently, as a second step, those embryos that show an alteration at this level can be further stained for bone as well as cartilage. Since the first step can be performed on live embryos, the same dish can be fixed and used in the second step for staining.

In addition, *in vivo* screening combined with subsequent histological stainings can also be an attractive approach for chemical compound screening. This can be effective not only for a general compound screen to study the effects of the compounds on wild type bone formation and osteoblast behaviour, but also to investigate if certain known compounds are able to rescue or phenocopy the mutant phenotypes identified in our forward genetic screen. For example, the BMP signaling inhibitor dorsomorphin has been described to result in inhibition of bone mineralization in zebrafish, with fewer calcein stained vertebral segments (Yu et al., 2008). It will be interesting to investigate if one of the class II mutants with fused vertebrae is affected in the BMP pathway and can be rescued by dorsomorphin treatment.

Taken together, we have shown that forward genetic screening in zebrafish is a very efficient and effective method to identify novel gene functions important for bone development. Analysis and positional cloning of identified mutants is currently ongoing. It is hoped that the powerful genetics will soon help us to elucidate the molecular nature of the mutations described and that the combination with the optical properties of zebrafish embryos, which have made it possible to establish osteoblast-specific transgenic lines, enable us to study the mutant phenotypes at a cellular level *in vivo*.

REFERENCES

Avaron, F., Hoffman, L., Guay, D. and Akimenko, M. A. (2006). Characterization of two new zebrafish members of the hedgehog family: atypical expression of a zebrafish indian hedgehog gene in skeletal elements of both endochondral and dermal origins. Dev Dyn 235, 478-89.

Beck, G. R., Jr. (2003). Inorganic phosphate as a signaling molecule in osteoblast differentiation. J Cell Biochem 90, 234-43.

Butler, W. T. and Ritchie, H. (1995). The nature and functional significance of dentin extracellular matrix proteins. Int J Dev Biol 39, 169-79.

Colnot, C. (2005). Cellular and molecular interactions regulating skeletogenesis. J Cell Biochem 95, 688-97.

Cubbage, C. C. and Mabee, P. M. (1996). Development of the Cranium and Paired Fins in the Zebrafish Danio rerio (Ostariophysi, Cyprinidae). Journal of Morphology 229, 121-160.

Draper, B. W., McCallum, C. M., Stout, J. L., Slade, A. J. and Moens, C. B. (2004). A high-throughput method for identifying N-ethyl-N-nitrosourea (ENU)-induced point mutations in zebrafish. Methods Cell Biol 77, 91-112.

Driever, W., Solnica-Krezel, L., Schier, A. F., Neuhauss, S. C., Malicki, J., Stemple, D. L., Stainier, D. Y., Zwartkruis, F., Abdelilah, S., Rangini, Z. et al. (1996). A genetic screen for mutations affecting embryogenesis in zebrafish. Development 123, 37-46.

Flores, M. V., Tsang, V. W., Hu, W., Kalev-Zylinska, M., Postlethwait, J., Crosier, P., Crosier, K. and Fisher, S. (2004). Duplicate zebrafish runx2 orthologues are expressed in developing skeletal elements. Gene Expr Patterns 4, 573-81.

Geisler, R. (2002). Mapping and Cloning. Zebrafish, a practical approach, 175-210.

Haffter, P., Granato, M., Brand, M., Mullins, M. C., Hammerschmidt, M., Kane, D. A., Odenthal, J., van Eeden, F. J., Jiang, Y. J., Heisenberg, C. P. et al. (1996). The identification of genes with unique and essential functions in the development of the zebrafish, Danio rerio. Development 123, 1-36.

Hogan, B. M., Bos, F. L., Bussmann, J., Witte, M., Chi, N. C., Duckers, H. J. and Schulte-Merker, S. (2009). Ccbe1 is required for embryonic lymphangiogenesis and venous sprouting. Nat Genet 41, 396-8.

Hughes, I., Thalmann, I., Thalmann, R. and Ornitz, D. M. (2006). Mixing model systems: using zebrafish and mouse inner ear mutants and other organ systems to unravel the mystery of otoconial development. Brain Res 1091, 58-74.

Inohaya, K., Takano, Y. and Kudo, A. (2007). The teleost intervertebral region acts as a growth center of the centrum: in vivo visualization of osteoblasts and their progenitors in transgenic fish. Dev Dyn 236, 3031-46.

Karsenty, G. and Wagner, E. F. (2002). Reaching a genetic and molecular understanding of skeletal development. Dev Cell 2, 389-406.

Kawasaki, K., Suzuki, T. and Weiss, K. M. (2004). Genetic basis for the evolution of vertebrate mineralized tissue. Proc Natl Acad Sci U S A 101, 11356-61.

Kimmel, C. B., Miller, C. T. and Moens, C. B. (2001). Specification and morphogenesis of the zebrafish larval head skeleton. Dev Biol 233, 239-57.

Kobayashi, T. and Kronenberg, H. (2005). Minireview: transcriptional regulation in development of bone. Endocrinology 146, 1012-7.

Komori, T. (2002). Runx2, a multifunctional transcription factor in skeletal development. J Cell Biochem 87, 1-8.

Lawson, N. D. and Weinstein, B. M. (2002). In vivo imaging of embryonic vascular development using transgenic zebrafish. Dev Biol 248, 307-18.

Li, N., Felber, K., Elks, P., Croucher, P. and Roehl, H. H. (2009). Tracking gene expression during zebrafish osteoblast differentiation. Dev Dyn 238, 459-66.

Mackie, E. J. (2003). Osteoblasts: novel roles in orchestration of skeletal architecture. Int J Biochem Cell Biol 35, 1301-5.

Nakashima, K., Zhou, X., Kunkel, G., Zhang, Z., Deng, J. M., Behringer, R. R. and de Crombrugghe, B. (2002). The novel zinc finger-containing transcription factor osterix is required for osteoblast differentiation and bone formation. Cell 108, 17-29.

Neuhauss, S. C., Solnica-Krezel, L., Schier, A. F., Zwartkruis, F., Stemple, D. L., Malicki, J., Abdelilah, S., Stainier, D. Y. and Driever, W. (1996). Mutations affecting craniofacial development in zebrafish. Development 123, 357-67.

Otto, S. P. and Yong, P. (2002). The evolution of gene duplicates. Adv Genet 46, 451-83.

Piotrowski, T., Schilling, T. F., Brand, M., Jiang, Y. J., Heisenberg, C. P., Beuchle, D., Grandel, H., van Eeden, F. J., Furutani-Seiki, M., Granato, M. et al. (1996). Jaw and branchial arch mutants in zebrafish II: anterior arches and cartilage differentiation. Development 123, 345-56.

Renn, J. and Winkler, C. (2009). Osterix-mCherry transgenic medaka for in vivo imaging of bone formation. Dev Dyn 238, 241-8.

Robinson-Rechavi, M., Marchand, O., Escriva, H., Bardet, P. L., Zelus, D., Hughes, S. and Laudet, V. (2001). Euteleost fish genomes are characterized by expansion of gene families. Genome Res 11, 781-8.

Schilling, T. F., Piotrowski, T., Grandel, H., Brand, M., Heisenberg, C. P., Jiang, Y. J., Beuchle, D., Hammerschmidt, M., Kane, D. A., Mullins, M. C. et al. (1996). Jaw and branchial arch mutants in zebrafish I: branchial arches. Development 123, 329-44.

Spoorendonk, K. M., Peterson-Maduro, J., Renn, J., Trowe, T., Kranenbarg, S., Winkler, C. and Schulte-Merker, S. (2008). Retinoic acid and Cyp26b1 are critical regulators of osteogenesis in the axial skeleton. Development 135, 3765-74.

Wienholds, E., Schulte-Merker, S., Walderich, B. and Plasterk, R. H. (2002). Target-selected inactivation of the zebrafish rag1 gene. Science 297, 99-102.

Witten, P. E., Hansen, A. and Hall, B. K. (2001). Features of mono- and multinucleated bone resorbing cells of the zebrafish Danio rerio and their contribution to skeletal development, remodeling, and growth. J Morphol 250, 197-207.

Yu, P. B., Hong, C. C., Sachidanandan, C., Babitt, J. L., Deng, D. Y., Hoyng, S. A., Lin, H. Y., Bloch, K. D. and Peterson, R. T. (2008). Dorsomorphin inhibits BMP signals required for embryogenesis and iron metabolism. Nat Chem Biol 4, 33-41.

CHAPTER 4

Retinoic acid and cyp26b1 are critical regulators of osteogenesis in the axial skeleton

Kirsten M. Spoorendonk, Josi Peterson-Maduro, Jörg Renn, Torsten Trowe, Sander Kranenbarg, Christoph Winkler, and Stefan Schulte-Merker

Development. 2008 Nov; 135(22): 3765-74.

SUMMARY

Retinoic acid (RA) plays important roles in diverse biological processes ranging from germ cell specification to limb patterning. RA ultimately exerts its effect in the nucleus, but how RA levels are being generated and maintained locally is less clear. Here, we have analyzed the zebrafish *stocksteif* mutant which exhibits severe over-ossification of the entire vertebral column. s*tocksteif* encodes *cyp26b1*, a cytochrome P450 member that metabolizes RA. The mutant is completely phenocopied by treating 4 dpf wild-type embryos with either RA or the pharmacological Cyp26 blocker R115866, thus identifying a previously unappreciated role for RA and *cyp26b1* in osteogenesis of the vertebral column. *Cyp26b1* is expressed within osteoblast cells, demonstrating that RA levels within these cells need to be tightly controlled. Furthermore, we have examined the effect of RA on osteoblasts *in vivo*. Since numbers of osteoblasts do not change upon RA treatment we suggest that RA causes increased activity of axial osteoblasts, ultimately resulting in defective skeletogenesis.

INTRODUCTION

Retinoic acid (RA) has been demonstrated to play important roles in processes as diverse as cardiac specification (Keegan et al. 2005), patterning of both the central nervous system (Hernandez et al. 2007) and the tetrapod limb (Yashiro et al. 2004), as well as specification of germ cell fate (Bowles et al. 2006). RA is synthesized intracellularly from its precursor, vitamin A (or retinol), by retinaldehyde dehydrogenases (Raldhs) and transported to the nucleus where it initiates transcription of target genes (Ross et al. 2000; Maden 2002). Levels of RA are determined by Raldhs and in addition by Cyp26 enzymes, members of the RA catabolizing cytochrome P450 family (White et al. 2000; MacLean et al. 2001). In vertebrates, three Cyp26 enzymes have been found: Cyp26a1, Cyp26b1, and Cyp26c1 (White et al. 1996; Nelson 1999; Gu et al. 2005).

In mice, a *Cyp26a1* knock out that exhibits spina bifida and tail truncation as a consequence of patterning defects, and also shows homeotic transformations of anterior vertebrae has been described (Abu-Abed et al. 2001; Sakai et al. 2001), while *Cyp26b1* knockout mouse embryos display craniofacial defects and reduced limbs (Yashiro et al. 2004). Homozygous mutants die immediately after birth due to respiratory distress before vertebral defects become obvious and hence no other bone defects have been reported. In zebrafish, the effects of Cyp26 enzymes have been studied in the context of hindbrain (Emoto et al. 2005; Hernandez et al. 2007; White et al. 2007) and neural crest patterning (Reijntjes et al. 2007).

In this study, we characterized a zebrafish mutant in *cyp26b1,* which exhibits severe over-ossification of the vertebral column. In both zebrafish and mouse, we report expression of *Cyp26b1* in osteoblasts of the pre-vertebrae regions. We suggest that it is the tight regulation of RA within osteoblasts by cyp26b1 activity which is critical for axial osteogenesis.

In zebrafish and medaka, which are considered to have highly similar modes of axial skeleton ossification (Inohaya et al. 2007), vertebrae form by intramembranous ossification without passing through a cartilage stage (Ekanayake and Hall 1987; Fleming et al. 2004). It has been suggested for both species that notochord cells are involved in the initial bone matrix formation of the centra during development of the vertebral column (Fleming et al. 2004; Inohaya et al. 2007). However, Inohaya et al. (2007) also could show that sclerotome derived progenitor cells differentiate into osteoblasts on the surface of the notochordal sheath, where they produce and mineralize bone matrix: this matrix is formed by cells distal to the notochord. Subsequent vertebral growth then proceeds from the anterior and posterior edges of the forming centra.

Until now, several *in vitro* studies have reported effects of RA exposure on mineralization, however with contradicting results. Some studies describe an increase in mineralization (Skillington et al. 2002; Wang and Kirsch 2002; Song et al. 2005; Yamashita et al. 2005; Malladi et al. 2006; Wan et al. 2007), while others

report a suppression of cell differentiation and therefore a decrease in mineralization (Cohen-Tanugi and Forest 1998; Iba et al. 2001) upon RA treatment of cultured cells. Here, we establish an *in vivo* model to follow early osteoblasts. We show that, upon RA treatment, axial osteoblasts in *osterix:nuGFP* transgenic zebrafish retain their normal positions. Moreover, also osteoblast numbers do not change. Therefore, over-ossification of the axial skeleton upon RA excess is caused most likely by increased activity of osteoblasts along the vertebral column.

MATERIALS AND METHODS

Transgenic osterix:mCherry and osterix:nuGFP zebrafish. A 4.1kb upstream regulatory region of the medaka *osterix* gene was amplified using the primers FW: 5'-TGAACATGTCAGTGCCATCA-3' and RV: 5'-CGGGACAGTTTGGAAGAAGT-3', and cloned in front of mCherry. Transgenic zebrafish were generated by injection into 1-cell stage embryos using the I-SceI meganuclease approach (Rembold et al. 2006). The same upstream region was cloned in front of a nuclear localization signal followed by GFP (nuGFP), and transgenic zebrafish were generated using the Tol2 transposon system (Kawakami et al. 1998). Cloning details are available upon request.

BAC recombineering. YFP was recombined directly after the ATG site of the gene of interest on a BAC clone, containing the genomic information of the gene of interest (Kimura et al. 2006). The following BACs and primers were used: DKEY-53014 (containing 73,5 kb upstream of the *cyp26b1* coding region, and >73,5 kb downstream of *cyp26b1*) ;
Cyp26b1_GFP_fw (ttgctcatcactccaaagagatatttgagacaagtccccggacgttcaca ACCATGGTGAGCAAGGGCGAGGAG),
Cyp26b1_Neo_rev (cacgcagccagcgtcgccaacgccgagacaaggtcaaaactctcgaagag TCAGAAGAACTCGTCAAGAAGGCG)
and CH211-51D23 (containing 111,6 kb upstream of the *osx* coding region, and 66,3 kb downstream of *osx*);
Osx_GFP_fw (cagctctcctctcccgcttttggattgaccctcactggactgcttcctcc ACCATGGTGAGCAAGGGCGAGGAG),
Osx_Neo_rev (gcagctgtgagatcgcagtgagttttccgtacctccagaatcgacgcggc TCAGAAGAACTCGTCAAGAAGGCG)

Meiotic Mapping. The *stocksteif* mutation was mapped to linkage group 7 using standard simple sequence length polymorphism mapping. The following six primers were used for fine mapping: R3.2-fw (5' ACCGTAATTGAAACCACGTC 3'), R3.2-rv (5' GCCAAATATTTCGATCTGTG 3'), R1.11-fw (5' GATGCTCAGACCTGTGTTTG 3'), R1.11-rv (5' TGAAGTCAATGCTGGTCAAC 3'), R2.22-fw (5' TCACCCTTCCATGAACTTAAC 3'), and R2.22-rv (5' AAACAGCCAGCGTAGATAAAC 3').

Skeletal staining. Embryos were fixed in 3.5% formaldehyde/0.1M sodium phosphate buffer for 1 hour and stored in 70% MeOH. The protocol for simultaneous bone and cartilage staining was adapted from what was previously described (Walker and Kimmel 2007). Briefly, embryos were rinsed in 50% EtOH and subsequently stained with 0.2mg/ml alcian blue 8 GX (Sigma) in 70% EtOH/80mM $MgCl_2$. After washes in 0.02% Triton, embryos were bleached in 1%

H_2O_2/1% KOH for 30 min, washed in a saturated sodiumtetraborate solution, and digested for 1 hour in 1 mg/ml trypsin (Sigma) in 60% saturated sodiumtetraborate. Bones were stained with 0.04mg/ml alizarin red S (Sigma) in 1% KOH. Destaining was done in an increasing glycerol series (10%, 30%, 70%) and specimens were stored at 4°C in 70% glycerol.
For alizarin red stainings only, the alcian blue step was omitted. Juvenile fish were fixed for 2 hours, incubated in acetone to remove fat (up to 24 hours) and digested with 10mg/ml trypsin in 60% sodiumtetraborate overnight. Scales were removed manually. *In vivo* skeletal stainings were done with 0.001% calcein (Sigma) in embryo water for at least 2 days.

Pharmacological treatments. Stock solutions of 10 mM all-trans retinoic acid (Sigma) and 10 mM R115866 (Janssen Pharmaceutica) in DMSO were diluted in embryo medium. Sibling controls were incubated in corresponding dilutions of DMSO. RA treatments were done in the dark and solutions were changed every ~ 12 hours.

MicroCT scans. Fixed samples were wrapped in parafilm and scanned with a Skyscan 1072 microCT system at 80 kV and 100 µA. The cubic voxelsize was 6.08 µm for the wild type and 2.73 µm for the *sst* animals. The scans were reconstructed and subsequently segmented as previously described (Feldkamp et al. 1984; Waarsing et al. 2004). The segmented images were visualized as a surface using a custom-written Matlab 7.3 script.

In situ hybridizations. For all sectioned zebrafish material, in situ hybridizations were carried out first on whole mount embryos (Schulte-Merker 2002), and only subsequently embryos were embedded either in 3% agarose and cut (100 µm sections) on a vibrotome (Microm HM650V), or embedded in plastic and cut (10 µm sections) on a microtome (Leica RM2035). For sections of mouse material, paraffin-embedded embryos where first sectioned and subsequently in situ hybridizations were performed, according to standard procedures (Moorman et al. 2001).

RESULTS

In a screen for genes affecting ossification in zebrafish, we identified a single allele of the *stocksteif* mutant, *sst*^{t24295}. Mutant embryos are characterized by an early onset over-ossification of the notochord, resulting in fused vertebral centra (Figure1A). In this original allele, *sst* mutants are comparable in size and external features to their wild type siblings, and therefore the phenotype can only be detected by skeletal staining at 8 days post fertilization (dpf) or later. Skeletal stainings of siblings show an equidistant distribution of vertebrae along the notochord, whilst in mutants most of the vertebrae are fused. Examining mutants that were not completely synchronous enabled us to conclude that initially centra are placed in a proper pattern along the notochord, but that later the excess of developing bone causes fusion of the vertebrae (insets in figure 1A).
To assess whether the phenotypic effects might be due to early patterning defects, we performed in situ hybridizations for somitic markers (*myoD, smad1)*, which did not show any differences between mutants and siblings (data not shown).

In a few exceptional cases mutants survived, when separated early from their siblings, until a maximum age of 6 months. These mutants remain smaller (figure 1B), have problems swimming, and exhibit a protruding jaw (figure 1C). In skeletal preparations most centra appear fused, and only about five distinct intervertebral boundaries can be observed along the body axis (figure 1C). Neural and haemal arches both exhibit fan-shaped expansions (figure 1C). Furthermore, the angles of the arches with respect to the body axis are more irregular and obtuse in mutants than in siblings. The phenotype is not restricted to the vertebral column at this later stage: hypurals partially fuse in the tail, and the head skeleton shows abnormalitites as well (figure 1C). Phenotypic analysis of three, six, and nine week old mutants showed that the severity of bone defects increases over time with the older mutants exhibiting the broadest arches (data not shown).

MicroCT scans demonstrate that in *sst* mutants excess bone can replace the notochord by proximal growth, leading to completely solid centra (figure 1D), while the notochord remains present as a continuous rod in the vertebral column of wild type siblings (see movies S1 and S2: http://dev.biologists.org/cgi/content/full/135/22/3765/DC1).

stocksteif encodes *cyp26b1*

In order to molecularly identify the *stocksteif* locus we positionally cloned the gene. The mutation mapped to linkage group 7 (figure 2A). Fine mapping identified two flanking markers on BAC clone zC197C14. In 839 embryos tested, R3.2 left two recombinants (<0.2cM) and R1.11 left one recombinant (<0.1cM). The single gene enclosed by both markers is *cyp26b1*. Sequence analysis of the coding region of

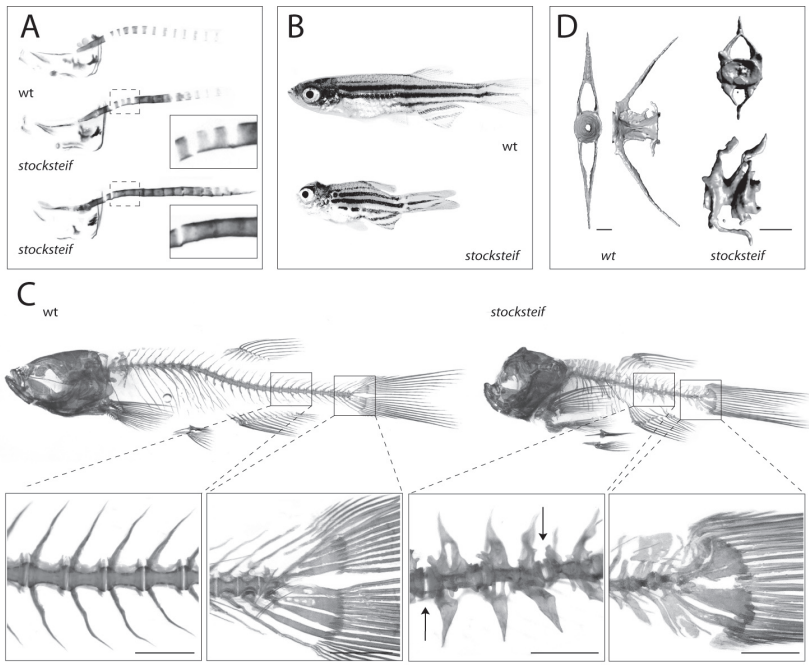

Figure 1: ***Stocksteif* mutants exhibit over-ossification of the larval and adult vertebral column.** (A) Alizarin red bone staining of wild type and *stocksteif* embryos at 8 dpf. Insets show that the initial spacing of vertebrae is normal, but that excessive bone formation causes fusion of the future vertebrae. (B) Sibling wild type and *stocksteif* juveniles (2 months). Pictures are taken with the same magnification. (C) Alizarin red bone staining of wild type and *stocksteif* juveniles (2 months) shown to scale with magnifications of part of the vertebral column and the tail. In mutants, vertebrae are usually fused with each other, and only few intervertebral boundaries can be observed (arrows). Hypural elements in the tail are also fused. Note expansion of both neural and haemal arches in mutants. Scalebars: 500 µm. (D) MicroCT scans of wild type (3 months) and *stocksteif* juveniles (2 months) show that mutants exhibit completely solid centra, with the central opening (area of the nucleus pulposus) completely filled by excess bone. Scalebars: 100 µm.

cyp26b1 as well as exon-intron-boundaries revealed no mutations causing amino acid alterations. Indeed, the sequence of mutant *cyp26b1* cDNA also showed no base changes.

To obtain additional alleles of *sst* we performed a reverse genetic screen (Wienholds et al. 2002). One allele, a nonsense mutation in exon 1, is predicted to change a lysine to a stop codon at position 46 (K46STOP; *sst*^{sa0002}) out of 512 amino acids in the putative wildtype protein. Another allele, a splice donor mutation (*sst*^{sa0003}), changes the most 5' nucleotide of intron 2 from G to A (figure 2B), likely resulting in deficient splicing of this intron and consequently a full knock-out of the encoded protein. Figures 2C and 2D show alizarin red stained progeny from a cross between the two original *sst*^{sa0002} and *sst*^{sa0003} founders. Identical stainings were also obtained

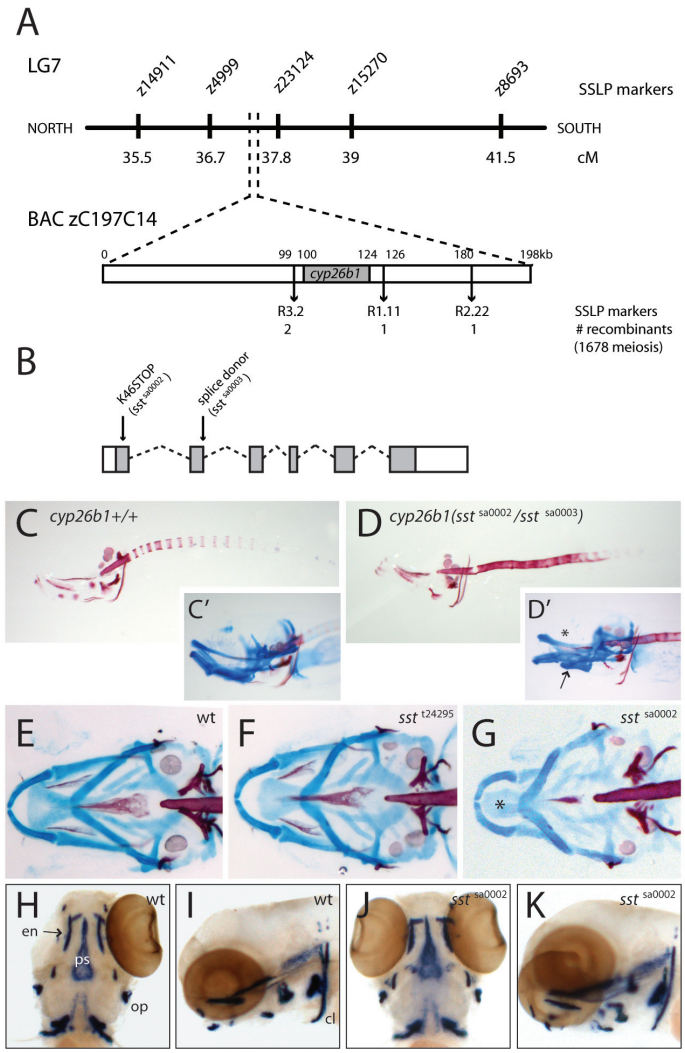

Figure 2: ***stocksteif* encodes *cyp26b1*.** (A) *stocksteif* was mapped to a narrow region on linkage group 7. Flanking SSLP markers are both located on BAC zC197C14. *Cyp26b1* appears to be the only gene present on the clone. (B) Schematic overview of *cyp26b1* structure on the genomic level with nonsense (K46STOP or *sst*^{sa0002}) and splice donor (*sst*^{sa0003}) mutation indicated. Translated parts of the exons are shaded. (C-D) Alizarin red bone staining of a *cyp26b1+/+* embryo and a transheterozygous *cyp26b1(sst*^{sa0002}*/ sst*^{sa0003}*)* embryo. (C',D', E-G) Double stainings with alcian blue for cartilage and alizarin red for bone. (C',D') a *cyp26b1+/+* embryo shows normal cartilage, while a transheterozygous *cyp26b1(sst*^{sa0002}*/ sst*^{sa0003}*)* embryo show missing tissue dorsal to the ethmoid plate (asterisk) and fusion of the ceratohyal with the basihyal (arrow). (E-G) Ventral views of a wild type embryo (E), a homozygous *sst*^{t24295} mutant (F) and a homozygous *sst*^{sa0002} mutant (G). Note the reduced and misshaped ethmoid plate (asterisk) in the *sst*^{sa0002} mutant. (H-K) Expression of *col10a1* is not changed in 4 dpf siblings (H and I) versus mutants (J and K). cl = cleithrum, en = entopterygoid, op = opercle, ps = parasphenoid.

for transheterozygous embryos from crosses between *sst*^{sa0002} and *sst*^{t24295} carriers, and homozygous mutant embryos for both newly obtained alleles, *sst*^{sa0002} and *sst*^{sa0003} (data not shown).

As described above, we have been able to raise a few homozygous mutants from the original *sst*^{t24295} allele. In contrast, all transheterozygous embryos (both *sst*^{sa0002}/ *sst*^{sa0003} and *sst*^{sa0002}/ *sst*^{t24295}) as well as the homozygous embryos for *sst*^{sa0002} and *sst*^{sa0003} die around day 8 of development, without developing a swim bladder. In addition to the over-ossification of the vertebral column, these mutants also exhibit a protruding jaw and miss some tissue dorsal to the ethmoid plate (figure 2C', D', E-G). The cartilage derived ethmoid plate itself (asterisk in figure 2G) is reduced in size and shows a more narrow morphology in homozygous *sst*^{sa0002} and *sst*^{sa0003} mutants than in siblings.
However, mRNA expression of bone specific markers such as *type X collagen* (*col10a1*), shown to be expressed in intramembranous bone in zebrafish (Avaron et al. 2006) and *osterix*, a specific marker for mature osteoblasts (Nakashima et al. 2002) is not altered in mutants. In situ hybridizations for both markers at 4 dpf do not show any differences between siblings and mutants (figure 2H-K and S3).
In situ hybridizations for *cyp26b1* showed that expression levels in homozygous mutants are upregulated in comparison with siblings (figure S4H-I), suggesting a positive feedback response to increased RA levels.
In summary, this shows that *cyp26b1* deficiency leads to cranial cartilage defects. In contrast, bone structures are not affected in the head at this stage, but show severe over-ossification in the trunk.

***Cyp26b1* is expressed in osteoblasts**
To further understand the role of Cyp26b1 in ossification we examined its expression pattern both in zebrafish and mice. In zebrafish, we confirmed previously reported *cyp26b1* expression up to 72hpf (Zhao et al. 2005) in the head region, covering expression in the hindbrain, branchial arches, and pectoral fins (figure 3A, S4A-C). In addition, we here show that previously unreported expression can also be found in bone elements (examples are shown in figure 3A (cleithrum), S4E (opercle), and S4F-G (parasphenoid)). Moreover, we report a segmented pattern in the area surrounding the notochord which is most clearly visible in *sst* mutants because of their upregulated *cyp26b1* levels (figure 3B). To determine whether the latter staining represents expression in sclerotome derived cells, we compared *cyp26b1* expression with expression of *twist* (figure 3C, D), which has been shown to be specific, within the somites, for sclerotome in zebrafish (Morin-Kensicki and Eisen 1997) as well as in medaka (Renn et al. 2006). Expression patterns of *cyp26b1* and *twist* do correspond with one another, indicating that *cyp26b1* in zebrafish is expressed in sclerotome derived cells.

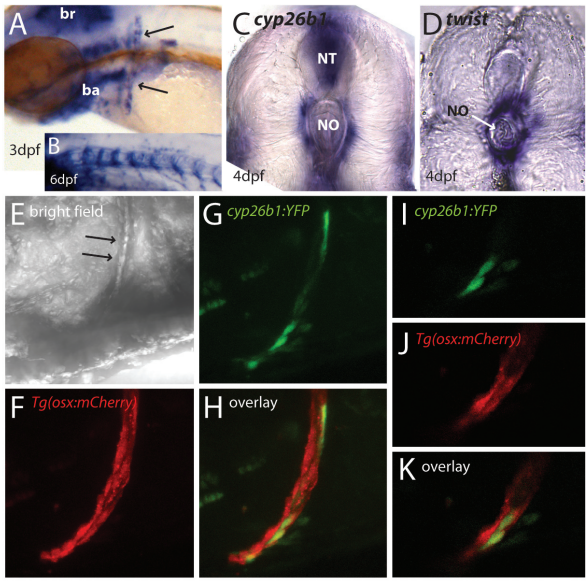

Figure 3: ***cyp26b1* is expressed in zebrafish osteoblasts.**
(A-C) *cyp26b1* expression in zebrafish. (A) Early *cyp26b1* expression in zebrafish is found in the hindbrain, branchial arches, pectoral fins and the cleithrum (arrows). (B) At 6 dpf *cyp26b1* expression is seen in a segmented pattern around the notochord. A mutant embryo is shown, as *cyp26b1* mRNA levels are higher in mutants than wildtype embryos. (C-D) 100 µm vibratome transversal sections (4 dpf) showing *cyp26b1* expression (C) surrounding the notochord (no) and in the neural tube (nt), and expression of the sclerotome marker *twist* in cells juxtaposed to the notochord (D), similar to *cyp26b1* expression. (E) Bright field view of an embryonic trunk with arrows pointing to the cleithrum. (F-K) Co-localization of *cyp26b1*:*YFP* and *osx*:*mCherry* in osteoblasts of the cleithrum. (F) Cleithrum cells are labeled in *Tg(osx:mCherry)* embryos. (G) Transient expression of *cyp26b1*:*YFP* in cells of the cleithrum at 4 dpf, with projection in (H) demonstrating co-localization of both genes in the same cells. (I-K) Single confocal scans of a part of the projections shown in F-H. Anterior is to the left, except where stated otherwise.

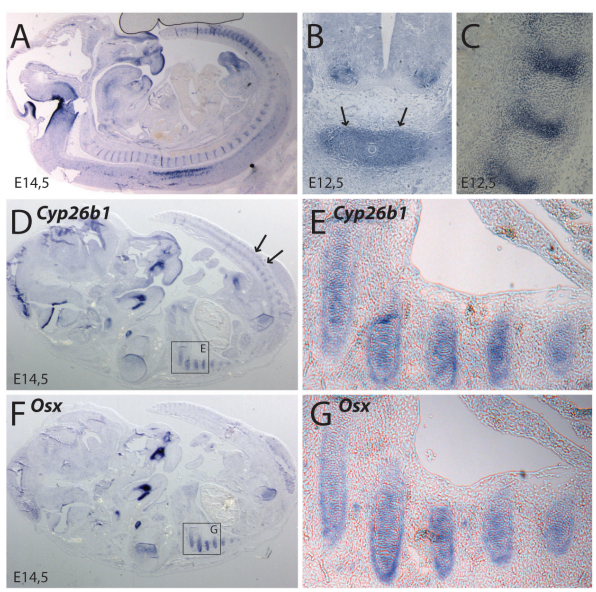

Figure 4: ***Cyp26b1* is expressed in mouse osteoblasts prior to *Osterix* expression.**
(A-E) *Cyp26b1* expression in mice. (A) At E14,5 *Cyp26b1* mRNA is present in the brain, neural tube, craniofacial structures, and in the pre-vertebrae regions. (B) Transversal section (E12,5) showing expression of *Cyp26b1* in the cells of the condensing sclerotome (arrows) around the notochord. (C) Detail of sagittal section (E12,5) confirming the segmented pattern in the pre-vertebrae regions. (D-G) Consecutive sections showing expression of *Cyp26b1* (D, enlargement in E) and *Osterix* (F, enlargement in G) in the forming vertebrae. Note that expression is seen in exactly the same region, showing that *Cyp26b1* is expressed in osteoblasts. Arrows in D are pointing to expression of *Cyp26b1* in posterior vertebrae where *Osterix* is not expressed yet.

To investigate whether *cyp26b1* is expressed in osteoblasts we first generated a new transgenic zebrafish reporter line, in which mCherry expression is controlled by the medaka *osterix* promoter (Renn and Winkler, unpublished). Briefly, in transgenic larvae, *osterix*:*mCherry* positive cells in the head are seen in all intramembranous bones, such as parasphenoid and cleithrum, and later in the opercle and branchiostegal rays, as well as in endochondral bones (data not shown).
In order to compare *osterix* expression with *cyp26b1* expression *in vivo*, we recombined YFP into a BAC clone that contained the genomic sequence of *cyp26b1*. This construct was injected into 1-cell stage *Tg(osx:mCherry)* embryos. Since in these transient assays not all cells will incorporate the *cyp26b1*:*YFP* construct, we expected patchy *cyp26b1*:*YFP* expression. Indeed, we were able to detect single YFP positive cells in *osx:mCherry* positive bone elements (figure 3F-K). In various embryos that we have analyzed, we have only seen YFP expression at places where we had previously observed *cyp26b1* mRNA expression. Ectopic expression was never observed. We conclude that *cyp26b1* is expressed in osteoblasts.

In mice, *Cyp26b1* is expressed during early embryonic development in the hindbrain, neural tube, craniofacial structures, in outgrowing limb buds (MacLean et al. 2001) and in the pre-vertebrae regions at E12.5 and E14.5 (Abu-Abed et al. 2002). We confirm and extend these findings by showing that also in mice it is the condensing sclerotome surrounding the notochord which expresses *Cyp26b1* (figure 4B, C), as in zebrafish.
Furthermore, in situ hybridizations on consecutive sections using probes against *Cyp26b1* and *Osterix* show expression of both genes in overlapping regions of the mouse axial skeleton (figure4D-G). Vertebrae are formed in an anterior-posterior progression with more posterior vertebrae being less mature than anterior ones. *Cyp26b1* is expressed in all forming vertebrae, including the most posterior ones (arrows in figure 4D), while *Osterix* is only expressed in the most mature vertebrae (figure 4F). Thus, C*yp26b1* expression precedes *Osterix* expression.
We conclude that, as in zebrafish, murine *Cyp26b1* is expressed in osteoblasts and that expression of *Cyp26b1* is conserved among vertebrates. The expression pattern of *Cyp26b1* is consistent with the axial skeletogenesis phenotype in *stocksteif* mutants.

***In vivo* observations of axial *osterix* expression**
In the course of these studies, we noticed that in zebrafish axial *osterix* expression could only be detected at points in time when neural and haemal arches were about to appear at day 17 (Fleming et al. 2004; Spoorendonk and Schulte-Merker, unpublished). We have failed to detect *osterix* mRNA in the axis prior to this point in time. This suggests that cells which form the calcified material of the centra do not express *osterix* at these stages in zebrafish.
Further support for this notion stems from the analysis of a transgenic zebrafish

line, in which mCherry is controlled by the medaka *osterix* promoter. Here, we only detect mCherry positive cells in the arches and at the anterior and posterior edges of the forming vertebrae, but not in the central part of the centra at this stage. Expression could only be detected shortly prior to the formation of neural and haemal arches (see figure 6A-D). To confirm that this is not a limitation of the transgene, we have recombined YFP into a BAC containing the zebrafish *osterix* gene. Again, after injections of this construct in one-cell stage embryos, we were able to detect expression only in cranial bone and, after day 17, in haemal and neural arches. The main bodies of the centra, however, were always devoid of YFP expression in these transient expression assays (data not shown). Both transgenic lines show identical results and exhibit expression patterns identical to what we observe with *osterix* mRNA in situs.
We conclude that zebrafish *osterix* is very likely not expressed in cells that are responsible for early ossification of the centra. *osterix* expression, in the axial skeleton, is restricted to the anterior and posterior edges of the forming vertebrae, as well as to neural and haemal arches.

Treatment of wild type embryos with either retinoic acid or R115866 phenocopies the *stocksteif* mutant phenotype

Since *sst* mutants lack Cyp26b1 activity and therefore should have at least a local excess of RA, we asked whether RA treatment of wild type embryos can phenocopy the mutant phenotype. Treatments were started at day 4 or later to avoid defects associated with early RA treatments of embryos (Keegan et al. 2005; Hernandez et al. 2007; Reijntjes et al. 2007). Wild type embryos were treated with 1 µM RA starting at day 4, 5, 6, or 7 of development. At 8 dpf, alizarin red staining was performed. Sibling controls received equivalent treatments of DMSO, with no detectable effect on ossification. RA treatments, however, resulted in three phenotypic classes, all exhibiting axial over-ossification, with the most severe one completely mimicking the *sst* mutant phenotype (figure 5A). As shown in figure 5B, all embryos for which treatment was started at 4 dpf showed a phenotype, with 35% exhibiting a completely over-ossified notochord. For treatments started at 5 dpf and 6 dpf, respectively, 90% and 70% showed a phenotype. Embryos treated for 24h with RA onwards from day 7 were indistinguishable from controls, presumably since 24 hours were insufficient to allow for mineralization to occur.

To investigate more specifically the effect of aberrant Cyp26b1 function, we treated wild type embryos with 0.5 µM of the R115866 compound, a selective antagonist for the three Cyp26 enzymes (Hernandez et al. 2007). Treatments were identical, and results near-identical to the described RA treatments: all embryos for which treatment was started at day 4 showed a phenotype resembling the *sst* mutant (figure 5C).

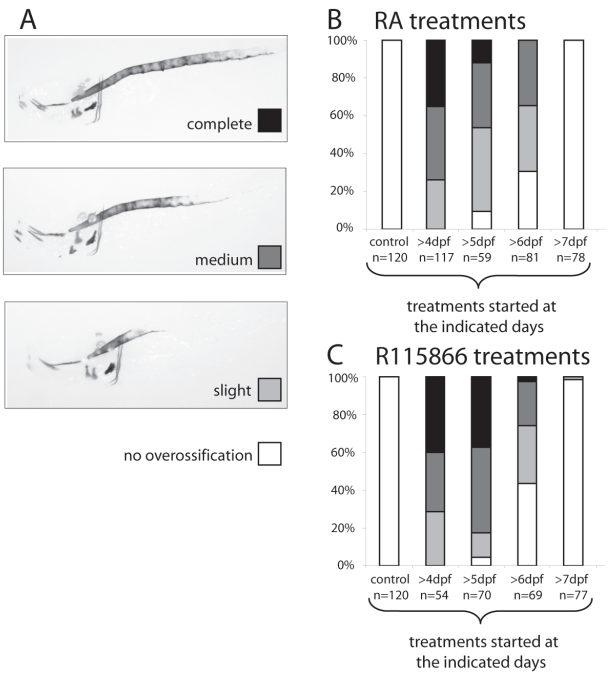

Figure 5: **Treatments of wild type embryos with either retinoic acid or R115866 phenocopy the *stocksteif* mutant phenotype.** (A) After treatments of wild type embryos with 1µM RA three phenotypic classes were observed, with the most severe phenotype completely mimicking the *sst* mutant phenotype. (B) Results are shown for RA treatments which were started at the days indicated and continued until the embryos were fixed at 8 dpf. Control treatments with only DMSO were started at day 4. (C) Treatment of wild type embryos with 0.5 µM R115866 resulted in the same three phenotypic classes as shown for the RA treatments in (A).

Osteoblast numbers do not alter upon retinoic acid treatment

Obvious explanations for the observed phenotype would be mislocalization of osteoblasts, an increased number of osteoblasts, or increased osteoblast activity. In order to distinguish between these scenarios, and in order to precisely quantify osteoblasts *in vivo*, we established, next to the described *osterix*:*mCherry* line, an additional line with nuclear GFP (nuGFP) controlled by the medaka *osterix* promoter region. Unfortunately, since even the hypomorphic *sst*^{t24295} allele is near-lethal, we have not been able to obtain homozygous *sst*^{t24295} larvae in this transgenic background. Therefore, we decided to directly visualize the response of osteoblasts to excess RA in the *osterix*:*nuGFP* zebrafish line.

When zebrafish embryos are treated with 0.1 µM RA from 17 dpf to 20 dpf, i.e. after onset of endogenous and transgenic *osterix* expression, over-ossification of the axial skeleton can be observed as evidenced by fusion of vertebrae (alizarin red bone staining in figure 6E-H), identical to our RA treatments described above

(compare with figure 5A). The localization of GFP-positive osteoblasts in RA treated embryos, however, is not altered in comparison with DMSO controls (compare figure 6I and L). In most treated cases, the space between centra was easily recognizable, even though anterior and posterior edges of centra were not delineated as straight as in DMSO control cases, probably due to the large amount of ectopic bone matrix which is laid down in the spaces between the centra.

Next, we performed cell counts. While in projections of confocal scans it is not always clear whether a spot of GFP expression refers to one or more nuclei, nuclei of separate cells can be clearly distinguished from each other in single confocal scans (e.g., the encircled spot in one projection (figure 6J) was resolved to represent two cells in a single scan (figure 6K)). Furthermore, cells that are seen in projections but belong to arches at the other side of the embryo can be discriminated in single scans (examples of such cells are indicated with arrows in projections (figure 6J, M)). Therefore, all cell counts were done in single confocal scans. In at least five different larvae per condition several segments were counted (schematic representation of counted area is seen in figure 6O). As shown in figure 6P, there is no significant difference in numbers of *osterix:nuGFP* positive cells between DMSO controls and RA treated larvae. In conclusion, RA treatment of embryos from 17 to 20 dpf does not alter localization of mature *osterix* expressing osteoblasts or their numbers.

Figure 6 (right): **RA treatment does not increase the number of *osterix:nuGFP* positive osteoblasts in the centrum.** (A-D) *Osx:mCherry* expressing osteoblasts in a vertebra of a 20 day old zebrafish. (A) *Osx* expressing cells are positioned around arches and at the anterior and posterior edges of each centrum, which is counterstained with calcein in (B). Part of the overlay in C is shown in D. Note that osteoblasts are positioned distal to the produced bone matrix (examples are indicated with arrows). (E-H) Alizarin red bone staining of 20 day old zebrafish embryos treated with DMSO (E, enlargement in F) or 0,1 µM RA (G, enlargement in H) showing over-ossification of the vertebral column in RA treated specimen. (I-N) *Osx:nuGFP* expressing osteoblasts in 20 day old zebrafish embryos treated with DMSO (I, enlargement in J) or 0,1 µM RA (L, enlargement in M). Single scans of one focal plane (K) were used to count cells. Cells indicated with arrows in projections (J, M) are not seen in single scans (K, N) since they belong to the arch at the opposite site. Note that in single scans cells can be distinguished from each other while in projections this is not always clear (encircled spot in J was resolved to represent two different cells in K). Panels M and N show high magnifications of a haemal arch, but were actually not used for countings. (O) Schematic representation of vertebrae shows defined area in which cells were counted per segment. (P) Cell counts show no difference between DMSO controls and treated embryos in amount of *osx:nuGFP* positive osteoblasts. Scalebars: (A-C) 25 µm; (E, G) 500 µm; (I, L) 50 µm.

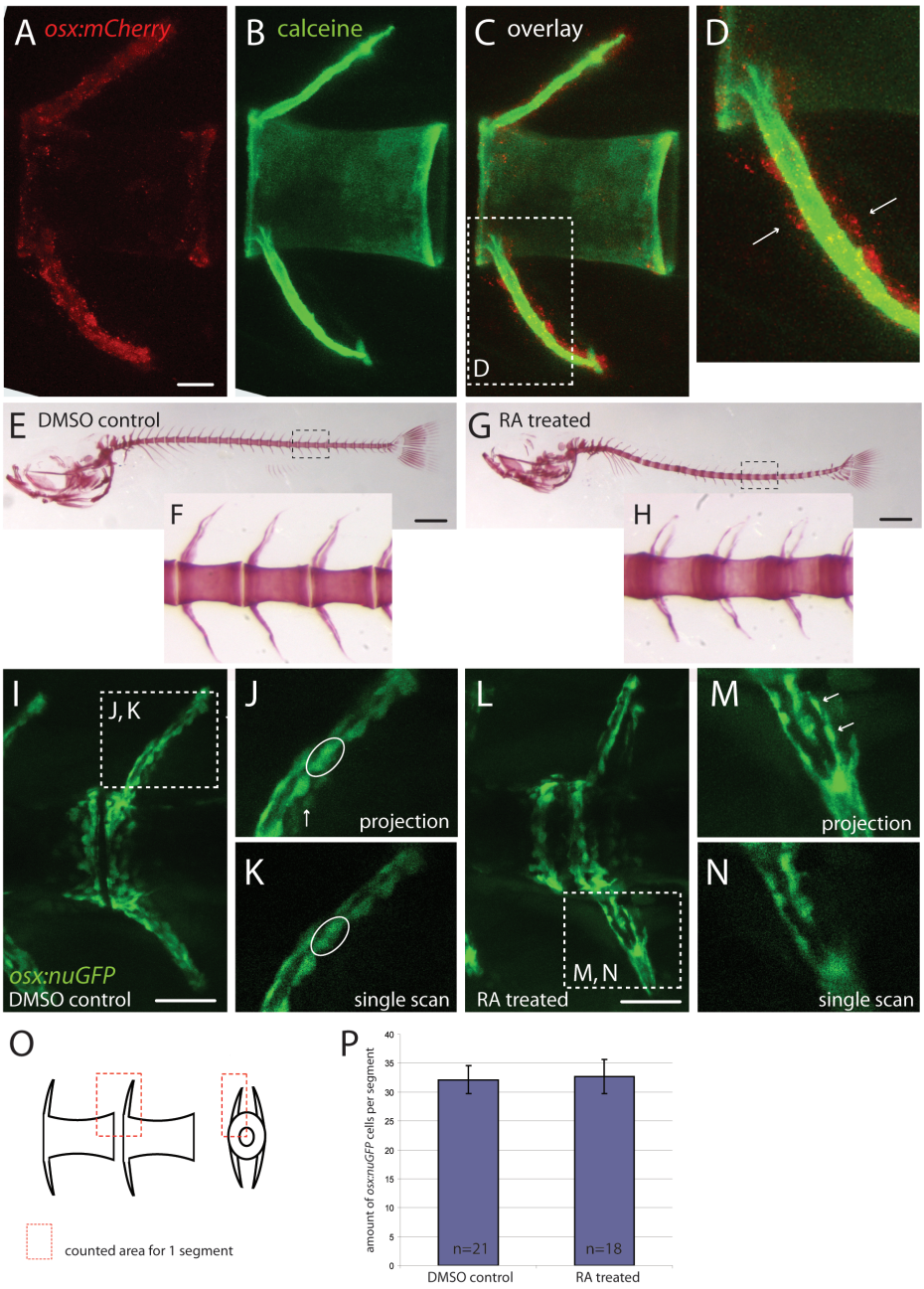
A osx:mCherry
B calceine
C overlay
D
D
E DMSO control
F
G RA treated
H
I
J, K
osx:nuGFP
DMSO control
J
projection
K
single scan
L
M, N
RA treated
M
projection
N
single scan
O
counted area for 1 segment
P
amount of osx:nuGFP cells per segment
0
5
10
15
20
25
30
35
40
n=21
n=18
DMSO control
RA treated

DISCUSSION

The *stocksteif* mutant phenotype

In this study, we characterized the zebrafish mutant *stocksteif* which exhibits severe over-ossification of the vertebral column. Initially, centra are placed in a wild type pattern along the notochord, but later the excess of developing bone causes fusion of the vertebrae. This suggests that over-ossification in *sst* mutants is not due to a defect in initial anterior-posterior patterning, and is therefore distinct from the *fused somites* mutant phenotype (van Eeden et al. 1996). Unchanged expression patterns of early somitic markers (*myoD, smad1)* confirmed this notion.

In a few exceptional cases, we have been able to raise homozygous mutants of the original *sst*^{t24295} allele to a later stage in life. Phenotypic analysis of larvae at different ages showed that the severity of bone defects increases over time, indicating that the gene affected in *sst* mutants is critical for controlling proper ossification not only during embryogenesis, but also in late larval and adult stages. We suggest that *sst* activity is required throughout life to control osteogenesis, at least in axial skeletogenesis. This notion is supported by the late RA treatments we performed (17-20 dpf) which also resulted in axial over-ossification, indicating sensitivity to RA at late larval stages.

Hypomorphic and loss-of-function mutants for *cyp26b1*

Positional cloning of *sst*^{t24295} revealed two flanking markers enclosing the retinoic acid metabolizing gene *cyp26b1*, but no causative mutation could be found in this allele. In order to identify additional alleles, we undertook a reverse genetic screen. We obtained two additional alleles of *sst*, both of which fail to complement the original *sst*^{t24295} allele. We focus in this study on *sst*^{sa0002}, which encodes a nonsense mutation in exon 1, predicted to change a lysine to a stop codon at position 46 (K46STOP; *sst*^{sa0002}) of the protein. Since this will truncate the protein even N-terminal to the cytochrome P450 domain (at amino acid 50), we conclude that this allele encodes a loss-of-funtion allele.

When comparing the *sst*^{t24295} and the *sst*^{sa0002} allele, there are a number of noteworthy differences. First, all *sst*^{sa0002} mutants die shortly after hatching, while we have been able to raise very few *sst*^{t24295} homozygotes to late larval and adult stages. Second, when examining the head cartilage, *sst*^{t24295} does not show alterations when compared to wildtype siblings, while the *sst*^{sa0002} allele shows a protruding jaw and a reduced and misshapen ethmoid plate. Both lines of evidence suggest that *sst*^{t24295} is a hypomorph and that it represents a slightly weaker allele than *sst*^{sa0002}*.* The observed jaw phenotype is most likely the reason for early lethality in the strong alleles and correlates with the adult head skeleton phenotype that we find in the hypomorphic *sst*^{t24295} allele (figure 1C).

In the original *stocksteif* allele we also observe over-ossification of neural and haemal arches, while the other two *sst* alleles die too early to analyze arch formation. In mice,

similar arch phenotypes can be observed by treatments with the Cyp26 inhibitor R115866 which results in over-ossification and fusion of arches of treated embryos (Laue and Hammerschmidt, personal communication). This suggests a conserved role for the function of Cyp26b1 among vertebrates.

Cyp26 mutants in mice

Cyp26b1 knockout mice die before the onset of vertebral deformities, due to respiratory distress. Mutant mouse embryos however manifest reduced limbs (Yashiro et al. 2004). In fish, we do not observe phenotypes related to fin outgrow, most probably because fin rays are evolutionary completely different from the digits of a mammalian limb (Grandel and Schulte-Merker 1998).

Jaw phenotypes mimicking what we observe in both embryonic and adult *cyp26b1* mutants were not described in *Cyp26a1* mutant mice (Abu-Abed et al. 2001; Sakai et al. 2001). The *Cyp26a1* mouse phenotype therefore is clearly distinct from what we observe in zebrafish *cyp26b1* mutants. Moreover, expression patterns of both genes are also distinct from each other: compared to *Cyp26b1*, *Cyp26a1* expression is restricted to the extremities of the vertebral arches and ribs, and has not been detected in the pre-vertebrae regions (Abu-Abed et al. 2002).

We conclude that *stocksteif* manifests a novel phenotype, which allows new insight into the function of *Cyp26b1* and retinoid signaling during vertebral ossification.

Retinoic acid treatment leads to axial over-ossification

Pharmacological treatments with either RA itself or the Cyp26 inhibitor R115866 completely phenocopy the *stocksteif* over-ossification phenotype, demonstrating a role for RA in ossification of the vertebral column. We propose that it is the regulation of Cyp26b1 activity which defines local concentrations of RA within the vertebral area. Disruption of the gene or altered RA levels result in over-ossification along the vertebral column, most likely due to a local excess of RA within osteoblasts.

To support this notion, we examined the axial expression of *Cyp26b1* in zebrafish and mice. Localization of *Cyp26b1* transcripts in both species was found abutting the notochord, and comparison with zebrafish *twist* expression suggests that *Cyp26b1* is indeed expressed in sclerotome derived cells of both teleosts and mammals. Furthermore, in both zebrafish and mice, we could clearly establish that *Cyp26b1* is expressed in cells that also express *Osterix* (figure 3F-K and 4D-G). Therefore, we suggest that Cyp26b1 activity controls RA levels within osteoblasts, possibly setting up a boundary of low versus high RA levels between cells that express *Cyp26b1* and those that do not.

Evidence for two populations of osteoblasts

In zebrafish we have never been able to detect *osterix* expression in the axial skeleton before arches appear, neither by in situ hybridizations nor in the described transgenic lines. However, there is mineralized matrix present as visualized by

alizarin red or calcein staining, raising the question which cells are responsible for initial ossification of the very earliest centrum material. We suggest the existence of two types of osteoblasts: both are osteoblasts in the functional sense of secreting matrix which is then mineralized. However, one group does not express *osterix*, while the other group does. The latter group includes the osteoblasts of the future head skeleton, the vertebral arches, and late-appearing osteoblasts at the anterior and posterior edges of the centra (figure 6A, C). The *osterix* negative cells provide the initial material of the centrum body.
Further evidence for this hypothesis stems from Fleming et al. (2004), who were never able to detect osteoblasts in centrum bone matrix, while they could detect them in developing skull bones. It remains to be seen whether the *osterix* negative cells are identical to cells of the notochord, which are postulated by Fleming et al. (2004) to initiate centrum formation. Finally, it is interesting to note that *Osterix* null mutant mice are born with mineralized centra , while they lack almost all craniofacial bone elements (Nakashima et al. 2002). While it is possible that centrum osteoblasts in mice express *Osterix*, but do not require it for osteoblast function, it does point to a difference between centrum osteoblasts and all other osteoblasts.

Effects of retinoic acid on osteoblast activity
We considered three models that may explain why excess RA results in over-ossification: (1) RA causes ectopic bone formation by mis-positioning of osteoblasts, (2) RA causes an increase in osteoblast number, or (3) RA increases the activity of osteoblasts while not affecting their number. To distinguish between these mechanisms, we made use of a zebrafish *osterix*:*nuGFP* transgenic reporter line, in order to directly visualize the response of mature osteoblasts to RA. We show that upon RA treatment *osterix* positive osteoblasts do not change position, nor do they increase in number. We therefore favor the third model and suggest that osteoblasts increase their mineralization activity upon exposure to excess RA.
As at present there is no marker available for the putative, *osterix* negative osteoblasts in the centra, we are unable to assess whether RA also acts on this type of osteoblasts. It is noteworthy that skeletons of the adult hypomorphic *sst* mutants show over-ossification at precisely the sites where we do see *osterix* expression: anterior and posterior edges of the centra, as well as neural and haemal arches. Therefore our results could be explained by postulating an increase in the activity of *osterix* positive osteoblasts for the later aspects of the phenotype. However, we do consider it likely that RA also has an effect on *osterix* negative osteoblasts, as the *sst* phenotype becomes apparent already at day 8 of development.

In the past, conflicting results have been reported about *in vitro* studies that have examined the effect of RA on mineralization. An increase in mineralization was reported (Skillington et al. 2002; Wang and Kirsch 2002; Song et al. 2005; Yamashita et al. 2005; Malladi et al. 2006; Wan et al. 2007), while different studies show suppression

of cell differentiation with a concomitant decrease in mineralization (Cohen-Tanugi and Forest 1998; Iba et al. 2001) upon RA treatment of cultured cells. Here, we show in an *in vivo* setting that RA increases bone formation and suggest this to occur by an increased activity of osteoblasts. We have demonstrated that zebrafish offer an attractive model for performing genetic and pharmacological studies on osteoblasts, allowing *in vivo* observations and histological read-outs at the same time. In a field where the interpretation of *in vitro* and *ex vivo* experiments is inherently difficult, the use of an *in vivo* model which allows monitoring osteoblasts in real time will be highly beneficial.

A model for RA activity in axial skeletogenesis

We have shown that systemic treatment of larvae with RA produces phenotypes very similar to *cyp26b1* loss-of-function situations, even though one might speculate that mis-regulation of RA in axial osteoblasts causes a more spatially restricted increase in local RA levels, than exposing all cells to excess RA. We have incorporated all data presented in this manuscript in the following model:

In the wildtype situation, expression of Cyp26b1 protein within osteoblasts leads to lower RA levels within *cyp26b1* positive cells (i.e. osteoblasts) than in neighboring cells that do not express *cyp26b1* (i.e. non-osteoblasts). We propose that the juxtaposition of areas with low versus high RA levels is significant in maintaining *cyp26b1* positive cells in a state in which they produce tightly controlled amounts of calcified matrix. Only when cells are exposed to comparatively higher levels of RA, e.g. in *cyp26b1* mutants or after exposure to exogenous RA, will they then begin to produce an excess of calcified tissue.

In RA treated embryos, all cells within the embryo experience high RA levels, and consequently there is no boundary between “RA low” and “RA high” regions. Accordingly, both *osterix* negative osteoblasts within the body of the centrum and *osterix* positive osteoblasts in the anterior and posterior regions of the centrum produce more matrix, leading to the observed over-ossification phenotype.

In loss-of-function *stocksteif* mutant embryos, RA levels are not lowered in osteoblasts (or only mildly lowered in the hypomorphic allele), again leading to increased osteoblast activity and resulting in the same events as just described for systemic RA exposure.

Conclusion

In summary, we have shown that regulation of RA levels and the tight control of Cyp26b1 activity are essential for regulation of skeletogenesis in zebrafish. Our data demonstrate a previously unappreciated role for RA and *cyp26b1* in osteogenesis of the vertebral column and provide novel insight into the regulation of bone formation.

ACKNOWLEDGEMENTS

The original *sst*^{t24295} allele was identified in by the members of the Tübingen 2000 Screen. Janssen Pharmaceutica kindly provided R115866. Ansa Wasim performed initial genomic mappings. Jeroen Bussmann performed BAC recombineering experiments. Identification of additional *sst* alleles by TILLING at the Hubrecht Institute and the Sanger Center would not have been possible without the enthusiastic help of (in alphabetical order) Ewart de Bruijn, Elisabeth Busch, Edwin Cuppen, Ross Kettleborough, and Derek Stemple. Kathrin Laue and Matthias Hammerschmidt shared results before publication. All members of the S.-M. lab are acknowledged for discussions. S.S.-M. gratefully recognizes the support of the Smart Mix Programme of the Netherlands Ministry of Economic Affairs and the Netherlands Ministry of Education, Culture and Science. In part, this work was funded by ESA (15452/01/NL/SH) and an A*STAR BMRC grant (07/1/21/19/544) to C.W.

REFERENCES

Abu-Abed, S., Dolle, P., Metzger, D., Beckett, B., Chambon, P. and Petkovich, M. (2001). The retinoic acid-metabolizing enzyme, CYP26A1, is essential for normal hindbrain patterning, vertebral identity, and development of posterior structures. Genes Dev 15, 226-40.

Abu-Abed, S., MacLean, G., Fraulob, V., Chambon, P., Petkovich, M. and Dolle, P. (2002). Differential expression of the retinoic acid-metabolizing enzymes CYP26A1 and CYP26B1 during murine organogenesis. Mech Dev 110, 173-7.

Avaron, F., Hoffman, L., Guay, D. and Akimenko, M. A. (2006). Characterization of two new zebrafish members of the hedgehog family: atypical expression of a zebrafish indian hedgehog gene in skeletal elements of both endochondral and dermal origins. Dev Dyn 235, 478-89.

Bowles, J., Knight, D., Smith, C., Wilhelm, D., Richman, J., Mamiya, S., Yashiro, K., Chawengsaksophak, K., Wilson, M. J., Rossant, J. et al. (2006). Retinoid signaling determines germ cell fate in mice. Science 312, 596-600.

Cohen-Tanugi, A. and Forest, N. (1998). Retinoic acid suppresses the osteogenic differentiation capacity of murine osteoblast-like 3/A/1D-1M cell cultures. Differentiation 63, 115-23.

Ekanayake, S. and Hall, B. K. (1987). The development of acellularity of the vertebral bone of the Japanese medaka, Oryzias latipes (Teleostei; Cyprinidontidae). J Morphol 193, 253-61.

Emoto, Y., Wada, H., Okamoto, H., Kudo, A. and Imai, Y. (2005). Retinoic acid-metabolizing enzyme Cyp26a1 is essential for determining territories of hindbrain and spinal cord in zebrafish. Dev Biol 278, 415-27.

Feldkamp, L. A., Davis, L. C. and Kress, J. W. (1984). Practical cone-beam algorithm. J Opt Soc Am A 1, 612-9.

Fleming, A., Keynes, R. and Tannahill, D. (2004). A central role for the notochord in vertebral patterning. Development 131, 873-80.

Grandel, H. and Schulte-Merker, S. (1998). The development of the paired fins in the zebrafish (Danio rerio). Mech Dev 79, 99-120.

Gu, X., Xu, F., Wang, X., Gao, X. and Zhao, Q. (2005). Molecular cloning and expression of a novel CYP26 gene (cyp26d1) during zebrafish early development. Gene Expr Patterns 5, 733-9.

Hernandez, R. E., Putzke, A. P., Myers, J. P., Margaretha, L. and Moens, C. B. (2007).

Cyp26 enzymes generate the retinoic acid response pattern necessary for hindbrain development. Development 134, 177-87.

Iba, K., Chiba, H., Yamashita, T., Ishii, S. and Sawada, N. (2001). Phase-independent inhibition by retinoic acid of mineralization correlated with loss of tetranectin expression in a human osteoblastic cell line. Cell Struct Funct 26, 227-33.

Inohaya, K., Takano, Y. and Kudo, A. (2007). The teleost intervertebral region acts as a growth center of the centrum: in vivo visualization of osteoblasts and their progenitors in transgenic fish. Dev Dyn 236, 3031-46.

Kawakami, K., Koga, A., Hori, H. and Shima, A. (1998). Excision of the tol2 transposable element of the medaka fish, Oryzias latipes, in zebrafish, Danio rerio. Gene 225, 17-22.

Keegan, B. R., Feldman, J. L., Begemann, G., Ingham, P. W. and Yelon, D. (2005). Retinoic acid signaling restricts the cardiac progenitor pool. Science 307, 247-9.

Kimura, Y., Okamura, Y. and Higashijima, S. (2006). alx, a zebrafish homolog of Chx10, marks ipsilateral descending excitatory interneurons that participate in the regulation of spinal locomotor circuits. J Neurosci 26, 5684-97.

MacLean, G., Abu-Abed, S., Dolle, P., Tahayato, A., Chambon, P. and Petkovich, M. (2001). Cloning of a novel retinoic-acid metabolizing cytochrome P450, Cyp26B1, and comparative expression analysis with Cyp26A1 during early murine development. Mech Dev 107, 195-201.

Maden, M. (2002). Retinoid signalling in the development of the central nervous system. Nat Rev Neurosci 3, 843-53.

Malladi, P., Xu, Y., Yang, G. P. and Longaker, M. T. (2006). Functions of vitamin D, retinoic acid, and dexamethasone in mouse adipose-derived mesenchymal cells. Tissue Eng 12, 2031-40.

Moorman, A. F., Houweling, A. C., de Boer, P. A. and Christoffels, V. M. (2001). Sensitive nonradioactive detection of mRNA in tissue sections: novel application of the whole-mount in situ hybridization protocol. J Histochem Cytochem 49, 1-8.

Morin-Kensicki, E. M. and Eisen, J. S. (1997). Sclerotome development and peripheral nervous system segmentation in embryonic zebrafish. Development 124, 159-67.

Nakashima, K., Zhou, X., Kunkel, G., Zhang, Z., Deng, J. M., Behringer, R. R. and de Crombrugghe, B. (2002). The novel zinc finger-containing transcription factor osterix is required for osteoblast differentiation and bone formation. Cell 108, 17-29.

Nelson, D. R. (1999). A second CYP26 P450 in humans and zebrafish: CYP26B1. Arch Biochem Biophys 371, 345-7.

Reijntjes, S., Rodaway, A. and Maden, M. (2007). The retinoic acid metabolising gene, CYP26B1, patterns the cartilaginous cranial neural crest in zebrafish. Int J Dev Biol 51, 351-60.

Rembold, M., Lahiri, K., Foulkes, N. S. and Wittbrodt, J. (2006). Transgenesis in fish: efficient selection of transgenic fish by co-injection with a fluorescent reporter construct. Nat Protoc 1, 1133-9.

Renn, J., Schaedel, M., Volff, J. N., Goerlich, R., Schartl, M. and Winkler, C. (2006). Dynamic expression of sparc precedes formation of skeletal elements in the Medaka (Oryzias latipes). Gene 372, 208-18.

Ross, S. A., McCaffery, P. J., Drager, U. C. and De Luca, L. M. (2000). Retinoids in embryonal development. Physiol Rev 80, 1021-54.

Sakai, Y., Meno, C., Fujii, H., Nishino, J., Shiratori, H., Saijoh, Y., Rossant, J. and Hamada, H. (2001). The retinoic acid-inactivating enzyme CYP26 is essential for establishing an uneven distribution of retinoic acid along the anterio-posterior axis within the mouse embryo. Genes Dev 15, 213-25.

Schulte-Merker, S. (2002). Looking at embryos. Zebrafish, a practical approach, 41-43.

Skillington, J., Choy, L. and Derynck, R. (2002). Bone morphogenetic protein and retinoic acid signaling cooperate to induce osteoblast differentiation of preadipocytes. J Cell Biol 159, 135-46.

Song, H. M., Nacamuli, R. P., Xia, W., Bari, A. S., Shi, Y. Y., Fang, T. D. and Longaker, M. T. (2005). High-dose retinoic acid modulates rat calvarial osteoblast biology. J Cell Physiol 202, 255-62.

van Eeden, F. J., Granato, M., Schach, U., Brand, M., Furutani-Seiki, M., Haffter, P., Hammerschmidt, M., Heisenberg, C. P., Jiang, Y. J., Kane, D. A. et al. (1996). Mutations affecting somite formation and patterning in the zebrafish, Danio rerio. Development 123, 153-64.

Waarsing, J. H., Day, J. S. and Weinans, H. (2004). An improved segmentation method for in vivo microCT imaging. J Bone Miner Res 19, 1640-50.

Walker, M. B. and Kimmel, C. B. (2007). A two-color acid-free cartilage and bone stain for zebrafish larvae. Biotech Histochem 82, 23-8.

Wan, D. C., Siedhoff, M. T., Kwan, M. D., Nacamuli, R. P., Wu, B. M. and Longaker, M. T. (2007). Refining retinoic acid stimulation for osteogenic differentiation of murine adipose-derived adult stromal cells. Tissue Eng 13, 1623-31.

Wang, W. and Kirsch, T. (2002). Retinoic acid stimulates annexin-mediated growth plate chondrocyte mineralization. J Cell Biol 157, 1061-9.

White, J. A., Guo, Y. D., Baetz, K., Beckett-Jones, B., Bonasoro, J., Hsu, K. E., Dilworth, F. J., Jones, G. and Petkovich, M. (1996). Identification of the retinoic acid-inducible all-trans-retinoic acid 4-hydroxylase. J Biol Chem 271, 29922-7.

White, J. A., Ramshaw, H., Taimi, M., Stangle, W., Zhang, A., Everingham, S., Creighton, S., Tam, S. P., Jones, G. and Petkovich, M. (2000). Identification of the human cytochrome P450, P450RAI-2, which is predominantly expressed in the adult cerebellum and is responsible for all-trans-retinoic acid metabolism. Proc Natl Acad Sci U S A 97, 6403-8.

White, R. J., Nie, Q., Lander, A. D. and Schilling, T. F. (2007). Complex regulation of cyp26a1 creates a robust retinoic acid gradient in the zebrafish embryo. PLoS Biol 5, e304.

Wienholds, E., Schulte-Merker, S., Walderich, B. and Plasterk, R. H. (2002). Target-selected inactivation of the zebrafish rag1 gene. Science 297, 99-102.

Yamashita, A., Takada, T., Narita, J., Yamamoto, G. and Torii, R. (2005). Osteoblastic differentiation of monkey embryonic stem cells in vitro. Cloning Stem Cells 7, 232-7.

Yashiro, K., Zhao, X., Uehara, M., Yamashita, K., Nishijima, M., Nishino, J., Saijoh, Y., Sakai, Y. and Hamada, H. (2004). Regulation of retinoic acid distribution is required for proximodistal patterning and outgrowth of the developing mouse limb. Dev Cell 6, 411-22.

Zhao, Q., Dobbs-McAuliffe, B. and Linney, E. (2005). Expression of cyp26b1 during zebrafish early development. Gene Expr Patterns 5, 363-9.

SUPPLEMENTARY FIGURES

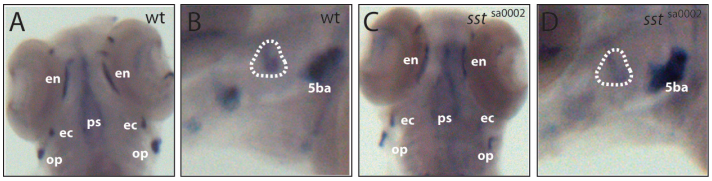

Figure S3: ***osterix* expression in siblings versus mutants.** Expression of *osterix* is not changed in 4 dpf siblings (A,B) versus mutants (C,D). Opercle is encircled in B,D. 5ba = 5th branchial arch, ec = ectopterygoid, en = entopterygoid, op = opercle, ps = parasphenoid.

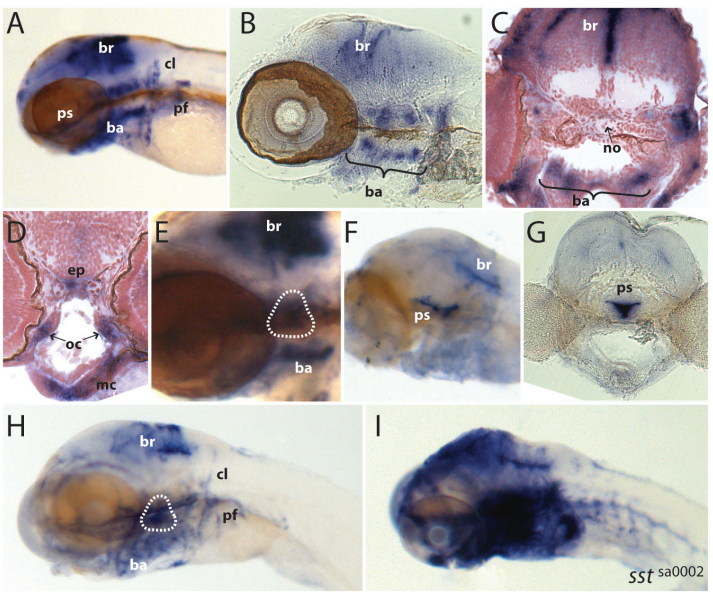

Figure S4: ***cyp26b1* expression in zebrafish.** (A-E) *cyp26b1* expression in zebrafish at 3 dpf. (F-I) *cyp26b1* expression in zebrafish at 6 dpf. For sectioned material, in situ hybridization was performed on whole-mount embryos, and subsequently sections were cut using a vibratome (100 µm; B,G) or a microtome (10 µm; C,D). Expression of *cyp26b1* is seen in the hindbrain, branchial arches, pectoral fins and ossified structures such as the opercle (encircled in E and H) and the parasphenoid (F,G). ba = branchial arches, br = brain, cl = cleithrum, ep = ethmoid plate, mc = meckel's cartilage, no = notochord, oc = orbital cartilage, pf = pectoral fin, ps = parasphenoid. (F,G) Embryos that were only shortly stained show extensive staining in the parasphenoid. (H,I) Sibling (H) and *sst*^{sa0002} mutant (I) embryos showing massive upregulation of *cyp26b1* expression in mutants. Identically treated sibling embryos are depicted. Genotypes were determined by sequence analysis. Other than the embryo in I, all embryos are wild type.

CHAPTER 5

Expression in vertebral centra preceding mineralization suggests a role for *cyp26b1* in the formation of the teleost chordacentrum

Kirsten M. Spoorendonk
Stefan Schulte-Merker

SUMMARY

The teleost vertebra consists of two types of centra: a chordacentrum and an autocentrum. The initial mineralized matrix of the chordacentrum is deposited before common markers for osteoblasts such as *osterix* or *osteocalcin* can be detected in the axial skeleton. An apparently different group of *osterix*-positive sclerotomal osteoblasts are responsible for the formation of the arches and eventually also cover the vertebral bodies forming autocentra. Until now no markers have been described for the cells that form the chordacentrum, which previously have been suggested to be synonymous with the notochord cells. Here, we show that *cyp26b1* is expressed in a segmented pattern in the axial skeleton. Expression overlaps with the future vertebral centra and precedes mineralization. Therefore, we suggest that *cyp26b1* might play a role in the formation of the teleost chordacentrum.

INTRODUCTION

The backbone or vertebral column is the defining feature of vertebrates. It has a clear metameric appearance with vertebrae as the functional segmental units. A vertebra consists of a vertebral body, or centrum, that develops around the embryonic notochord with neural arches extending dorsally and haemal arches extending ventrally. In between the consecutive vertebrae intervertebral discs, soft gel-like cushions, join adjacent vertebral bodies.
Evolutionary studies have shown that four morphologically different types of vertebral bodies have evolved, based on the origin of the cells producing mineralized matrix. In general, in primitive species, all types are present and eventually form one compact vertebral body, whereas in more advanced species, some types are reduced. In birds and mammals, it is well known that the centra of the vertebrae originate from the somite-derived sclerotome and form via endochondral ossification, the type of bone formation responsible for their complete vertebral column. This type of centrum is called a holocentrum (Arratia et al., 2001).

In teleosts two types of centra are present: chordacentra and autocentra (Arratia et al., 2001; Grotmol et al., 2003). Mineralization of the chordacentra starts in the notochordal sheath, a thin layer of extracellular matrix surrounding the notochord believed to resist the internal pressure building up during vacuolization of the notochord (Cerda et al., 2002). Studies in salmon showed that initially, notochordal segments are formed within the layer of notochordal cells (chordoblasts) by metameric changes in the axial orientation of groups of chordoblasts. Formation of the chordoblast segments closely precedes formation of the chordacentra, which form as calcified rings within the adjacent notochordal sheat (Grotmol et al., 2003). Eventually, sclerotomal osteoblasts then differentiate on the surface of these chordacentra, using them as foundations to form autocentra for further vertebral growth (Grotmol et al., 2003).
Thus, the notochord plays a central role in the formation of the centrum of teleost vertebrae. Also in zebrafish, it is proposed that the notochord cells (chordoblasts) themselves are responsible for the secretion of the initial bone matrix of the chordacentra. Isolated notochords secrete bone matrix *in vitro* and ablation of notochord cells prevents centrum formation (Fleming et al., 2004).

Osteoblasts in the developing skull bones of the zebrafish can be labeled with the zns5 antibody, while zns5 labeling could not be detected in the developing centra around the embryonic notochord (Fleming et al., 2004), indicating that there might be at least two different types of osteogenic cells at that stage.
Additionally, in a medaka transgenic reporter line, *twist:eGFP* positive cells which first appear in the sclerotome, could be traced until they became distributed around the notochord (Inohaya et al., 2007). By using a double transgenic medaka line

(*twist:eGFP* and *osteocalcin:dsRed*), it has been shown that some eGFP-positive cells in the sclerotome were able to differentiate into mature osteoblasts, expressing *osteocalcin:dsRed*. However, the initial *osteocalcin:dsRed* expression in the vertebral column was only observed around the arches and not around the centra. At a later stage, expression was detected at the edges of the centra, and eventually around the whole centra as well (Inohaya et al., 2007).
For another osteoblast marker, *osterix*, the same expression pattern has been described in zebrafish (Spoorendonk et al., 2008) as well as in medaka (Renn and Winkler, 2009): expression in the vertebral column is observed as soon as the first arches appear. Expression subsequentially broadens to the edges of the centra and only finally it can also be observed around the vertebral bodies.
These findings suggest that the arches originate out of sclerotomal osteoblasts while other cells, most likely the notochord cells but in any case cells which are negative for *osterix* and *osteocalcin* expression, initially form the bone matrix of the centra. Grotmol and colleagues (2003) have described the formation of the teleost vertebrae in a dual segmentation model: the segmentation of vertebral bodies arises as a primary pattern within the chordoblast layer of the notochord, while the segmental appearance of neural and haemal arches appears to arise from the sclerotome.

Taken together, it is proposed that there are two different cell types responsible for the formation of the teleost vertebral centra: notochord cells form the initial chordacentra and sclerotomal osteoblasts form the autocentra, which will eventually cover the chordacentra. These latter cells are characterized by the well-known osteoblast markers such as *osterix* and *osteocalcin*. However, for the subset of notochord cells suggested to be responsible for the chordacentrum formation, no reliable marker has been identified until now. Two transgenic reporter lines for genes expressed in the embryonic notochord have been generated, but the expression of *sonic hedgehog* (*shh:GFP*) completely disappeared by 4 dpf, while the expression of *tiggy-winkle hedgehog* (*twwh:GFP*, also known as *indian hedgehog* (*ihh*)) located to the intervertebral discs and not to the centra (Haga et al., 2009).

Previously, we were able to show that *cyp26b1* is expressed in osteoblasts by co-localization studies with *osterix* in the zebrafish head skeleton (this thesis, chapter 4: Spoorendonk et al., 2008). *cyp26b1* is a member of the retinoic acid (RA) catabolizing cytochrome P450 family (MacLean et al., 2001; White et al., 2000). Through controlling RA levels within osteoblasts, *cyp26b1* has been proposed to regulate the activity of osteoblasts especially in the axial skeleton (Laue et al., 2008; Spoorendonk et al., 2008). The *cyp26b1* zebrafish mutant is characterized by over-ossification of the entire vertebral column, resulting in fusion of the vertebral centra. This phenotype can already be observed from 8 dpf onwards, before neural and haemal arches appear (Spoorendonk et al., 2008).

Here, we show that *cyp26b1* is expressed in the future vertebral centra preceding mineralization. Sclerotomal osteoblasts expressing *osterix* are not yet detected during these stages, suggesting a role for *cyp26b1* in the initial ossification of the teleost chordacentrum.

MATERIALS & METHODS

BAC recombineering. YFP was recombined into BAC clone DKEY-53014 (containing 73.5 kb upstream of the *cyp26b1* coding region, and >73.5 kb downstream of *cyp26b1*) (Kimura et al., 2006) directly after the ATG site of *cyp26b1*. The following primers were used:
Cyp26b1_GFP_fw (ttgctcatcactccaaagagatatttgagacaagtccccggacgttcaca ACCATGGTGAGCAAGGGCGAGGAG);
Cyp26b1_Neo_rev (cacgcagccagcgtcgccaacgccgagacaaggtcaaaactctcgaagag TCAGAAGAACTCGTCAAGAAGGCG).

Zebrafish transgenic lines. *osx:mCherry* and *osx:nuGFP* were used as previously described (Renn and Winkler, 2009; Spoorendonk et al., 2008).

***In vivo* skeletal stainings.** Transgenic embryos were incubated in 0.01 % calcein (Sigma) or 0.005 % alizarin red (Sigma) in embryo medium for 10 min, subsequently washed in embryo medium only, and analyzed on a Leica TCS SPE confocal system.

RESULTS

Previously, we have reported that *osterix* expression in the axial skeleton of the zebrafish is restricted to the anterior and posterior edges of the forming vertebrae, as well as to the neural and haemal arches (this thesis, chapter 4: Spoorendonk et al., 2008). Expression of *osterix* could be detected only shortly prior to the formation of neural and haemal arches. Vertebral bodies were always devoid of *osterix* expression at that point in time.

Figure 1A-C shows a lateral view of the trunk of a 7 day old *osx:mCherry* transgenic zebrafish embryo counterstained for mineralized tissue with calcein. While vertebral centra have already formed, visualized by the ring-shape appearance of calcein stained material around the notochord (figure 1A), indeed *osx:mCherry* positive cells can only be detected in bone elements of the craniofacial skeleton but not in the forming vertebral centra (figure 1B: *osx:mCherry* expression is shown in the cleithrum (cl) but not in the vertebral column). The very first detectable expression of *osterix* in the axial skeleton is shown in figure 1E-F. Here, the first neural arches have just started to develop: *osx:mCherry* positive cells surround the first mineralized structures forming the future arches. It is interesting to note that the arches do not grow out of the vertebral centra. Instead, they appear as independent structures and are not yet connected to the vertebral centra (in figure 1D and 1F the distance between arch and centrum is marked with a bracket).

Subsequently, we followed the expression of *osterix* over time. Figure 1G-I shows a lateral view of the trunk of a 19 day old *osx:nuGFP* transgenic zebrafish larva counterstained with alizarin red. In the three most anterior vertebrae depicted, the neural arches have started to form. *osx:nuGFP* positive cells surround them and are also detectable at the anterior and posterior edges of the vertebral centra (arrows mark anterior edges of centra, asterisks mark posterior edges). The anterior edge of the most posterior vertebra shown already exhibit some *osx:nuGFP* positive cells, while the formation of its neural arch has not started yet. Thus, as we previously reported, *osterix* expression precedes the formation of the neural and haemal arches in the development of the zebrafish axial skeleton.

cyp26b1 is expressed in osteoblasts and chondrocytes

In our previous study we furthermore reported that *cyp26b1* is expressed in osteoblasts. In order to compare *osterix* expression with *cyp26b1* expression *in vivo*, we recombined YFP into a BAC clone that contained the genomic sequence of *cyp26b1*. Transient co-localization studies in which we injected this construct into one cell-stage transgenic *osx:mCherry* embryos resulted in bone elements with cells positive for YFP as well as mCherry. Here, we extend these findings and show that *cyp26b1* is expressed in osteoblasts: figure 2A-C shows colocalization of *cyp26b1:YFP* and *osx:mCherry* in the cells of the opercle. Additionaly, *cyp26b1* is

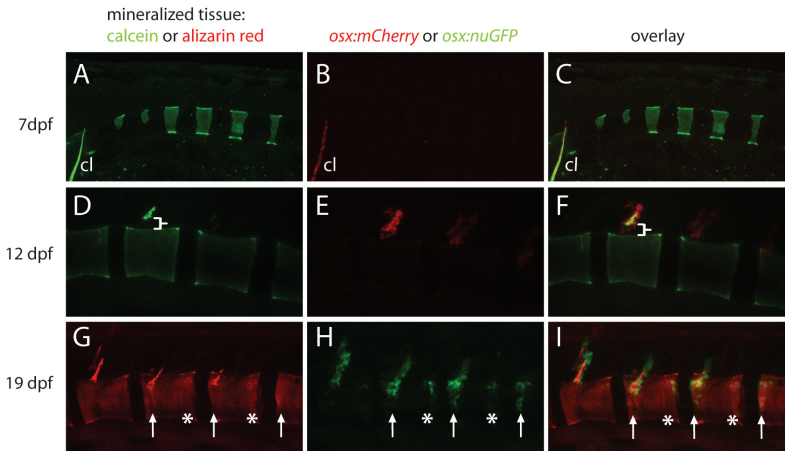

Figure 1: **Expression of *osterix* in the axial skeleton.** (A-F) Lateral view of the trunk of an *osx:mCherry* transgenic embryo counterstained with calcein. At 7 dpf (A-C), *osx:mCherry* is only detected in the craniofacial skeleton (not shown) and the cleithrum (cl) but not in the axial skeleton. At 12 dpf (D-F), the first osterix expression is detected around the forming arches. Note that arches and centra develop independent from each other. The distance between them is marked with a bracket. (G-I) Lateral view of the trunk of a 19 day old *osx:nuGFP* transgenic larva counterstained with alizarin red. *osx:nuGFP* positive osteoblasts are observed around neural arches and at the edges of the vertebral centra. Anterior edges are marked with arrows, posterior edges are marked with asterisks.

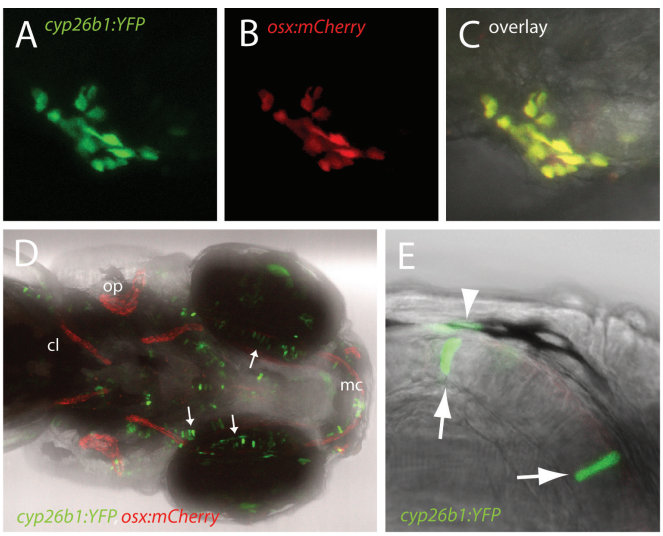

Figure 2: ***cyp26b1* is expressed in osteoblasts and chondrocytes of the craniofacial skeleton.** (A-C) Colocalization of *cyp26b1:YFP* (A) and *osx:mCherry* (B) in osteoblasts of the opercle. In the overlay (C) cells clearly express both *cyp26b1:YFP* and *osx:mCherry*. (D) Ventral view of the head of a 5 day old transgenic *osx:mCherry* embryo injected with *cyp26b1:YFP*. Transient expression is observed in typical columnar cartilage cells (some indicated with arrows). cl = cleithrum, mc = Meckel's cartilage, op = operculum. (E) Higher magnification of Meckel's cartilage (ventral view, anterior is to the top). Arrows point to two cartilage cells expressing *cyp26b1:YFP*. The arrowhead indicates another *cyp26b1:YFP* positive cell, most likely an osteoblast of the bone collar.

not solely expressed in osteoblasts. Expression has also been reported in the hindbrain and the cartilaginous skeleton including the branchial arches and pectoral fins (Zhao et al., 2005): figure 2D shows that chondrocytes express *cyp26b1* as well (arrows in figure 2D point to typical columnar stacked chondrocytes). Since this is still a transient assay we expect patchy expression of *cyp26b1:YFP* because not all the cells will have incorporated the injected construct.
In the example which is depicted in figure 2E, two chondrocytes in Meckel's cartilage clearly express *cyp26b1:YFP* (arrows). Moreover, another cell also shows expression of *cyp26b1:YFP* (arrowhead): this cell is most likely an osteoblast forming the bone collar around the cartilage structure. We conclude that *cyp26b1* is expressed in both osteoblasts as well as chondrocytes of the zebrafish craniofacial skeleton.

Expression of *cyp26b1* in the developing centra precedes mineralization
Next to expression in osteoblasts, chondrocytes, and in the hindbrain, we also detected *cyp26b1:YFP* around the notochord. Figure 3A-C shows a 5 day old *osx:mCherry* transgenic embryo injected with *cyp26b1:YFP*. In this example *cyp26b1:YFP* is clearly detected in a segmented pattern along the axis (figure 3A). However, as described above, the *osx:mCherry* positive cells are at this early point in development not yet detected in the region of the future vertebral column (figure 3B). In order to examine whether the expression overlaps with the future vertebrae or with the intervertebral discs we followed the injected embryos over time. Figure 3D-F shows that the observed segmented pattern of *cyp26b1:YFP* positive cells overlaps with the centra of the vertebrae. The *osx:mCherry* positive cells localize around the neural and haemal arches and to the edges of the centra.
Subsequently, we counterstained *cyp26b1:YFP* injected embryos with alizarin red to study the relation between early *cyp26b1* expression and the mineralization of the centra (figure 4). In zebrafish, centra of the axial skeleton are formed sequentially. The third and fourth centra are the first two to form, followed by the addition of the first two centra anteriorly and the other centra posteriorly of the third and fourth ones (Bird and Mabee, 2003; Du et al., 2001). In figure 4C the centra are numbered. Of note, *cyp26b1:YFP* is observed in all the 8 centra depicted, while only centra 3, 4, and 5 are mineralized yet. These results indicate that expression of *cyp26b1* precedes mineralization of the future vertebral centra and suggest that *cyp26b1* might play a role in the formation of these centra.

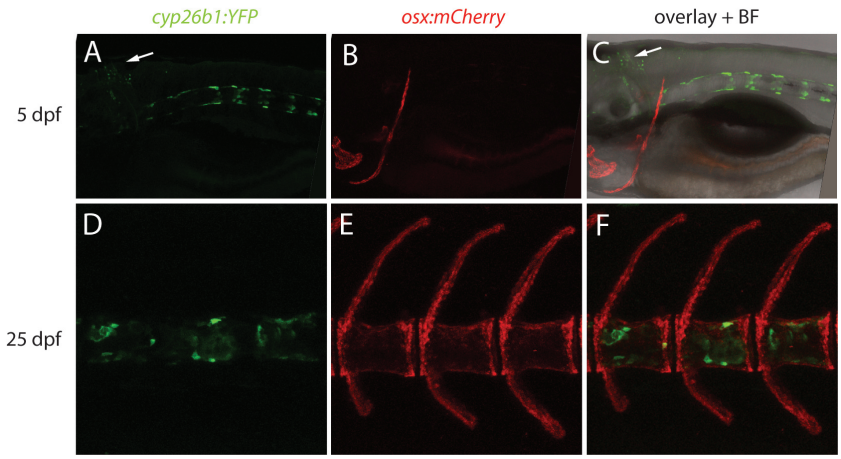

Figure 3: ***cyp26b1* expression overlaps with future positions of the centra.**
Lateral views of the trunk of a 5 day old (A-C) and 25 day old (D-F) transgenic *osx:mCherry* embryo injected with *cyp26b1:YFP*. (A-C) Transient *cyp26b1:YFP* expression is observed in a segmented pattern along the notochord (A) where at this point in time *osterix* is not expressed yet (B). Note that in this example *cyp26b1:YFP* positive cells are also found in the brain (arrow). (D-F) At 25 dpf *cyp26b1:YFP* expression is detected around the vertebral centra. *osx:mCherry* positive cells are detected around the arches and at the edges of the centra. BF = bright field.

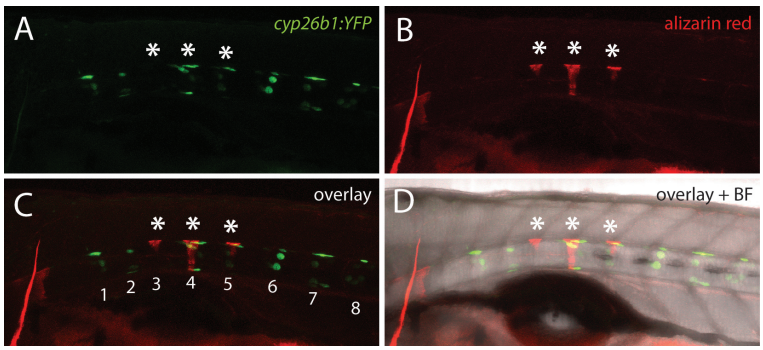

Figure 4: **Expression of *cyp26b1* precedes mineralization of centra.**
Counterstaining of a *cyp26b1:YFP* injected embryo (5 dpf) with alizarin red shows that at this stage only centra 3, 4, and 5 have started to mineralize (marked with asterisks, centra are numbered in C). However, *cyp26b1:YFP* expression is observed in all the 8 centra depicted, indicating that expression of *cyp26b1* precedes mineralization of the future vertebral centra. BF = bright field.

DISCUSSION

In this study, we have shown that *cyp26b1* is expressed in osteoblasts as well as chondrocytes of the zebrafish craniofacial skeleton. Expression of *cyp26b1* is observed at the places where the initial centrum material of the vertebrae is formed. Moreover, *cyp26b1* expression precedes mineralization of these centra.
Additionally, we have shown the experimental data covering the issue we already reported previously: we have never been able to detect *osterix* expression in the axial skeleton before arches appear. In our previous study (this thesis, chapter 4: Spoorendonk et al., 2008) we have suggested the existence of two populations of osteoblasts: *osterix*-positive osteoblasts and *osterix*-negative osteoblasts. The first group are the sclerotomal osteoblasts found in the head skeleton and around the arches of the vertebrae and subsequently also at their edges. The second group is responsible for the production of the initial centrum material.

A role for *cyp26b1* in chordacentrum formation?

The presence of *cyp26b1* expression at the places where centra of vertebrae will be formed before the onset of *osterix* expression suggests a role for *cyp26b1* in the production of the early centrum material, especially since *cyp26b1* expression precedes mineralization of the centra. Moreover, *cyp26b1* mutants are characterized by over-ossification of the axial skeleton resulting in fused vertebrae, an early phenotype that can be picked up before the sclerotomal osteoblasts can be detected (this thesis, chapter 4: Spoorendonk et al., 2008). This suggests that, next to its described expression in *osterix*-positive osteoblasts, *cyp26b1* is also expressed in the *osterix*-negative osteoblasts that form the chordacentra.

Chordacentra develop, at least in salmon, as calcified rings within the notochordal sheath (Arratia et al., 2001; Grotmol et al., 2003). The notochord sheath consists of three layers, which are all acellular (Grotmol et al., 2005). Also in zebrafish, it has been proposed that the notochord cells themselves are responsible for the production of the mineralized matrix, since ablation of notochord cells prevented chordacentrum formation (Fleming et al., 2004).
Osterix-negative osteoblasts responsible for the formation and mineralization of the chordacentra could theoretically be localized either adjacent to the inside or to the outside of the sheath. In case of the first option this would mean that it are indeed the notochord cells themselves, as postulated by Fleming et al. (2004), to initiate centrum formation. Up to now no markers have been described to label this subset of notochord cells. Therefore, electron microscopy studies in which YFP could be labeled with gold particles are probably the best way to get a definitive answer for the localization of *cyp26b1*. Thus, further research is necessary to examine the exact localization of *cyp26b1* and its role in the teleost chordacentrum formation.

The dual segmentation model and *cyp26b1*

According to the dual segmentation model the segmentation of vertebral bodies arises as a primary pattern within the chordoblast layer of the notochord, while the segmental appearance of neural and haemal arches appears to arise from the sclerotome (Grotmol et al., 2003). In the zebrafish *fused somites* mutants (*fss*) for example, sclerotome patterning is abnormal (van Eeden et al., 1996). Subsequently, indeed the patterning of the neural and haemal arches is disorganized, yet the centra develop normal in number and shape.

The *stocksteif* mutant phenotype is characterized by fusion of vertebral centra, suggesting that, according to the dual segmentation model, the patterning of the notochord should be disrupted, simultaneously introducing another argument that *cyp26b1* would indeed be expressed in the notochord cells. On the other hand, sclerotomal patterning in *stocksteif* mutants is normal. However, in older mutants haemal and neural arches are misshaped as well, which contradicts with the dual segmentation model. Interestingly, we have only found *cyp26b1:YFP* expression around the centra of the vertebrae and never around the arches (see figure 3D, F), which makes the misshapen arches in mutants a phenomenon which is difficult to interpret. A possible explanation could be that the misformed arches are actually a secondary effect of the fusion of the vertebral centra.

Chordacentrum formation: a conserved mechanism of bone development?

Also in other species, the notochord plays a central role in the formation of vertebrae. In mice for example, *Shh*, which is secreted by the notochord, has been shown to be the key molecule required for the sclerotomal expression of *Pax1* and *Pax9. Pax1* expression is rapidly lost and none of the skeletal elements of the vertebral column form in *Shh*-deficient mice (Chiang et al., 1996). Vertebrae of mice and chick form via endochondral ossification out of sclerotome derived mesenchymal cells. These cells first differentiate into chondrocytes to form a cartilage template, which is later on replaced by bone.

In mice, *Osterix* expression in the condensed mesenchymes of the developing vertebrae is detected from E14.5 onwards (Nakashima et al., 2002), indicating that sclerotomal osteoblasts are involved in the ossification of their vertebral centra. *Osterix* null mice lack almost all craniofacial bone elements. However, it is interesting to note that they are born with mineralized centra (Nakashima et al., 2002). This raises the question whether mice share a mechanism of bone formation, comparable to the teleost chordacentrum, which is formed independently of sclerotomal osteoblasts marked with *Osterix*.

Additionally, some genes characteristic of cartilage are also expressed in the notochord. In zebrafish, collagen type II, marking early chondrocytes (Karsenty and Wagner, 2002), has been described to be expressed in the notochord (Yan et al., 1995). Moreover, in our own unpublished studies we have observed expression of

collagen type X, marking hypertrophic chondrocytes (Karsenty and Wagner, 2002) and at least in zebrafish also osteoblasts (Avaron et al., 2006), in a segmented pattern in the notochord. The expression patterns of both collagens are conserved: it has been reported that the expression of type II as well as type X collagen appears in a segmented pattern in the chick notochord (Linsenmayer et al., 1986).
It has even been hypothesized that there might be a direct relationship between the notochord and cartilage in which the notochord is likely to represent a primitive form of cartilage (Stemple, 2005). This could explain why the notochord in teleosts has a more direct role in the formation of vertebrae. In mammalian and avian species cartilage could have taken over the function of the notochord: future research has to elucidate whether or not their notochord still has a function in the formation of vertebral centra.

REFERENCES

Arratia, G., Schultze, H. P. and Casciotta, J. (2001). Vertebral column and associated elements in dipnoans and comparison with other fishes: development and homology. J Morphol 250, 101-72.

Avaron, F., Hoffman, L., Guay, D. and Akimenko, M. A. (2006). Characterization of two new zebrafish members of the hedgehog family: atypical expression of a zebrafish indian hedgehog gene in skeletal elements of both endochondral and dermal origins. Dev Dyn 235, 478-89.

Bird, N. C. and Mabee, P. M. (2003). Developmental morphology of the axial skeleton of the zebrafish, Danio rerio (Ostariophysi: Cyprinidae). Dev Dyn 228, 337-57.

Cerda, J., Grund, C., Franke, W. W. and Brand, M. (2002). Molecular characterization of Calymmin, a novel notochord sheath-associated extracellular matrix protein in the zebrafish embryo. Dev Dyn 224, 200-9.

Chiang, C., Litingtung, Y., Lee, E., Young, K. E., Corden, J. L., Westphal, H. and Beachy, P. A. (1996). Cyclopia and defective axial patterning in mice lacking Sonic hedgehog gene function. Nature 383, 407-13.

Du, S. J., Frenkel, V., Kindschi, G. and Zohar, Y. (2001). Visualizing normal and defective bone development in zebrafish embryos using the fluorescent chromophore calcein. Dev Biol 238, 239-46.

Fleming, A., Keynes, R. and Tannahill, D. (2004). A central role for the notochord in vertebral patterning. Development 131, 873-80.

Grotmol, S., Kryvi, H., Nordvik, K. and Totland, G. K. (2003). Notochord segmentation may lay down the pathway for the development of the vertebral bodies in the Atlantic salmon. Anat Embryol (Berl) 207, 263-72.

Grotmol, S., Nordvik, K., Kryvi, H. and Totland, G. K. (2005). A segmental pattern of alkaline phosphatase activity within the notochord coincides with the initial formation of the vertebral bodies. J Anat 206, 427-36.

Haga, Y., Dominique, V. J., 3rd and Du, S. J. (2009). Analyzing notochord segmentation and intervertebral disc formation using the twhh:gfp transgenic zebrafish model. Transgenic Res.

Inohaya, K., Takano, Y. and Kudo, A. (2007). The teleost intervertebral region acts as a growth center of the centrum: in vivo visualization of osteoblasts and their progenitors in transgenic fish. Dev Dyn 236, 3031-46.

Karsenty, G. and Wagner, E. F. (2002). Reaching a genetic and molecular understanding of skeletal development. Dev Cell 2, 389-406.

Kimura, Y., Okamura, Y. and Higashijima, S. (2006). alx, a zebrafish homolog of Chx10, marks ipsilateral descending excitatory interneurons that participate in the regulation of spinal locomotor circuits. J Neurosci 26, 5684-97.

Laue, K., Janicke, M., Plaster, N., Sonntag, C. and Hammerschmidt, M. (2008). Restriction of retinoic acid activity by Cyp26b1 is required for proper timing and patterning of osteogenesis during zebrafish development. Development 135, 3775-87.

Linsenmayer, T. F., Gibney, E. and Schmid, T. M. (1986). Segmental appearance of type X collagen in the developing avian notochord. Dev Biol 113, 467-73.

MacLean, G., Abu-Abed, S., Dolle, P., Tahayato, A., Chambon, P. and Petkovich, M. (2001). Cloning of a novel retinoic-acid metabolizing cytochrome P450, Cyp26B1, and comparative expression analysis with Cyp26A1 during early murine development. Mech Dev 107, 195-201.

Nakashima, K., Zhou, X., Kunkel, G., Zhang, Z., Deng, J. M., Behringer, R. R. and de Crombrugghe, B. (2002). The novel zinc finger-containing transcription factor osterix is required for osteoblast differentiation and bone formation. Cell 108, 17-29.

Renn, J. and Winkler, C. (2009). Osterix-mCherry transgenic medaka for in vivo imaging of bone formation. Dev Dyn 238, 241-8.

Spoorendonk, K. M., Peterson-Maduro, J., Renn, J., Trowe, T., Kranenbarg, S., Winkler, C. and Schulte-Merker, S. (2008). Retinoic acid and Cyp26b1 are critical regulators of osteogenesis in the axial skeleton. Development 135, 3765-74.

Stemple, D. L. (2005). Structure and function of the notochord: an essential organ for chordate development. Development 132, 2503-12.

van Eeden, F. J., Granato, M., Schach, U., Brand, M., Furutani-Seiki, M., Haffter, P., Hammerschmidt, M., Heisenberg, C. P., Jiang, Y. J., Kane, D. A. et al. (1996). Mutations affecting somite formation and patterning in the zebrafish, Danio rerio. Development 123, 153-64.

White, J. A., Ramshaw, H., Taimi, M., Stangle, W., Zhang, A., Everingham, S., Creighton, S., Tam, S. P., Jones, G. and Petkovich, M. (2000). Identification of the human cytochrome P450, P450RAI-2, which is predominantly expressed in the adult cerebellum and is responsible for all-trans-retinoic acid metabolism. Proc Natl Acad Sci U S A 97, 6403-8.

Yan, Y. L., Hatta, K., Riggleman, B. and Postlethwait, J. H. (1995). Expression of a type II collagen gene in the zebrafish embryonic axis. Dev Dyn 203, 363-76.

Zhao, Q., Dobbs-McAuliffe, B. and Linney, E. (2005). Expression of cyp26b1 during zebrafish early development. Gene Expr Patterns 5, 363-9.

CHAPTER 6

Over-ossification and pathological mineralization *in vivo*: the *dragonfish* mutant phenotype

Kirsten M. Spoorendonk
Stefan Schulte-Merker

SUMMARY

Osteoarthritis, atherosclerosis, Alzheimer's disease, and Parkinson's disease are examples of chronic disorders in which pathological mineralization can occur. Little is known about the molecular biology behind these uncommon bone formation processes. In a forward genetic screen in zebrafish we identified two non-complementing alleles of the *dragonfish* mutant phenotype. Mutants are characterized by over-ossification of the axial skeleton resulting in fused vertebrae. Additionally, they exhibit pathological mineralization in the head and neural tube. Here, we describe the analysis of the *dragonfish* mutant including *in vivo* observations in osteoblast-specific transgenic zebrafish lines. Despite the phenotypic similarities with the *stocksteif* mutant, *dragonfish* does not appear to function in the retinoic acid pathway.

INTRODUCTION

Under normal conditions, bone tissue is the only tissue in which the extracellular matrix, laid down by osteoblasts, will be mineralized. However, under certain pathological conditions some soft tissues like articular cartilage and (cardio)vascular tissues are prone to mineralization (Giachelli, 1999). Patients with osteoarthritis suffer from articular cartilage mineralization, leading to cartilage destruction. The prevalence of osteoarthritis is high: prevalences ranging from 5 to 20% in a certain population have been reported, depending on differences in lifestyle and age (Das and Farooqi, 2008). Similarly, vascular calcification most often occurs at older age. The most common one is atherosclerosis, a vascular disease characterized by the accumulation of lipid material in the arterial wall: over time, more than 90% of these fatty plaques undergo calcification (Danilevicius et al., 2007).
A relatively rare inherited disease is fibrodysplasia ossificans progressiva (FOP), a syndrome causing severe disability and life-threatening complications. FOP is characterized by skeletal abnormalities and by the progressive development of bone-forming lesions in tendons and muscles (Job-Deslandre, 2004) and has recently been linked to dysregulation of the BMP4 signaling pathway (Kaplan et al., 2006).
Pathological calcifications in the brain have been described in patients suffering from neurodegenerative diseases such as Alzheimer's and Parkinson's disease (Ramonet et al., 2006), but are also symptoms of the congenital sporadic Sturge-Weber disease (Di Trapani et al., 1982).

Unfortunately, for many bone diseases the underlying genetic cause remains unknown and only a few effective treatments for chronic skeletal diseases and other diseases where pathological mineralizations are common are available. Therefore, it is necessary to gain more insight in the molecular mechanisms underlying bone development and diseases.
In order to identify new genes essential in bone formation and bone homeostasis we performed a forward genetic screen in zebrafish (described in chapter 3 of this thesis). Here, we analyze one of the mutants we identified in this screen: *dragonfish* mutants are characterized by over-ossification of the axial skeleton resulting in fusion of the future vertebrae, and, additionally, exhibit ectopic pathological mineralizations in the head and neural tube.
Since transgenic zebrafish lines for osteoblast markers are available and bone stainings can be performed on live embryos, the *dragonfish* mutant phenotype serves possibly as an instructive model to study pathological mineralizatons *in vivo*.

MATERIALS & METHODS

Skeletal stainings. Embryos were fixed at 8 dpf and subsequently stained simultaneously for bone and cartilage as described before (this thesis, chapter 4: Spoorendonk et al., 2008). For exclusive alizarin red stainings the alcian blue step was omitted. Embryos were analyzed and photographed with a Leica 480C camera on a Zeiss Axioplan microscope.When sections were required, embryos were first stained, subsequently embedded in 3% agarose and cut (200 µm sections) on a vibratome (Microm HM650V). Sections were counterstained with DAPI (1:2000, 1 mg/ml stock) and analyzed on a Leica TCS SPE confocal system.
Bone stainings *in vivo* (analysis of transgenic embryos) were carried out with 0.005 % alizarin red (Sigma) in embryo medium for 10 min. Subsequently, embryos were analyzed on a Leica TCS SPE confocal system.

Meiotic mapping. Positional cloning of the *dragonfish* mutation was carried out as previously described (Geisler, 2002). Briefly, linkage was determined using a genome wide single nucleotide polymorphism (SNP) panel. This panel with 384 markers was tested on genomic DNA of 48 pooled mutants and 48 pooled siblings. 8 SNPs in linkage group 20 showed linkage, from which D6 (CASCAD 057597) and H6 (CASCAD 039178) were confirmed at a single embryo level as two markers localized at the same side of the mutation. Primer sequences for additional SNPs used for fine mapping are as follows:
1.16-FW: CTCCCGATCTGAAAACATCA
1.16-RV: AACTGTATGTGTGCGCGTATG
2.12- FW: TGGTTGCTCAAGTGAACGAG
2.12-RV: CATTGTCACCCACACGATTC
5.10-FW: TCAAGCCTATTCACTCAAACC
5.10-RV: TGCAATTGACCTCCATAAAC
6.1-FW: ACGGGGAGTTGAGGAACTTT
6.1-RV: AGGTGACGTTGGGCATGT
7.12-FW: AGCTTAAGGCCCGATACC
7.12-RV: GCATGTTGCAGAAATAGGAG

Zebrafish transgenic lines. *osx:nuGFP* and *osc:GFP* were used as previously described (Inohaya et al., 2007; Renn and Winkler, 2009; Spoorendonk et al., 2008).

In situ hybridizations. In situ hybridizations were performed as previously described (Schulte-Merker, 2002).

DEAB treatments. A stock solution of 10 mM 4-(diethylamino)benzaldehyde (DEAB, Sigma) in DMSO was diluted in embryo medium to a final concentration of 10 or 50 µM. Sibling controls were incubated in corresponding dilutions of DMSO only. Embryos were treated from 4 dpf onwards and fixed and stained with alizarin red at 8 dpf.

RESULTS

In a forward genetic screen to identify novel genes playing a role in bone development in the zebrafish, we isolated two mutants which exhibit an identical over-ossification phenotype. Both alleles, *dragonfish* (*dgf*) 1.027 and 1.093 failed to complement each other, and are therefore considered to be allelic.
While siblings show an equidistant distribution of vertebrae along the notochord (figure 1A), mutant embryos are characterized by an early onset over-ossification of the notochord, resulting in fused vertebral centra (figure 1B-B'). Additionally, ectopic mineralizations are observed at several places in *dragonfish* mutants. Figure 1B" shows ectopic alizarin red staining immediately dorsal to the notochord. In the head region, pathological mineralizations are observed in the brain area (arrowheads in figure 1B) and in the surroundings of the cleithrum (arrowhead in figure 1D). In wild type siblings, the cleithrum is a long smooth bone element (asterisk in figure 1C), whereas most *dragonfish* mutants exhibit an expansion filled with extra mineralized tissue located approximately in the middle of the structure and always protruding to the posterior site of the embryo (arrow in figure 1D). On the other hand, the cartilaginous skeleton is never affected in mutants.

Variabilities in the *dragonfish* mutant phenotype

Mutant embryos are comparable in size to their wild type siblings. Concerning their external features, most mutants exhibit a slight lateral bending in the posterior end of the tail and do not develop a swim bladder. However, both the external phenotype as well as the bone phenotype are largely variable. Therefore, mutants can only reliably be detected by skeletal staining at 8 dpf or later. Figure 1E shows three *dgf* mutants varying from a severe to mild over-ossification of the notochord (arrows indicated the area of over-ossification in the lower two mutants). The two milder versions of the phenotype indicate that the patterning of the vertebrae is not necessarily disturbed since the anterior ones are placed properly. In order to confirm that the phenotype is not due to an early patterning defect, we performed in situ hybridization for the somitic marker *myoD*, which did not show any alterations between mutants and siblings (data not shown).

The variability of the phenotype also includes the overall ossification of the head skeleton. Whereas some mutants are comparable to wild type siblings, other mutants show premature mineralization of several jaw elements and branchial arches at 8 dpf, while in wildtype siblings, mineralization of these elements occurs only around day 10 to 12. Figure 1F shows a sibling, a comparable mutant, and a mutant where ossification of the head skeleton occurred prematurely (arrows point to the mineralized jaw and first branchial arch), respectively. In figure 1G a magnification of the marked area in 1F is depicted, showing spotted mineralization of the proximal part of the ceratohyal.

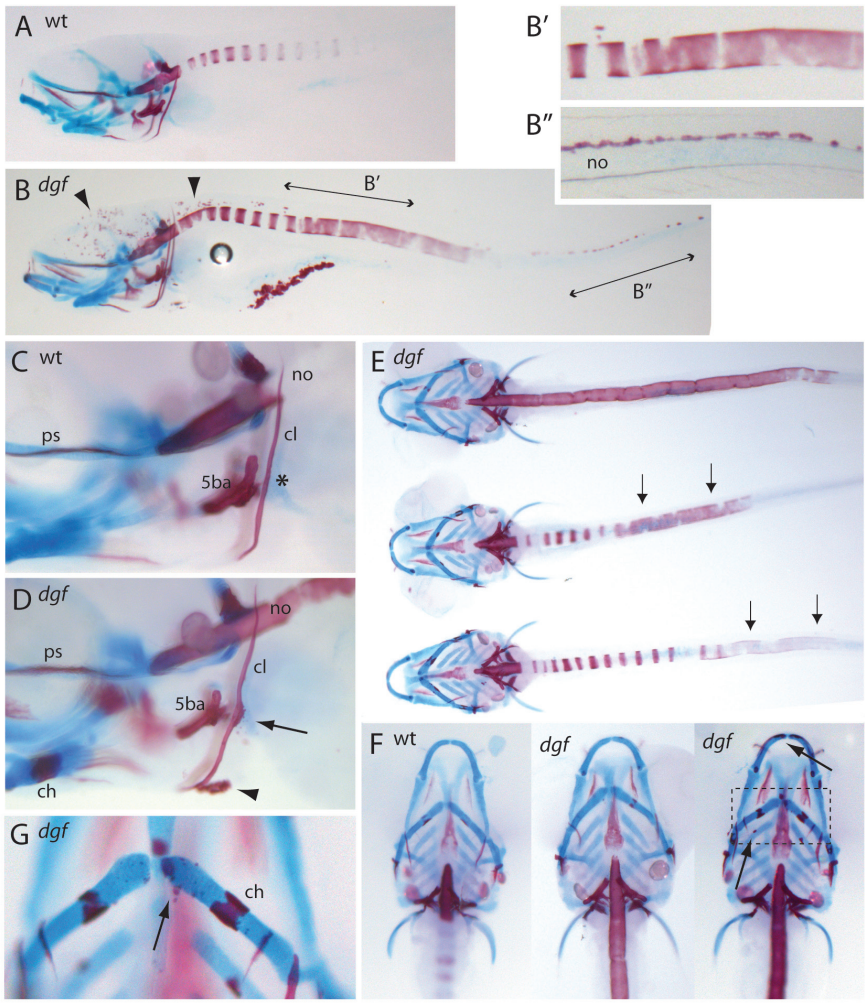

Figure 1: ***dragonfish* mutants exhibit axial over-ossification and ectopic mineralization.** (A-D) Lateral views of wild type siblings (A, C) and *dragonfish* mutant embryos (B, D). Mutants show over-ossification of the notochord resulting in fused vertebral centra (B') and exhibit ectopic mineralizations dorsal to the notochord (B"), in the brain area (arrowheads in B), and in immediate proximity to the cleithra (arrowhead in D). Note that the wild type cleithrum is smooth (asterisk in C) while the mutant cleithrum exhibits a nodule-like expansion (arrow in D). (E) Ventral views of three *dragonfish* mutants are shown, their over-ossification phenotype of the notochord varying from severe (top embryo) to mild (bottom embryo). Arrows indicate the area of over-ossification in the milder phenotypes. (F) Ventral views of the head skeleton of a sibling, a mutant with a comparable phenotype (middle), and a mutant where there is significant premature ossification; arrows are pointing to the mineralized jaw and first branchial arch. Note that the cartilaginous skeleton is not affected in mutants. (G) Magnification of the marked area in F is depicted, showing spotted mineralization of the proximal part of the ceratohyal (arrow). All embryos shown are stained for both bone (alizarin red) and cartilage (alcian blue) at 8 dpf. 5ba = fifth branchial arch, ch = ceratohyal, cl = cleithrum, no = notochord, ps = parasphenoid.

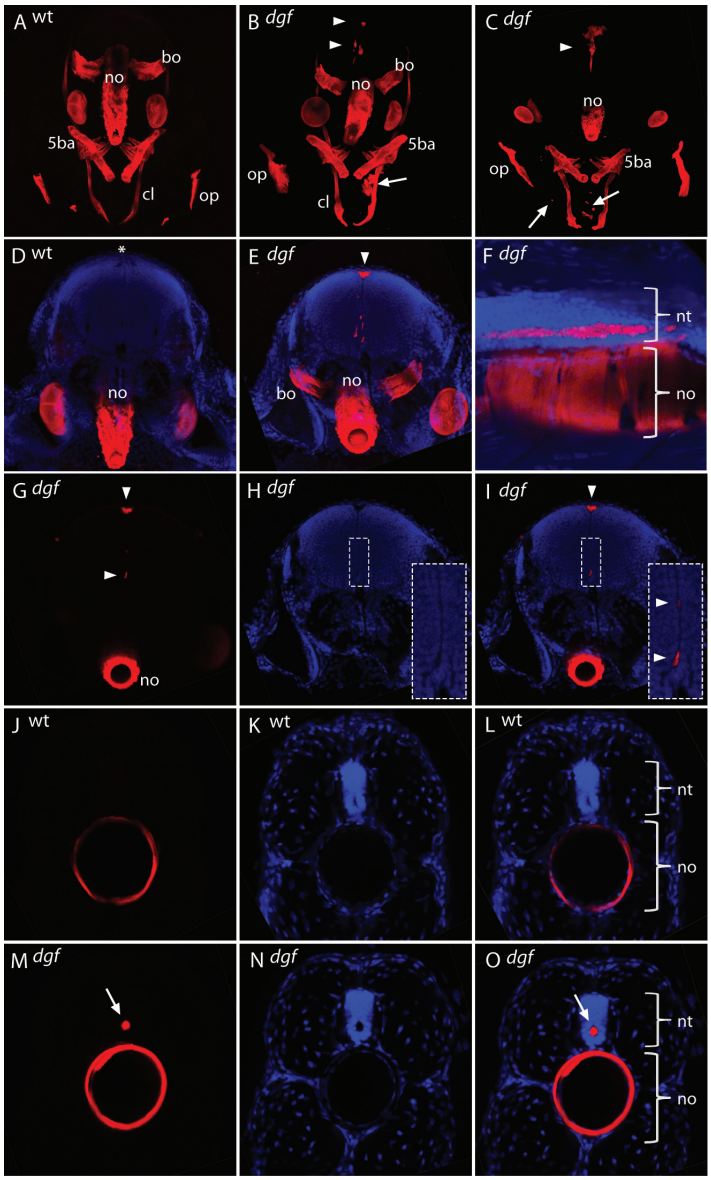

Figure 2: **Ectopic mineralization in the head and neural tube of *dragonfish* mutants.** Vibratome sections of wild type siblings (A, D, J-L) and *dragonfish* mutants (B, C, E-I, M-O) stained for bone (alizarin red) and counterstained with DAPI (blue) at 8 dpf. Transverse sections of the head show ectopic mineralization in the brain (arrowheads in B, C, E, G, and I) located in the extracellular space in between the two brain halves, and at random places close to the cleithra (arrows in B and C) in mutants. (F) Sagital section of a *dragonfish* mutant trunk showing ectopic mineralization in the neural tube. (J-O) Transverse sections of the trunk show a central canal in siblings (J-L), which is filled with mineralized material (arrow) in mutants (M-O). A-F are confocal projections, G-O are single confocal scans. 5ba = fifth branchial arch, bo = basioccipital, cl = cleithrum, no = notochord, nt = neural tube, op = opercle.

Ectopic mineralization in the head and neural tube

In order to examine where the ectopic mineralizations in dragonfish mutants are precisely localized, we made vibratome sections of alizarin red stained embryos and counterstained the sections with DAPI before analyzing them by confocal microscopy. Confocal projections of transverse sections of the head showed ectopic mineralization in the brain area and in the area surrounding the two cleithra (figure 2A-C, arrowheads point to the brain area, arrows indicate mineralization spots around cleithra). In the latter region the mineralizations were randomly distributed, varied between mutants and were not restricted to a particular place (compare figure 2B with 2C). In the brain, the pathological mineralizations were located in between the two brain halves (figure 2D-E). Single confocal scans confirmed that mineralizations were only observed in the extracellular space and never inside cells (figure 2G-I).

A projection of saggital confocal scans of the trunk showed that the ectopic mineralizations dorsally to the notochord are located inside the neural tube (figure 2F). Single scans indicate that, where siblings exhibit a central canal in the neural tube (figure 2J-L), this canal is completely filled with mineralized tissue in *dragonfish* mutants (figure 2M-O).

The juvenile *dragonfish* phenotype

In a few cases, mutants survived until juvenile stages when separated early enough from their siblings. These mutants remain smaller with a maximum length of approximately half the size of a wild type sibling and have problems swimming. All centra of the vertebral column of a three weeks old mutant appear fused to each other. At several spots the chain of fused vertebrae is interrupted by what may be a fracture or an incomplete ossification of the intervertebral space (arrows in figure 3D). Neural arches in mutants start to form but are much broader then in wild type siblings and are triangular shaped. Some juvenile *dragonfish* mutants exhibit ectopic mineralization in the brain area (figure 3E), similar to the ones observed in mutant embryos.

At five weeks of age, the axial phenotype has increased in severity: neural and haemal arches have grown out irregularly, are still much broader, and most of them fuse with the adjacent arch anterior or posterior (arrows in figure 3J indicate some examples of fusion events). Furthermore, the head skeleton shows abnormalities as well. One striking example is a spotted mineralization pattern in the lower jaw (figure 3K, compare with 3H).

Positional cloning of the *dragonfish* mutation

To identify the affected gene in the *dragonfish* mutant, genetic mapping was performed with single nucleotide polymorphism markers (SNPs) (figure 4). Two SNPs on linkage group 20, H6 (CASCAD 039178; Ensembl Zv8, release 54: 28.8 Mb) and D6 (CASCAD 057597; 20.1 Mb), were determined on a single embryo level to be linked to the phenotype. Both markers are localized south of the mutation.

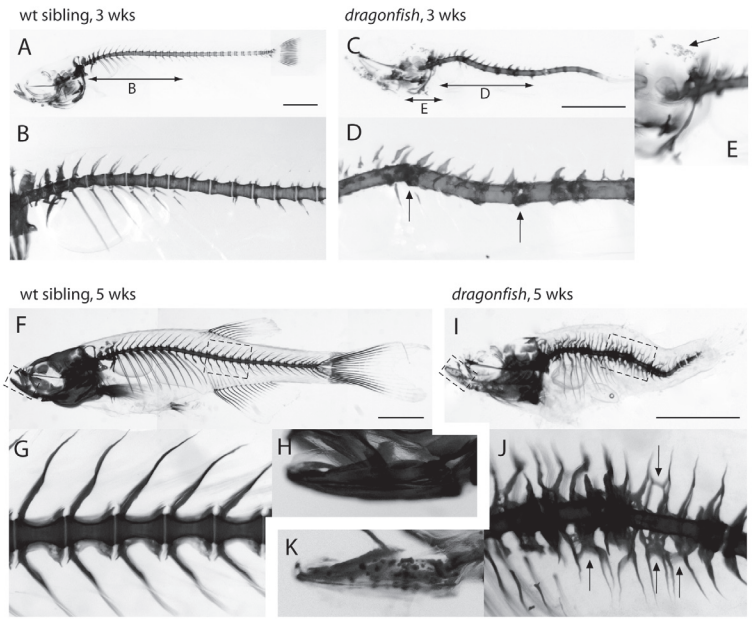

Figure 3: **The juvenile *dragonfish* phenotype.** (A-E) 3 week old wild type sibling (A, B) and *dragonfish* mutant (C-E) stained with alizarin red. Mutants remain smaller and all their vertebral centra appear fused to each other. Arrows in D indicate presumed fractures of the fused mutant vertebral column. Arrow in E points to ectopic mineralization in the brain. Scale bars in A and C: 1 mm. (F-K) 5 week old wild type sibling (F-H) and *dragonfish* mutant (I-K) stained with alizarin red. While wild type vertebrae show the normal organization (G), mutant vertebrae are fused and arches grow out irregularly resulting in fusions with adjacent arches (J, arrows indicate examples of fusion events between arches). (K) Spotted mineralization pattern in the lower jaw of a dragonfish mutant; compare with smooth and solid ossification in wild type sibling (H). Scale bars in F and I: 2 mm.

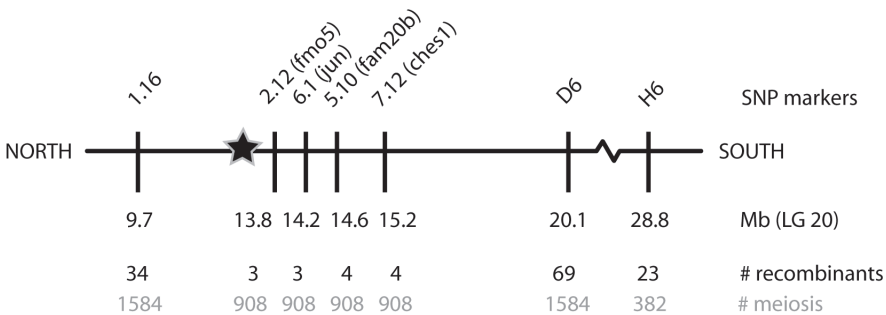

Figure 4: **Schematic overview of the area of linkage group 20 to which the *dragonfish* mutation was mapped.** SNP markers are depicted and the number of recombinants found is shown, together with the number of meioses tested. SNP 2.12 in the *fmo5* gene was found closest to the mutation. The star indicates the estimated position of the mutation.

SNP 1.16 (9.7 Mb) was subsequently found as a linked marker north of the mutation. Additional SNPs in the genes fmo5 (SNP 2.12), jun (SNP 6.1), fam20b (SNP 5.10), and ches1 (SNP 7.12) were found to be in close proximity of the *dragonfish* mutation (3, 3, 4, and 4 recombinants in 908 meiosis, respectively).

Unchanged expression of bone-specific markers in the *dragonfish* mutant

Remarkably, and despite the very obvious skeletal problems in *dragonfish* mutants, in situ hybridizations for bone-specific markers such as type X collagen (*col10a1*), shown to be expressed in intramembranous bone in zebrafish (Avaron et al., 2006), did not show any alterations between siblings and mutants in the head skeleton (figure 5). Moreover, *dgf* mutants in an Tg(*osterix:nuGFP)* transgenic background, specifically marking the osteoblast lineage (Nakashima et al., 2002), did also not show any differences in expression compared to siblings. In the wild type situation, axial *osterix* expression appears only after the onset of arch development (figure 6A)(see also this thesis, chapter 5, figure 1). And whereas in *dragonfish* mutants fusion of vertebral centra and ectopic mineralization in the neural tube is observed, *osx:nuGFP* expression is still absent in their trunk (figure 6B). Similar results were obtained with mutants in an *osteocalcin* transgenic background, Tg(*osc*:*GFP*), marking mature osteoblasts: again, no alterations between the expression in siblings (figure 6C) versus mutants (figure 6D) could be detected.

Interestingly, while in the wild type situation osteoblasts always surround the mineralized matrix of bone elements, the expansion of the mutant cleithrum is not enclosed by osteoblasts (inset in figure 6D: arrow).

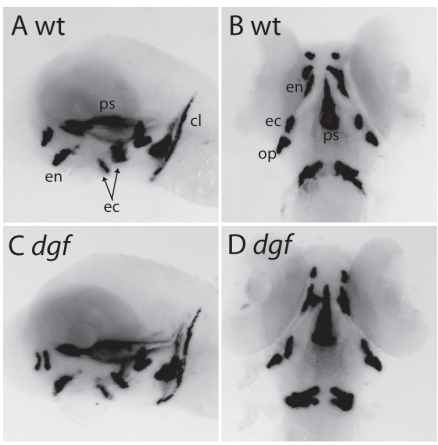

Figure 5: ***collagen type X* expression in *dragonfish* mutants.** mRNA expression of *col10a1* is unaltered in 4 dpf wild type siblings (A, B) versus mutants (C, D). cl = cleithrum, ec = ectopterygoid, en = entopterygoid, op = opercle, ps = parasphenoid.

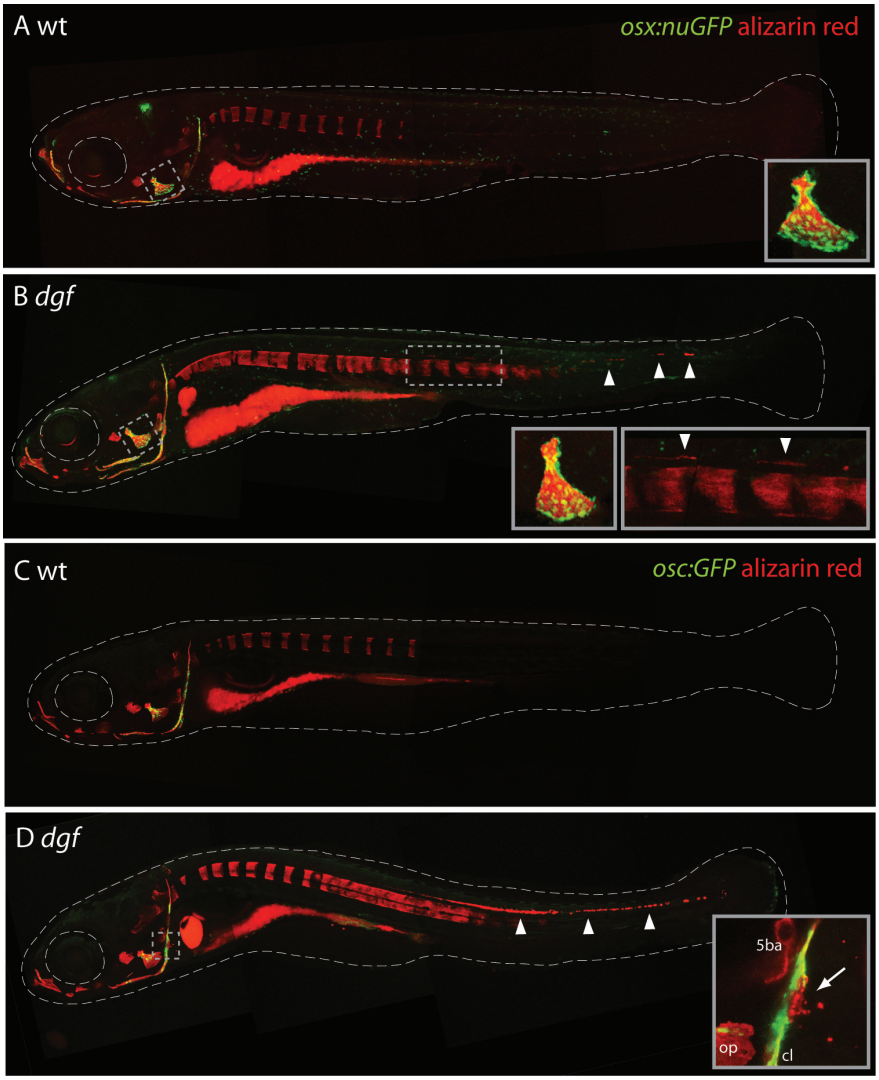

Figure 6: **Visualization of osteoblast-specific markers in *dragonfish* mutants.**
(A, B) *osx:nuGFP* expression is not altered in 8 dpf wild type siblings (A) versus mutants (B). Insets show magnifications of the operculum and the mutant trunk. (C, D) *osc:GFP* expression is not changed in 8 dpf wild siblings (C) versus mutants (D). Note that the expansion of the mutant cleithrum is not surrounded by *osc:GFP* positive cells (inset in D: arrow). Arrowheads point to sites of ectopic mineralization in all panels. 5ba = fifth branchial arc, cl = cleithrum, op = opercle.

DEAB treatment rescues *stocksteif* mutants but not *dragonfish* mutants

The *dragonfish* over-ossification phenotype of the vertebrae resulting in their fusion is very similar to the axial over-ossification phenotype reported for the *stocksteif* mutant (this thesis, chapter 4: Spoorendonk et al., 2008). Therefore, we hypothesized that *stocksteif* and *dragonfish* might function in the same pathway. *stocksteif* encodes *cyp26b1*, a cytochrome P450 member that catabolizes retinoic acid (RA). Here, we show that *stocksteif* mutants can be rescued with 4-(diethylamino)benzaldehyde (DEAB), an inhibitor of RA synthesis.

An incross of two *stocksteif* heterozygous carriers was split into three groups with an equal amount of embryos. The groups were treated from 4 dpf onwards with 10 µM DEAB, 50 µM DEAB, or DMSO as a control, respectively. At 8 dpf embryos were fixed and stained with alizarin red and subsequently divided into 'sibling' and 'mutant' phenotypes. Only after phenotyping, all embryos were genotyped.

Figure 7A shows that, for the control group treated with DMSO, all embryos scored as sibling phenotypically were confirmed as either homozygous wild type or heterozygous, and all embryos with a mutant phenotype were indeed genotyped as mutants. In the group treated with 10 µM DEAB, however, 6 embryos scored as siblings were resolved to be mutants after genotyping. Thus, 6 out of 38 mutants (16%) were rescued by DEAB treatment. Increasing the dose of DEAB treatment from 10 to 50 µM also increased the percentages of mutants being rescued: 32% of mutants (9 out of 28) was rescued when treating with 50 µM DEAB. Interestingly, treating wild type siblings with DEAB also has an effect on bone development in general (figure 7B): while DMSO treated siblings exhibited approximately 6 mineralized centra, embryos treated with 10 µM DEAB only showed around 2 mineralized centra, and for siblings treated with 50 µM DEAB none of the vertebral centra were mineralized yet.

In order to examine the hypothesis whether *stocksteif* and *dragonfish* might function in the same pathway, we studied the effects of DEAB treatment on *dragonfish* mutants (figure 8). Again, the siblings showed a slight concentration dependent delay in bone development resulting in less mineralized vertebral centra when treated with a higher dose of DEAB. However, all *dragonfish* mutants exhibited the very same phenotype independent of a certain treatment. Fusion of vertebral centra along the complete notochord was observed in all treated groups and moreover, all mutants exhibited ectopic mineralizations in the brain and neural tube. Since we have not identified the causative mutation yet, we were not able to reliably genotype the *dragonfish* mutants and siblings. However, in every group approximately 25% of the embryos showed the mutant phenotype, indicating that the mutants were not rescued by DEAB treatment. Taken together, these results indicate that *dragonfish* does not function in the RA pathway.

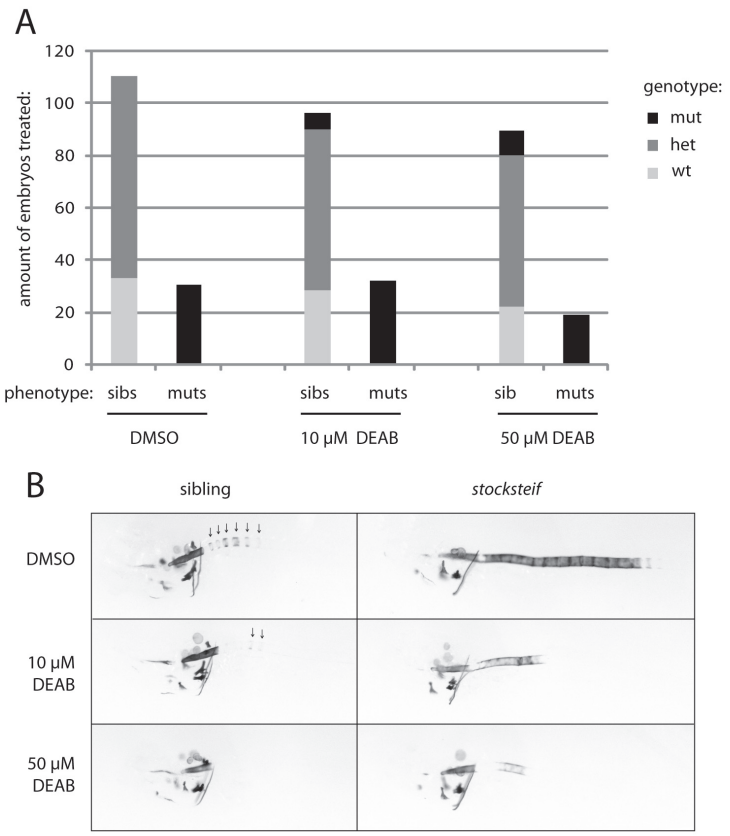

Figure 7: **The *stocksteif* mutant phenotype can be rescued with DEAB treatment.**
(A) Graph showing the results of phenotyping (columns: siblings (sibs) versus mutants (muts)) and genotyping (homozygous wild types (wt) in light gray, heterozygous embryos (het) in gray, and mutants (mut) in black) of an egg-lay of two *stocksteif* carriers treated with either 10 µM DEAB, 50 µM DEAB, or DMSO as a control group. 16% (6 out of 38) of mutants treated with 10 µM DEAB and 32% (9 out of 28) of mutants treated with 50 µM DEAB were rescued.
(B) Representative examples of alizarin red stained siblings versus *stocksteif* mutants for the three treated groups. Arrows indicate the amount of mineralized centra in the siblings.

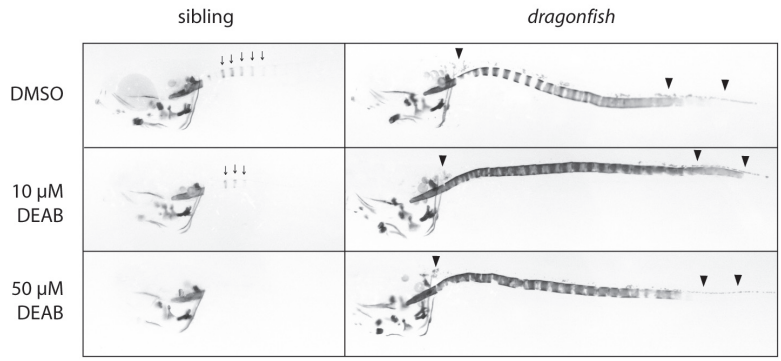

Figure 8: **The *dragonfish* mutant phenotype cannot be rescued with DEAB treatment.** Alizarin red stained siblings versus *dragonfish* mutants treated with either 10 µM DEAB, 50 µM DEAB, or DMSO as a control group. Arrows indicate the number of mineralized centra in the siblings. While siblings are delayed in bone development when treated with DEAB, the *dragonfish* mutant phenotype is not altered. Arrowheads point to ectopic mineralizations in the brain and neural tube.

DISCUSSION

In this study, we have analyzed the *dragonfish* mutant phenotype. Mutants are characterized by over-ossification of the vertebral column, resulting in fusion of vertebral centra. Additionally, ectopic pathological mineralizations are observed in the head and inside the central canal of the neural tube. Neural and haemal arches of juvenile mutants grow out irregularly, are broader, and fusions with adjacent arches either anterior or posterior occur often.

Pathological mineralizations

The ectopic mineralization in the brain is also observed in some juvenile mutants. We have not observed any juvenile mutant with ectopic mineralization in the neural tube. This, however, is most likely explainable by the fact that only a few (less than 5%) of the mutants with a weak phenotype were able to survive. In humans, a blockage of the cerebrospinal fluid in the central canal of the spinal cord causes hydrocephalus (excess of fluid in the cranial vault), a condition that can lead to brain damage (Rekate, 2009). It will be interesting to investigate whether lethality of *dgf* mutants is the reason that we have not observed juvenile mutants with ectopic mineralization in the neural tube or that, for example, this specific aspect of the phenotype is transient.

In some mutant embryos as well as juveniles, we observed a spotted mineralization pattern in certain bone elements (figure 1G: ceratohyal, figure 3K: lower jaw). Despite the considerable smaller size of the juvenile mutants, this is unlikely to be a consequence of a possible delay since we have never observed this mineralization pattern in wild type siblings. Moreover, when this spotted pattern is observed in 8 day old mutant embryos it is often accompanied by premature ossification of the head skeleton (figure 1F,G). A more likely explanation for this phenomenon could be that part of the osteoblasts have increased their mineralization activity, while others have not yet. Unraveling the molecular lesion in *dragonfish* mutants and understanding the function of the affected gene in bone development will help us in answering this and other questions.

Predicted expression of *dragonfish*

Since some *dragonfish* mutant embryos show premature ossification in the head skeleton compared to siblings, we predict that the affected *dragonfish* gene is expressed in classic osteoblasts (*osterix* positive osteoblasts (this thesis, chapter 4: Spoorendonk et al., 2008)). Moreover, the gene is most likely also expressed in the cells forming the initial mineralized matrix of the vertebral centra at times when we do not see *osterix:nuGFP* expression in the axial skeleton yet (*osterix*-negative osteoblasts (this thesis, chapter 4: Spoorendonk et al., 2008)), as this would explain the premature formation of centrae in mutants, and would be consistent with *cyp26b1* expression. Possibly, these cells are similar to the notochord cells, which have been proposed to be responsible for the initial centrum material (Fleming et al., 2004).
Furthermore, the affected gene is probably expressed in the neural tube explaining the pathological mineralizations in the central canal in mutants. A mis-regulation in the homeostasis of calcium, which is necessary for the release of neurotransmitters into the synaptic cleft under normal conditions (Parnas and Parnas, 1994), likely causes these pathological mineralizations.

***dragonfish* does not function in the retinoic acid/cyp26b1 pathway**

The axial over-ossification of the *dragonfish* mutant phenotype is very similar to the phenotype observed in *stocksteif* mutants. In both mutants, vertebrae are initially correctly placed, but an excess of bone production fuses the vertebral centra to each other. Moreover, for both mutants none of the expression patterns of specific bone-markers tested so far seem to be altered.
Therefore, we hypothesized that *dragonfish* might function in the same pathway as *stocksteif* which encodes *cyp26b1*, a retinoic acid metabolizing enzyme. However, we showed that, while *stocksteif* mutants can be rescued by treatment with DEAB (an inhibitor of RA synthesis), *dragonfish* mutants cannot be rescued by this treatment.
It turned out that DEAB treatment has an overall delaying effect on bone development as well, which complicates the analysis of this rescue experiment: there is a possibility that delayed mutants are scored as phenotypically sibling because of the delay, not

because of the rescue. However, *dragonfish* mutants treated with DEAB do not show any effect of delayed bone formation and are therefore distinct to *stocksteif* mutants. Moreover, two other observations support the thoughts that *dragonfish* does not function in the RA pathway: first, RA treatment of wild type embryos completely phenocopied the *stocksteif* mutant phenotype (this thesis, chapter 4: Spoorendonk et al., 2008), and thus also the axial over-ossification (fusion of vertebral centra) of the *dragonfish* mutants. However, the other characteristic of the *dragonfish* mutant phenotype, ectopic mineralizations in the head and neural tube, was never observed in RA treated embryos. Second, when exposed to increased RA levels, *cyp26b1* expression itself is highly upregulated in *stocksteif* mutants compared to the levels in siblings in what appears to be a positive feedback response. In situ hybridizations for *cyp26b1* in *dragonfish* mutants, however, did not show any alterations in *cyp26b1* expression levels in siblings versus mutants (data not shown).
Taken together, we conclude that *dragonfish* functions in a pathway different from that of retinoic acid.

An *in vivo* model to study over-ossification and pathological mineralizations
The combination of powerful genetics and *in vivo* imaging of osteoblast-specific transgenic lines in zebrafish have resulted in a unique model to study the biology of over-ossification and pathological mineralizations: the *dragonfish* mutant phenotype. Interestingly, expression of osteoblast markers is not altered in *dragonfish* mutants versus siblings. Preliminary data indicate moreover that the number of osteoblasts in the mutant versus the sibling cleithrum is unchanged (data not shown). Remarkably, the expansion of the mutant cleithrum is not enclosed by osteoblasts (inset in figure 6D: arrow). This suggests that the over-ossification is likely a consequence of enhanced osteoblast activity.
However, the other possibility is that this is a process occurring independently of osteoblasts and that other cells are responsible for the over-ossification. This last scenario is also likely to occur at places where we do not detect osteoblasts, like the sites of the future vertebral centra and the ectopic mineralizations throughout the embryo: connective or neuronal tissue are prone to mineralize under pathological circumstances in *dragonfish* mutants. Future research including finishing the positional cloning of the affected gene will help us to get more insights into the molecular mechanisms of bone development and disease.

REFERENCES

Avaron, F., Hoffman, L., Guay, D. and Akimenko, M. A. (2006). Characterization of two new zebrafish members of the hedgehog family: atypical expression of a zebrafish indian hedgehog gene in skeletal elements of both endochondral and dermal origins. Dev Dyn 235, 478-89.

Danilevicius, C. F., Lopes, J. B. and Pereira, R. M. (2007). Bone metabolism and vascular calcification. Braz J Med Biol Res 40, 435-42.

Das, S. K. and Farooqi, A. (2008). Osteoarthritis. Best Pract Res Clin Rheumatol 22, 657-75.

Di Trapani, G., Di Rocco, C., Abbamondi, A. L., Caldarelli, M. and Pocchiari, M. (1982). Light microscopy and ultrastructural studies of Sturge-Weber disease. Childs Brain 9, 23-36.

Fleming, A., Keynes, R. and Tannahill, D. (2004). A central role for the notochord in vertebral patterning. Development 131, 873-80.

Geisler, R. (2002). Mapping and Cloning. Zebrafish, a practical approach, 175-210.

Giachelli, C. M. (1999). Ectopic calcification: gathering hard facts about soft tissue mineralization. Am J Pathol 154, 671-5.

Inohaya, K., Takano, Y. and Kudo, A. (2007). The teleost intervertebral region acts as a growth center of the centrum: in vivo visualization of osteoblasts and their progenitors in transgenic fish. Dev Dyn 236, 3031-46.

Job-Deslandre, C. (2004). Inherited ossifying diseases. Joint Bone Spine 71, 98-101.

Kaplan, F. S., Fiori, J., LS, D. L. P., Ahn, J., Billings, P. C. and Shore, E. M. (2006). Dysregulation of the BMP-4 signaling pathway in fibrodysplasia ossificans progressiva. Ann N Y Acad Sci 1068, 54-65.

Nakashima, K., Zhou, X., Kunkel, G., Zhang, Z., Deng, J. M., Behringer, R. R. and de Crombrugghe, B. (2002). The novel zinc finger-containing transcription factor osterix is required for osteoblast differentiation and bone formation. Cell 108, 17-29.

Parnas, H. and Parnas, I. (1994). Neurotransmitter release at fast synapses. J Membr Biol 142, 267-79.

Ramonet, D., de Yebra, L., Fredriksson, K., Bernal, F., Ribalta, T. and Mahy, N. (2006). Similar calcification process in acute and chronic human brain pathologies. J Neurosci Res 83, 147-56.

Rekate, H. L. (2009). A contemporary definition and classification of hydrocephalus. Semin Pediatr Neurol 16, 9-15.

Renn, J. and Winkler, C. (2009). Osterix-mCherry transgenic medaka for in vivo imaging of bone formation. Dev Dyn 238, 241-8.

Schulte-Merker, S. (2002). Looking at embryos. Zebrafish, a practical approach, 41-43.

Spoorendonk, K. M., Peterson-Maduro, J., Renn, J., Trowe, T., Kranenbarg, S., Winkler, C. and Schulte-Merker, S. (2008). Retinoic acid and Cyp26b1 are critical regulators of osteogenesis in the axial skeleton. Development 135, 3765-74.

CHAPTER 7

General discussion

For many years two model organisms have dominated the area of bone research: mice have been mainly used to generate mutants in sclerotome and bone specific genes, while the chick has been the organism of choice for many grafting experiments and other embryologic manipulation studies. Furthermore, many studies have made use of *in vitro* cell culture systems or human material from the clinic.
In the research described in this thesis, we have used the zebrafish (*Danio rerio*) as a model system to study bone development. This small teleost offers possibilities which makes it a great complement to the other model systems available: first, forward genetic screens are possible in fish due to the extra-uterine development and large brood size. Second, the transparency of the zebrafish embryos has allowed the recent generation of osteoblast-specific reporter lines, which make *in vivo* visualization of osteoblasts possible.

Forward genetics as a powerful tool to identify novel genes
Using an unbiased forward genetic ENU-mutagenesis screen for defects in bone formation we identified, after screening 700 families, 27 specific mutants representing a maximum of 23 genetic loci (chapter 3). Two mutants, one with a delayed onset of ossification (p.03.14 or *lenny*) and one with over-ossification and pathological mineralizations (1.027/1.093 or *dragonfish*), were analyzed in detail (chapter 3 and chapter 6, respectively). Furthermore, we have reported the analysis of the *stocksteif* mutant, which was isolated in the Tübingen 2000 screen. *stocksteif* encodes *cyp26b1*, a retinoic acid metabolizing enzyme with a previously unappreciated role in osteogenesis (chapter 4). Although *lenny* and *dragonfish* have not been molecularly identified yet, they most likely also encode genes with a previously unappreciated function in bone development, since the regions to which both mutants are mapped do not contain genes with a known function in osteogenesis. Thus, so far we have not identified mutants for genes that had already been described to play a role in bone development.
The explanation for this might partly be found in the redundancy of genes. Many zebrafish genes have been evolutionary duplicated (Robinson-Rechavi et al., 2001). For example, zebrafish have two *runx2* genes, *runx2a* and *runx2b* (Flores et al., 2004). If one of these genes was mutated, there is a good possibility that the other gene would take over its function and thus, no phenotype will be observed. To overcome this problem, a reverse genetic set up (Wienholds et al., 2002) would have to be employed. On the other hand, we have just started to molecularly identify the lesions in a few of the mutants. Therefore, it is probably too early to draw any conclusions on the overlap in genes identified in our screen and genes characterized previously in mice.

Osteoblast-specific transgenic zebrafish lines: *in vivo* observations
It is often hard to determine the extent to which *in vitro* findings effectively mirror the *in vivo* situation. Similarly, it is not always clear how much of the characteristics of

a specific osteoblastic cell isolated from its local environment is actually transmitted into the culture system and whether the original features of isolated primary cells are well-preserved *in vitro*. Alternatively, the cells may represent a rather generalized population that has the potential or tendency to differentiate according to the osteoblast lineage upon exposure to a specific environmental factor provided by the growth medium. Moreover, *in vitro* models represent a system where osteoblasts are not exposed to other cell types, and for this reason it is impossible to characterize aspects such as origin and destiny of osteoblasts.
In mice, a few bone-specific reporter lines marked by lacZ have been generated (Lu et al., 2007; Zha et al., 2008). However, to be able to visualize this lacZ expression, mice have to be sacrificed and histologically stained. Therefore, in order to study the osteoblast lineage *in vivo*, we developed transgenic osteoblast-specific reporter lines in zebrafish: due to their transparency, zebrafish and medaka are currently the only model systems available to allow visualization of osteoblasts *in vivo* over time. In the research described in this thesis we have established two stable osteoblast-specific transgenic zebrafish lines: *osterix:nuGFP* (or *osterix:mCherry*) (chapter 4: Spoorendonk et al., 2008)(Renn and Winkler, 2009), labeling the osteoblast lineage (Nakashima et al., 2002), and *osteocalcin:GFP* (chapter 1)(Inohaya et al., 2007), marking mature osteoblasts (Gavaia et al., 2006). Furthermore we have made use of transient transgenic embryos injected with *cyp26b1:YFP* (a construct in which YFP was recombined into a BAC clone that contained the genomic sequence of *cyp26b1*) (chapter 5). Currently, we are screening these injected embryos for germline transmission.

In situ hybridizations for type X collagen (*col10a1*) in *lenny* mutants versus siblings did not show any alterations, indicating that the osteoid matrix in *lenny* mutants is formed correctly. No other cells than osteoblasts produce osteoid matrix. Thus, it was not surprising that *lenny* mutants do contain *osterix:nuGFP* expressing osteoblasts. Remarkably, unpublished data from our lab have shown that for all the mutants we studied so far and that exhibit delayed bone formation or no ossification at all, we could not detect differences in expression of the *osterix* transgenic line in mutants versus siblings (L. Huitema and S. Schulte-Merker, personal communication). Therefore, we have not been able yet to study mutants lacking osteoblasts. For future forward genetic approaches we suggest to screen in the *osterix:nuGFP* line that will permit counting of osteoblasts. At the same time, this way of screening might be profitable for compound screenings in order to investigate if a certain drug is able to enhance or lower the amount of active osteoblasts.
Also in *stocksteif* and *dragonfish* mutants, we did not detect an altered *osterix* expression pattern: at places where we observed over-ossification, *osterix:nuGFP* expression did not show any differences and moreover, at the sites of ectopic mineralizations we did not detect *osterix* expression at all. Furthermore, for both mutants also the expression of *osteocalcin:GFP* did not change between

mutants and siblings. These results indicate that at places where we do observe osteoblasts, it could be that the over-ossification is caused by an increased activity of osteoblasts. At sites of ectopic mineralizations, where we do not detect *osterix*-positive osteoblasts, it suggests that here mineralizations arise without involvement of classical osteoblasts.

Phenotypic consequences of excess retinoic acid

In chapter 4 we have shown that *stocksteif* encodes *cyp26b1*, a retinoic acid (RA) catabolizing enzyme, which is expressed in osteoblasts. We reported that the *stocksteif* mutant phenotype could be completely phenocopied by treating wild type embryos with RA. Subsequently, we studied the effects of RA on osteoblasts *in vivo* and showed that upon RA treatment osteoblast localization as well as numbers do not change. This indicates that in the *stocksteif* mutant it is indeed the increased activity of osteoblasts causing over-ossification.

On the other hand, the over-ossification resulting in fused vertebral centra of *stocksteif* mutants is already observed before we can detect *osterix*-positive osteoblasts in the axial skeleton. Therefore, we hypothesized that a second population of osteoblasts, referred to as *osterix*-negative osteoblasts, is responsible for the formation of the initial centrum material of zebrafish and that RA most likely also acts on this type of osteoblast.

Until now, several *in vitro* studies already reported effects of RA exposure on mineralization, however with contradicting results. Some studies describe an increase in mineralization (Malladi et al., 2006; Skillington et al., 2002; Song et al., 2005; Wan et al., 2007; Wang and Kirsch, 2002; Yamashita et al., 2005), while others report a suppression of cell differentiation with a concomitant decrease in mineralization (Cohen-Tanugi and Forest, 1998; Iba et al., 2001). As mentioned above, *in vitro* studies can suffer from intrinsic limitations and results are extremely dependent on the type of cell and the culture conditions used. Taken together, in a field where interpretation of *in vitro* experiments is inherently difficult, we have established an *in vivo* model to follow osteoblasts and we have shown that RA upregulates osteoblast activity resulting in increased mineralization.

The involvement of the notochord in axial osteogenesis

stocksteif and *dragonfish* mutants are both characterized by over-ossification of the future vertebral column, ultimately resulting in fusion of the vertebral centra (chapter 4 and 6). These phenotypes can be observed at 8 dpf or later. As mentioned above, at this point in time *osterix* expressing osteoblasts are not present yet in the axial skeleton (chapter 5, figure 1) and we have proposed that *osterix*-negative osteoblasts are responsible for the production of mineralized centra around the notochord.

Interestingly, in *lenny* mutants that are rescued by an excess of calcium the tip of the notochord is never mineralized, suggesting that indeed there is a difference between the mineralization of the notochord and the other bone elements in the zebrafish.

It has been proposed that the notochord cells (chordoblasts) themselves are responsible for the secretion of the initial bone matrix of the vertebral centra (chordacentra) in teleosts, since isolated notochords secrete bone matrix *in vitro* and ablation of notochord cells prevents centrum formation *in vivo* (Fleming et al., 2004). In order to study whether the *osterix*-negative osteoblasts are identical to the notochord cells a marker for these cells is necessary. Until now such a marker has not been described yet. In chapter 5 we reported that expression of *cyp26b1* in the axial skeleton is restricted to the places of the future vertebral centra preceding mineralization. Since a lack of *cyp26b1* (in *stocksteif* mutants) causes over-ossification and fusion of these vertebral centra, we propose that *cyp26b1* is expressed in the *osterix*-negative osteoblasts responsible for the formation of the chordacentra. Future research is necessary to elucidate whether these cells are identical to the notochord cells postulated by Fleming et al. (2004) to initiate centrum formation.

Additionally, in our forward genetic screen we identified four other mutants characterized by over-ossification of the notochord resulting in fused vertebrae: they resemble the *stocksteif* mutant, but not the *dragonfish* mutant because these mutants do not show additional ectopic mineralizations. However, in complementation tests with *stocksteif* carriers all four alleles could complement the *stocksteif* allele. Moreover, also all other possible complementation tests between these four mutants did not result in mutant embryos. Thus, these four mutants encode four different genes involved in the formation of the vertebral centra. Positional cloning and the subsequent analysis of the expression patterns of the mutated genes will greatly contribute to our understanding of axial osteogenesis.

A model for different RA levels in sibling versus *stocksteif* mutant embryos

We have demonstrated that RA levels within osteoblasts need to be tightly controlled for proper axial osteogenesis. When wild type embryos are exposed to elevated RA levels they start to increase the activity of osteoblasts which results in over-ossification between centra. Counter-intuitively, we have shown that expression of *cyp26b1* is restricted to the places of the vertebral centra. In the following model we have incorporated all the data about *cyp26b1* and RA presented in this thesis (figure 1): In the embryonic wild type situation (younger than 17 dpf), expression of *cyp26b1* is found around (future) vertebral centra, which leads to lower RA levels at places where the centra develop compared to the RA levels in between centra (the future intervertebral disc (IVD) spaces). In this model, we assume that only osteoblasts (either *osterix*-negative or *osterix*-positive, which appear later) react on RA levels. Under normal circumstances osteoblasts need a low RA level in order to produce tightly controlled amounts of calcified matrix. In the IVDs osteoblasts are not present and therefore here bone formation does not occur unless RA levels are dramatically higher. In loss-of-function *stocksteif* mutants, however, *cyp26b1* is not functional and thus, RA levels are not lowered at the places where the centra develop. Therefore,

osteoblasts react on the high RA levels and increase their activity resulting in an overproduction of mineralized matrix. Consequently, centra grow out in anterior and posterior directions as well as in the proximal direction, resulting in the fusion of centra adjacent to each other and completely solid centra, respectively. Whether or not centra also grow out in the distal direction is difficult to determine because of difficulties to correlate a possible centrum expansion distally with the size difference between mutants versus siblings: mutants stay considerably smaller.
The situation in older larvae (from 17 dpf onwards) is similar concerning the RA levels. The only difference is that *osterix*-positive osteoblasts have appeared at the anterior and posterior edges of the centra and that in the mutant situation these osteoblasts will also react on the elevated RA levels leading to even more matrix production. Additionally, the *osterix*-positive osteoblasts have also started to form the arches. Remarkably, we have not detected *cyp26b1* expression in the arches. Therefore it remains unclear how the wild type RA levels are lowered at these places in order to control the production of calcified matrix. A possible explanation could be that in arch-osteoblasts there is an additional regulator expressed controlling the RA levels.

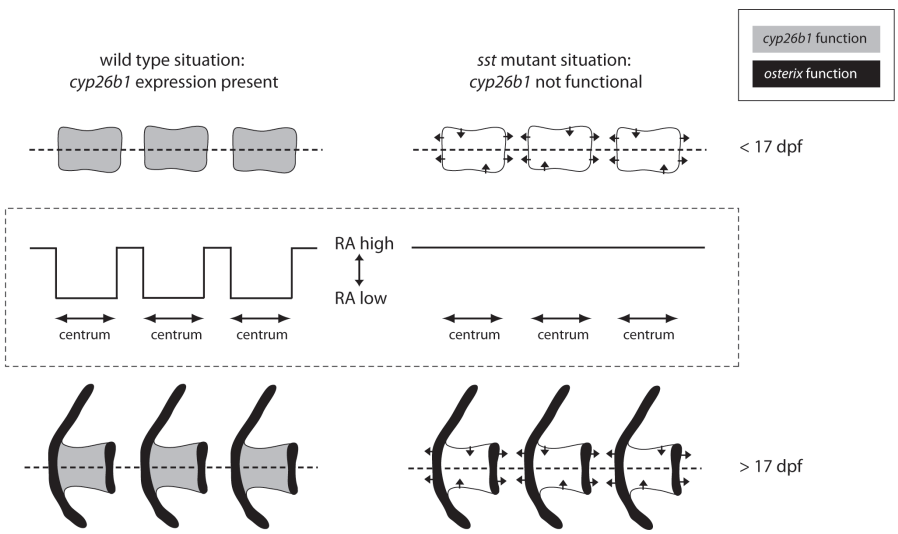

Figure 1: **A model for RA levels and the consequences in siblings versus *stocksteif* mutants.** In the wild type situation (left) *cyp26b1* is expressed around vertebral centra (three of them are depicted, anterior is to the left). From 17 dpf onwards *osterix*-expressing osteoblasts appear at the places where arches develop and at the anterior and posterior edges of the centra. The RA levels along the dotted line are indicated in the lower panel. We propose that only osteoblasts (which are present around each centrum) react on RA levels: when in the mutant situation (right) *cyp26b1* is not able anymore to lower the RA levels in centra, osteoblasts increase their activity resulting in overproduction of mineralized matrix in multiple directions (arrows). Arrows pointing to the inside of the centra indicate growth in the proximal direction.

Translation from fish to mammals

In order to study whether Cyp26 enzymes might have a similar role in restricting ossification during mammalian development, in two independent studies pregnant mice were treated with either the Cyp26 inhibitor R115866 or with RA itself. Laue and colleagues performed daily treatments (E13 till E18) with R115866: at E18.5 this resulted in fusions of neural arches of the cervical vertebrae and precocious fusions of neural arches with centra in the more posterior regions (Laue et al., 2008).

In a similar study we have treated mice with RA (figure 2). We performed one-time only treatments either at E10, E11, E12, or E13. At E16.5 the treated embryos exhibit overgrowth of ribs. The phenotype was clearly dependent on the timing of the treatment: the earlier the embryos were treated the more severe the phenotype. Embryos treated at E13 did not show a phenotype at all. In both studies, the ribs of treated embryos were significantly thicker than in untreated embryos.

These results suggest that, as in zebrafish, in mouse Cyp26b1 tightly controls RA levels and that both regulators are required for mammalian osteogenesis. The phenotypes in mouse however, do not completely mimic the situation observed in the *stocksteif* mutants. Most likely this is due to a systemic effect in the treated mice, while in *stocksteif* mutants a local effect of the loss-of-function of *cyp26b1* is observed. Moreover, in our study the RA treated mice only got one dosis. This implies that not only the levels of RA are critical for proper bone development but that also the timing is very important.

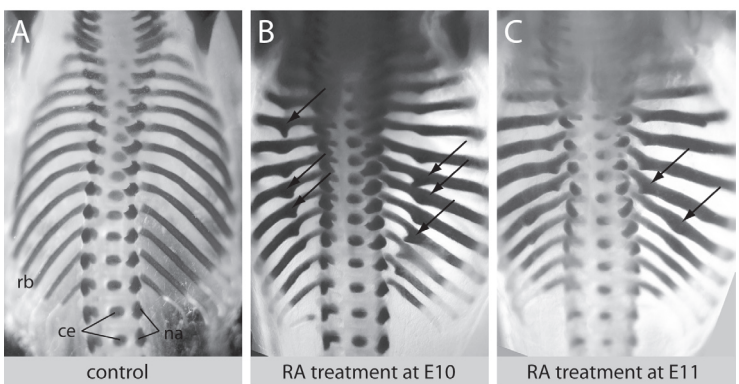

Figure 2: **Treatment of mice with retinoic acid causes overgrowth of ribs.**
Dorsal views of mouse embryos (E16.5) stained with alizarin red are shown (anterior is to the top). The embryos in B and C show thickenings of ribs (arrows) upon RA treatment. Note that ribs of treated embryos (B, C) are generally broader than in control embryos (A). ce = centra, na = neural arches, rb = ribs.

What exactly is the definition of an osteoblast?

Traditionally the simplest definition of an osteoblast is a cell that makes bone. This is a definition in the functional sense: every cell that produces bone is an osteoblast. However, nowadays, every report or review on osteogenesis will also state that osteoblasts derive from mesenchymal cells and that the transcription factors *osterix* is required for osteoblasts differentiation (Karsenty and Wagner, 2002; Kobayashi and Kronenberg, 2005; Nakashima et al., 2002). Therefore, a cell expressing this marker, characteristic of osteoblasts, has been accepted over time as being synonymous with an osteoblast.

Contradictory, in the research described in this thesis we have shown that not only under pathological conditions (the ectopic mineralizations observed in the *dragonfish* mutants) but also under normal circumstances ossification can occur without involvement of *osterix* expression: the mineralization of the vertebral centra in zebrafish starts before *osterix*-postive osteoblasts can be detected. We have proposed that *osterix*-negative osteoblasts are responsible for the initial matrix deposition. These osteoblasts are osteoblasts according to the definition in the functional way: these cells make bone. However, they do not match the criterion of expressing *osterix*. Therefore, we propose that the definition of an osteoblast, which includes *osterix* as a marker should be reconsidered and that the traditional definition, which only refers to the function of a cell should be re-introduced: every cell that makes bone under normal non-pathological conditions is an osteoblast.

Concluding remarks

In summary, the zebrafish has been demonstrated to be a powerful model system especially in forward genetics to identify novel gene functions and to study their role in osteogenesis. For example, our data have demonstrated a previously unappreciated role for *cyp26b1* in axial osteogenesis, in which *cyp26b1* tightly controls RA levels.

The zebrafish can be used as a tool to complement genetic and embryological studies in mice and avians in order to clarify the molecular mechanisms underlying bone development and disease. In addition, zebrafish and medaka are ideally suited and currently the only model system available to allow visualization of osteoblasts *in vivo* over time. Moreover, while most mouse mutants with a defect in bone formation are embryonic lethal or die at birth because of respiratory distress (Komori et al., 1997; Nakashima et al., 2002; Yashiro et al., 2004), many zebrafish bone mutants are sub-viable and can survive to early adulthood, enabling analysis not only of embryonic but also of adult effects on bone formation in these mutants. The combination of these advantageous features will greatly contribute to our understanding of osteogenesis in the future.

REFERENCES

Cohen-Tanugi, A. and Forest, N. (1998). Retinoic acid suppresses the osteogenic differentiation capacity of murine osteoblast-like 3/A/1D-1M cell cultures. Differentiation 63, 115-23.

Fleming, A., Keynes, R. and Tannahill, D. (2004). A central role for the notochord in vertebral patterning. Development 131, 873-80.

Flores, M. V., Tsang, V. W., Hu, W., Kalev-Zylinska, M., Postlethwait, J., Crosier, P., Crosier, K. and Fisher, S. (2004). Duplicate zebrafish runx2 orthologues are expressed in developing skeletal elements. Gene Expr Patterns 4, 573-81.

Gavaia, P. J., Simes, D. C., Ortiz-Delgado, J. B., Viegas, C. S., Pinto, J. P., Kelsh, R. N., Sarasquete, M. C. and Cancela, M. L. (2006). Osteocalcin and matrix Gla protein in zebrafish (Danio rerio) and Senegal sole (Solea senegalensis): comparative gene and protein expression during larval development through adulthood. Gene Expr Patterns 6, 637-52.

Iba, K., Chiba, H., Yamashita, T., Ishii, S. and Sawada, N. (2001). Phase-independent inhibition by retinoic acid of mineralization correlated with loss of tetranectin expression in a human osteoblastic cell line. Cell Struct Funct 26, 227-33.

Inohaya, K., Takano, Y. and Kudo, A. (2007). The teleost intervertebral region acts as a growth center of the centrum: in vivo visualization of osteoblasts and their progenitors in transgenic fish. Dev Dyn 236, 3031-46.

Karsenty, G. and Wagner, E. F. (2002). Reaching a genetic and molecular understanding of skeletal development. Dev Cell 2, 389-406.

Kobayashi, T. and Kronenberg, H. (2005). Minireview: transcriptional regulation in development of bone. Endocrinology 146, 1012-7.

Komori, T., Yagi, H., Nomura, S., Yamaguchi, A., Sasaki, K., Deguchi, K., Shimizu, Y., Bronson, R. T., Gao, Y. H., Inada, M. et al. (1997). Targeted disruption of Cbfa1 results in a complete lack of bone formation owing to maturational arrest of osteoblasts. Cell 89, 755-64.

Laue, K., Janicke, M., Plaster, N., Sonntag, C. and Hammerschmidt, M. (2008). Restriction of retinoic acid activity by Cyp26b1 is required for proper timing and patterning of osteogenesis during zebrafish development. Development 135, 3775-87.

Lu, Y., Xie, Y., Zhang, S., Dusevich, V., Bonewald, L. F. and Feng, J. Q. (2007). DMP1-targeted Cre expression in odontoblasts and osteocytes. J Dent Res 86, 320-5.

Malladi, P., Xu, Y., Yang, G. P. and Longaker, M. T. (2006). Functions of vitamin D, retinoic acid, and dexamethasone in mouse adipose-derived mesenchymal cells. Tissue Eng 12, 2031-40.

Nakashima, K., Zhou, X., Kunkel, G., Zhang, Z., Deng, J. M., Behringer, R. R. and de Crombrugghe, B. (2002). The novel zinc finger-containing transcription factor osterix is required for osteoblast differentiation and bone formation. Cell 108, 17-29.

Renn, J. and Winkler, C. (2009). Osterix-mCherry transgenic medaka for in vivo imaging of bone formation. Dev Dyn 238, 241-8.

Robinson-Rechavi, M., Marchand, O., Escriva, H., Bardet, P. L., Zelus, D., Hughes, S. and Laudet, V. (2001). Euteleost fish genomes are characterized by expansion of gene families. Genome Res 11, 781-8.

Skillington, J., Choy, L. and Derynck, R. (2002). Bone morphogenetic protein and retinoic acid signaling cooperate to induce osteoblast differentiation of preadipocytes. J Cell Biol 159, 135-46.

Song, H. M., Nacamuli, R. P., Xia, W., Bari, A. S., Shi, Y. Y., Fang, T. D. and Longaker, M. T. (2005). High-dose retinoic acid modulates rat calvarial osteoblast biology. J Cell Physiol 202, 255-62.

Spoorendonk, K. M., Peterson-Maduro, J., Renn, J., Trowe, T., Kranenbarg, S., Winkler, C. and Schulte-Merker, S. (2008). Retinoic acid and Cyp26b1 are critical regulators of osteogenesis in the axial skeleton. Development 135, 3765-74.

Wan, D. C., Siedhoff, M. T., Kwan, M. D., Nacamuli, R. P., Wu, B. M. and Longaker, M. T. (2007). Refining retinoic acid stimulation for osteogenic differentiation of murine adipose-derived adult stromal cells. Tissue Eng 13, 1623-31.

Wang, W. and Kirsch, T. (2002). Retinoic acid stimulates annexin-mediated growth plate chondrocyte mineralization. J Cell Biol 157, 1061-9.

Wienholds, E., Schulte-Merker, S., Walderich, B. and Plasterk, R. H. (2002). Target-selected inactivation of the zebrafish rag1 gene. Science 297, 99-102.

Yamashita, A., Takada, T., Narita, J., Yamamoto, G. and Torii, R. (2005). Osteoblastic differentiation of monkey embryonic stem cells in vitro. Cloning Stem Cells 7, 232-7.

Yashiro, K., Zhao, X., Uehara, M., Yamashita, K., Nishijima, M., Nishino, J., Saijoh, Y., Sakai, Y. and Hamada, H. (2004). Regulation of retinoic acid distribution is required for proximodistal patterning and outgrowth of the developing mouse limb. Dev Cell 6, 411-22.

Zha, L., Hou, N., Wang, J., Yang, G., Gao, Y., Chen, L. and Yang, X. (2008). Collagen1alpha1 promoter drives the expression of Cre recombinase in osteoblasts of transgenic mice. J Genet Genomics 35, 525-30.

NEDERLANDSE SAMENVATTING

Ieder mens, elke plant en elk dier bestaat uit cellen. De blauwdruk van alle processen die in een cel kunnen plaats vinden ligt opgeslagen in het erfelijke materiaal (DNA). Het DNA is opgebouwd uit vier verschillende bouwstenen en bevindt zich opgerold in chromosomen in de kern van een cel. Het DNA van de mens bestaat uit ongeveer drie miljard bouwstenen. Een lange streng van bouwstenen wordt een gen genoemd: ieder gen maakt een bepaald eiwit. Eiwitten zijn essentieel voor de ontwikkeling en het behoud van de processen in alle lichaamscellen.
Er zijn verschillende soorten cellen: een paar voorbeelden zijn zenuwcellen, bloedcellen, spiercellen en botcellen. Alle cellen bevatten echter precies hetzelfde DNA en dus dezelfde genen en zijn daarom in principe in staat om allemaal dezelfde eiwitten te maken, maar omdat men sommige eiwitten niet overal nodig heeft, zijn niet alle genen overal actief. In elk type cel is een bepaalde groep genen actief die uiteindelijk bepaalt wat de functie van die cel wordt. De mens heeft naar schatting zo'n 25.000 genen. Veel van deze genen zijn ook aanwezig in lagere organismen, zoals de muis, de zebravis en de fruitvlieg. Zo is 80 procent van de menselijke genen terug te vinden in de muis. Voor de zebravis is dit ongeveer 75 procent. Dit laat zien dat veel genen door de evolutie heen dezelfde rol zijn blijven vervullen.

Een levend organisme ontstaat uit een enkele bevruchte eicel. Deze cel moet zich gaan vermenigvuldigen maar ook specialiseren om de verschillende celtypes te kunnen vormen. Dit is een zeer complex proces waarbij een kleine fout zeer grote gevolgen kan hebben en kan leiden tot aangeboren afwijkingen of ziektes. Momenteel wordt er veel onderzoek gedaan om uit te vinden welke genen een specifieke rol spelen tijdens zulke ontwikkelingsprocessen.
Het onderzoek dat beschreven staat in dit proefschrift is toegespitst op botontwikkeling. Hiervoor hebben we de zebravis gebruikt als modelsysteem. Twee cellen zijn van groot belang bij de vorming van bot: osteoblasten maken bot en osteoclasten breken bot juist weer af. Hierdoor is in een volwassen organisme de aanmaak en afbraak van bot in evenwicht. In de zebravis zijn beide cellen ook aanwezig maar worden osteoclasten pas actief in 12 dagen oude visjes. Dit maakt de jonge zebravis een uitermate geschikt modelsysteem om onderzoek te doen naar osteoblasten: simpelweg omdat osteoclasten nog niet actief zijn en je dus zeker weet dat het bot dat gevormd is alleen het werk is geweest van osteoblasten.

Door met een DNA-beschadigende stof fouten (mutaties) te maken in het DNA van model organismen kunnen genen defect raken waardoor ze verkeerde of geen eiwitten meer maken. Hierdoor mislukken de ontwikkelingsprocessen waarbij deze genen betrokken zijn, wat kan leiden tot de meest uiteenlopende ziektes. De zebravis is een organisme waarmee het relatief gemakkelijk is om grote zogeheten *forward genetic* screens uit te voeren: het DNA van de vissen muteren, kijken wat het effect

is en vervolgens het gen achterhalen wat dit specifieke defect veroorzaakt. In deze manier van onderzoek doen bestuderen we dus de functie van genen door ze uit te schakelen om zo te kijken wat er fout gaat als het gen defect is. Een organisme met een defect in een bepaald gen noemen we een mutant voor dat gen.

Tot op heden werd de zebravis nog niet veelvuldig gebruikt als modelsysteem voor onderzoek naar botontwikkeling. In **hoofdstuk 1** van dit proefschrift beschrijven we de voordelen van de zebravis voor dit soort onderzoek. Naast de zojuist beschreven mogelijkheid om genetische screens uit te voeren is het andere grote voordeel van de zebravis de transparantie: de embryo's van de zebravis zijn tot zo'n twee weken oud transparant. Dit maakt het mogelijk om verschillende processen gemakkelijk te bekijken: het enige wat je nodig hebt is een microscoop. Bovendien is het hierdoor mogelijk om zebravissen te creëren die een fluorescerend transgen bevatten. In deze vissen wordt een niet-eigen gen (transgen) tot expressie gebracht dat een flourescerend eiwit maakt. De aanmaak van dit eiwit kan worden gekoppeld aan de activiteit van een bepaald gen: overal waar dit bepaalde gen actief is (tot expressie komt) zien we nu ook het fluorescerende eiwit. In dit proefschrift maak ik gebruik van twee van zulke lijnen die fluorescerende eiwitten tot expressie brengen in botcellen.

Hoofdstuk 2 geeft een algemene introductie in de biologie van botontwikkeling, de celtypes die van belang zijn en de genen waarvan bekend is dat die een rol spelen bij de vorming van bot. Voor veel botziektes, zoals osteoporose (broze botten) of osteo-artrose (verbening van kraakbeen rond de gewrichten) is echter nog geen onderliggende genetische achtergrond gevonden. Daarom is het van groot belang om nieuwe genen te vinden die een rol spelen bij botontwikkeling en veroorzaker kunnen zijn van de verschillende botafwijkingen.

In **hoofdstuk 3** beschrijven en bediscussiëren we de genetische screen die we uitgevoerd hebben om nieuwe gen functies te vinden. De nakomelingen van de gemuteerde vissen hebben we gescreend voor botafwijkingen. Dit doen we door de acht dagen oude visjes te kleuren voor zowel bot (rode kleuring) als kraakbeen (blauwe kleuring). Botvorming is één van de laatste processen tijdens de ontwikkeling van een organisme en is onder andere afhankelijk van de ontwikkeling van het kraakbeen. Door voor beide weefsels aan te kleuren kunnen we mutanten oppikken die enkel en alleen een botdefect hebben.
De mutanten die we gevonden hebben zijn te verdelen in drie verschillende groepen:
1. mutanten die te weinig of geen bot aanmaken
2. mutanten die bot aanmaken op plekken waar normaal geen bot wordt gemaakt
3. mutanten die sneller en meer bot aanmaken dan normaal

De focus van mijn onderzoek lag vooral bij mutanten uit de tweede groep. Een van deze mutanten is de *stocksteif* mutant. Deze mutant beschrijven we in **hoofdstuk 4**. De wervelkolom van normale vissen bestaat uit een aaneenschakeling van losse wervels (vergelijkbaar met een kralenketting: er is relatief veel beweging mogelijk tussen de verschillende wervels/kralen). Bij de *stocksteif* mutant zijn alle wervels aan elkaar gegroeid en kunnen niet meer onderling bewegen. Wij laten zien dat dit komt door een defect in het gen *cyp26b1*. Dit gen maakt een enzym dat retinoïne zuur (een product afgeleid van vitamine A) afbreekt. In feite hebben de *stocksteif* mutanten dus te veel retinoïne zuur omdat het niet meer afgebroken kan worden.
Het bleek dat de osteoblasten (botvormende cellen) in de mutanten niet veel afwijken van de osteoblasten in gezonde vissen: hun plek en hun aantal zijn niet veranderd. Daarom denken we dat het de activiteit van de osteoblasten is die bij een teveel aan retinoïne zuur wordt verhoogd waardoor er meer bot gevormd wordt zodat de wervels aan elkaar groeien.

In **hoofdstuk 5** gaan we verder in op de expressie van *cyp26b1*. We beschrijven dat *cyp26b1* tot expressie komt in de wervelkolom: precies op die plekken waar later de wervels gevormd zullen worden. Interessant genoeg komen de genen die tot voor kort verantwoordelijk werden gehouden om een cel tot een osteoblast te maken, hier in eerste instantie nog niet tot expressie terwijl we al wel bot kunnen detecteren. Hoogstwaarschijnlijk speelt *cyp26b1* dus een belangrijke rol in de initiële botontwikkeling van de wervelkolom.

In **hoofdstuk 6** bestuderen we een andere mutant uit de tweede groep, de *dragonfish* mutant. Deze mutant lijkt veel op de *stocksteif* mutant: ook hier groeien de wervels door een overproductie van bot aan elkaar. Vanwege deze overeenkomst hebben we gekeken of er ook in de *dragonfish* mutant iets mis is met de retinoïne zuur huishouding. Dit bleek niet het geval te zijn, in andere woorden: beide mutanten zijn duidelijk verschillend van elkaar. De *dragonfish* mutant wordt bovendien nog gekarakteriseerd door een extra kenmerk. In de hersenen en in de neurale buis (de neurale buis loopt boven langs de wervels en gaat het ruggenmerg vormen) zien we namelijk ook bot ontstaan. Het bleek dat juist op deze plekken de genen, waarvan bekend is dat die een rol spelen bij botvorming, niet tot expressie komen.
Als we kunnen achterhalen waardoor dit bot zomaar wordt gevormd (en welke genen hier dan wel een rol bij spelen), kan dit waardevolle informatie opleveren voor verder wetenschappelijk onderzoek naar botontwikkeling.

Hoofdstuk 7 geeft tenslotte een samenvattende discussie van alle resultaten die in dit proefschrift beschreven staan.

DANKWOORD

Zo. Vier jaar later: klaar! Wat is er veel gebeurd in die tijd, maar wat heb ik vooral ook een hele leuke tijd gehad. En nu? Nooit meer zebravissen-eitjes verzamelen? Nooit meer op belachelijke tijden confocallen? Me nooit meer verbazen dat er op die belachelijke tijden nog altijd mensen heel serieus aan het werk zijn? Wat dat betreft blijf ik het een vreemd wereldje vinden, maar aan de andere kant... misschien ga ik dat juist ook wel missen: de vrijheid.
Promoveren doe je niet alleen en daarom wil ik op de laatste bladzijdes van dit proefschrift dan ook iedereen, en een aantal in het bijzonder, bedanken die me de afgelopen jaren hiermee geholpen heeft en zonder wie het onmogelijk was geweest dit boekje bij elkaar te schrijven.

First of all, Stefan, thank you for giving me the opportunity to work in your lab. I have had a great time and I have learned a lot about science and politics. Thank you for your never-ending enthusiasm, your straightforward thinking, and your 'scientific' jokes. Edwin, bedankt dat je mijn Utrechtse promotor wilt zijn.

The one and only cool people of the bone group! Leonie and Chrissy, when you two joined the lab all of a sudden I wasn't the only person working on bone anymore:
Leonie jij bestormde me met allerlei vragen over het hoe en wat van de proeven, waar ik zelf vaak nog niet echt over had nagedacht. Bovendien was je moleculaire achtergrond erg welkom. Laat je vooral niet opjagen, hè! Chrissy, if an experiment was going to fail for whatever reason the only thing I had to do was walk up to you and ask: you already tried everything! So cool! I think you will be a great groupleader some day. Thank you both - en ook Jo - for all the discussions and fun in the lab!
Josi, ook jij hoort zeker bij de bone group: je hebt me onwijs geholpen met alle cyp26b1 in situs die je gedaan hebt! Bedankt voor al je hulp en adviezen. En in ieder geval weet ik zeker dat er iemand is die dit proefschrift helemaal gaat lezen ☺.
Ansa, dankjewel voor het werk dat je gedaan hebt voordat ik kwam, hierdoor heb ik zeker weten een super-start gehad!

Maja, you are such a sweet girl. There is probably no other supervisor who have had so many problems as I had with keeping a student out of the lab! I have had a lot of fun and adventure supervising you. I really liked it. Thank you for all the work you did, which resulted in a nice addition to the screen chapter.

Met vier mannen een kamer delen is niet altijd even gemakkelijk... maar ik heb er helemaal geen problemen mee gehad. Sterker nog, het was onwijs gezellig!
Frank, sjarrel, ik heb genoten van jouw vrolijkheid. De disco en happy hardcore uurtjes in het lab en Tiësto in het kantoor doen het altijd goed... Wat fijn dat je achter me wilt staan tijdens de promotie. Ik kom zeker nog eens een biefstukje bij je halen!

Ben and Robert, I have enjoyed your conversations: 90% of them start serious and end up in complete bullshit... Ben, good luck with starting up your own group in Australia! Robert, samen begonnen en bijna samen klaar: succes met jouw laatste loodjes.
Jeroen, als jij niet ooit professor wordt dan kan iedereen het wel shaken! Dankjewel voor de interessante artikelen die jij al te pakken had bijna nog voordat ze uitkwamen, je Ensembl-kennis en je BAC recombineering experimenten. Al is er nog geen stabiele cyp26b1 transgene lijn, het heeft al wel kunnen resulteren in hoofdstuk 5 van dit boekje.

In vier jaar tijd is de Schulte-Merker groep behoorlijk gegroeid. Thanks to all the (ex) labmembers. I have enjoyed working with you. Thank you all for discussions, help, advices, and a lot of fun. Evisa and Ellen, good luck in the States! Merlijn, gelukkig is er nog iemand in het lab die zich zo af en toe bekommerd om de veiligheid ☺.
Ive, zo'n klein meisje met zo veel mensenkennis. Als er iets aan de hand was had jij het soms nog eerder door dan ikzelf. Dankjewel voor al je gezelligheid.

Jorg Renn and Christoph Winkler, thank you for our fruitful collaboration. Your medaka constructs were of great help for us to generate the zebrafish transgenic lines.
Sander Kranenbarg, bedankt voor de mooie micro CT scans die je gemaakt hebt.

Het grote voordeel van het Hubrecht instituut is toch wel dat, ondanks de verdeling in onderzoeksgroepen, het stiekem toch ook gewoon één groot lab is: Mannen van het Cuppenlab, bedankt voor jullie technische hulp en het gebruik van de multi-channels als die van ons het weer eens hadden begeven. Vrouwen van het Bakkerslab, bedankt voor de zo af en toe geleende reagentia.
Toen de Mummery groep de andere helft van onze labruimte leeg achterliet kwam daar gelukkig snel weer leven in de brouwerij: bedankt voor jullie gezelligheid (Tamaraaaa, Petraaaa). Verder wil ik iedereen bedanken die wel eens een biertje drinkt/heeft gedronken op de (vrijdagmiddag)borrels. Volgens mij is er geen betere manier om het weekend in te gaan en lekkerder krijg je de bitterballen nergens!
Joram, in 't Pandje kun je inderdaad echt wel knakworsten eten ☺.

Een tweede grote voordeel van het Hubrecht is de aanwezigheid van alle ondersteunende diensten: Bert, wie kan er beter op mijn vissen passen dan jij! Heren van de IT, bedankt voor het vele malen terughalen van mijn data dat ergens op een al gewiste I schijf stond. Ira, wat moet een AIO toch zonder jou... dankjewel voor al je geregel!

Tenslotte wil ik dan nog graag een aantal mensen - buiten het werk om - bedanken voor hun vriendschap en steun van de afgelopen jaren. En alhoewel ze dus stiekem eigenlijk helemaal niet thuishoren in een werk-gerelateerd bedankje, zijn ze,

misschien daarom wel, juist heel belangrijk voor me. Want wat is het fijn om mensen om je heen te hebben bij wie je altijd terecht kan:
Ireentje, Maev, Ellen en Sil: vriendinnetjes vanaf het eerste jaar van de studie. Nu allemaal wat anders of ergens anders. Bedankt voor alle eetdates, stapavonden, zomibo'tjes, sauna bezoekjes, geklets (wat gelukkig maar weinig over werk gaat) en nog veel meer...
Nienke, jou opzoeken in Nieuw-Zeeland was geweldig! Niet alleen hebben we een vet mooie reis gemaakt maar ook kwam het voor mij nog eens precies op het goede moment. Jammer genoeg is Utrecht-Maastricht niet echt op een avond te doen... ach, in ieder geval een goede reden om er dan maar meteen een weekendje van te maken!

Dan mijn grote broer en grote zus. Al zien we elkaar niet echt heel vaak (waarom gaan jullie dan ook in Enschede en Deventer wonen?), we kunnen gelukkig altijd verder gaan waar we gebleven waren. Broertje (ja, dat is dezelfde als mijn grote broer), het zijn jouw woorden: "Wat moet ik doen? paranimf zijn? wat is dat? oh, met zo'n pinguinpak aan..." Ik denk inderdaad dat het je heel goed gaat staan hoor! ☺ Superfijn dat je achter me wilt staan tijdens de promotie.
Lieve papa en mama, het klinkt te cliché maar ik moet toch toegeven dat jullie een groot voorbeeld voor me zijn. Al zo lang samen en, alhoewel het voor jullie zelf misschien niet zo heeft gevoeld het afgelopen jaar, ik vind dat jullie enorm sterk in jullie schoenen staan! Bedankt dat jullie er altijd voor me zijn.

Lieve Ewart, wie had dat ooit gedacht, toen ik vier jaar geleden het Hubrecht kwam binnen wandelen, dat deze laatste woorden voor jou bedoeld waren. Ikzelf in ieder geval niet! Onze start samen was dan ook verre van briljant. Het was te snel, te chaotisch, te onhandig, maar het was vooral ook te mooi om waar te zijn. Langzaamaan hebben we samen ons plekje weer gevonden en voel ik me bij jou nu helemaal thuis. Ik ben ontzettend blij met je en heb enorm veel zin in onze toekomst: heb ik vandaag al verteld dat...

Kirsten

CURRICULUM VITAE

Kirsten Spoorendonk werd geboren in Hendrik-Ido-Ambacht op 22 augustus 1982. Na het behalen van haar gymnasium diploma aan het Johan de Witt Gymnasium te Dordrecht in 2000, begon ze in september van datzelfde jaar met de studie Biomedische Wetenschappen in Utrecht. Tijdens de master Biology of Disease deed ze onderzoekservaring op bij de afdeling Experimentele Neurologie van het Universitair Medisch Centrum Utrecht (UMCU) onder begeleiding van dr. Freek van Muiswinkel. Een tweede stage werd uitgevoerd bij de afdeling Celbiologie in het UMCU onder leiding van dr. Vangelis Kondylis en dr. Catherine Rabouille. Na het afronden van haar studie in oktober 2005, begon ze in november 2005 met haar promotie onderzoek in het Hubrecht Instituut te Utrecht in de groep van prof. dr. Stefan Schulte-Merker. De resultaten van dit onderzoek staan beschreven in dit proefschrift.

LIST OF PUBLICATIONS

Spoorendonk KM, Hammond CL, Huitema LFA, Vanoevelen J, and Schulte-Merker S. Zebrafish as a unique model system in bone research: the power of genetics and *in vivo* imaging. *Journal of Applied Ichthyology, in press.*

Spoorendonk KM, Peterson-Maduro J, Renn J, Trowe T, Kranenbarg S, Winkler C, Schulte-Merker S. Retinoic acid and cyp26b1 are critical regulators of osteogenesis in the axial skeleton. *Development. 2008 Nov; 135(22): 3765-74.*

Publications not related to this thesis:

Ivan V, de Voer G, Xanthakis D, **Spoorendonk KM**, Kondylis V, Rabouille C. Drosophila Sec16 mediates the biogenesis of tER sites upstream of Sar1 through an arginine-rich motif. *Mol Biol Cell. 2008 Oct; 19(10): 4352-65.*

Kondylis V, **Spoorendonk KM**, Rabouille C. dGRASP localization and function in the early exocytic pathway in Drosophila S2 cells. *Mol Biol Cell. 2005 Sep; 16(9): 4061-72.*